ANALYZING THE PARTS BEHAVIOR IN A VIBRATORY BOWL FEEDER TO PREDICT THE DYNAMIC PROBABILITY PROFILE

By

Abigail Santos Cordero

A Thesis Submitted in Partial Fulfillment
of the Requirements for the Degree of

MASTER OF SCIENCE
In
MECHANICAL ENGINEERING

UNIVERSITY OF PUERTO RICO
MAYAGUEZ CAMPUS
2004

Approve by:

_____	_____
Frederick A. Just-Agosto, Ph.D. Member, Graduate Committee	Date
_____	_____
Agustin Rullán-Toro, Ph.D. Member, Graduate Committee	Date
_____	_____
Lourdes M. Rosario, Ph.D. President, Graduate Committee	Date
_____	_____
Hamed Parsiani, Ph.D. Graduate Studies Representative	Date
_____	_____
Paul Sundaram, Ph.D. Mechanical Engineer Department Director	Date

ABSTRACT

The vibratory bowl feeder is used in automated assembly to sort and orient a variety of parts. To design a part feeder the engineer needs knowledge related to the tendency of the parts to fall in different aspects and production requirements. The investigation proposes the development of a model that predicts the influence or the effect of the vibration amplitude in the orientation efficiency. The model was based on the identified parameters, such as part's geometry and orientation, to optimize the design and performance of the vibratory bowl feeder. In addition, experiments were conducted using five different parts in the bowl feeder to estimate the probabilities that the parts have when resting in all possible aspects while moving through a surface in movement. These experiments provided information that will help in the development of the model. The results were compared with the method of the centroid solid angle and the stability method, and a good correlation was obtained.

RESUMEN

El alimentador vibratorio se usa en la línea de ensamblaje automático para ordenar y orientar una gran variedad de piezas. Para diseñar un alimentador el ingeniero necesita tener conocimiento relacionado a la tendencia de las piezas a caer en diferentes aspectos. La investigación propone el desarrollar un modelo que prediga la influencia o el efecto de la amplitud de vibración en la eficiencia de orientación. El modelo se basó en parámetros identificados, como la geometría y la orientación de la pieza, para así optimizar tanto el diseño como el rendimiento del alimentador vibratorio. Además, se realizaron experimentos usando cinco piezas de diferentes geometrías en el alimentador vibratorio para estimar la probabilidad de descanso de las piezas para todos los posibles aspectos mientras viajan por una superficie en movimiento. Estos experimentos proveyeron buena información que ayudo al desarrollo del modelo. Estos resultados se compararon con el método del centroide del ángulo sólido y el método de la estabilidad, obteniéndose una buena correlación.

DEDICATION

To **God** who guides me through all my life permitted me to reach my goals and take another step in my professional life.

To my **parents**, Enos and Ramona, for their immeasurable support, and for laying the foundation of what I am and will be.

To my **Sister**, Keila, for her support, for the good times and moments we shared together

To my **friends,** Carla, Luisa, Edwar and Amílcar, who helped me to reach the goal of finishing this work and teach me that friendship is a special gift from God.

ACKNOWLEDGEMENT

I acknowledge the guidance of my thesis advisor Dr. Lourdes M. Rosario for her advice and support throughout the course of this study. I would like to thank the Mechanical Engineering Department, University of Puerto Rico Mayagüez Campus for giving me the opportunity to work in my master degree and supporting me economically during those years. Also I would like to thanks the Industrial Engineering Department University of Puerto Rico Mayagüez Campus for giving me the opportunity to work in the Manufacturing Laboratory where the experimental workstation is located. I wish to express my gratitude to Dr. Agustin Rullán for his interest in my research and the new ideas. My special thanks to my friends Amílcar Rincón, Carla Carrasquillo, Edwar Romero and Luisa Feliciano for their help in preparing the experiments and thesis.

TABLE OF CONTENTS

LIST OF TABLES

LIST OF FIGURES

NOMENCLATURE

E_{ab}	Area of change in aspect from *a* to *b*.
P_i	Probability of the natural resting aspects in aspect *i*.
Q_i	Centroid solid angle subtended by aspect *i*.
h_i	Height of the Centroid from aspect *i*.
$\bar{y}_i$	Center of gravity from the base in aspect *i*.
A_i	Contact area of the aspect *i*
m_1	Base mass.
m_2	Bowl mass.
I_1	Base Mass Moment of Inertia.
I_2	Bowl Mass Moment of Inertia.
θ	Leaf Spring Angle.
r_1	Radius of leaf spring connection at base.
r_2	Radius of leaf spring connection at bowl.
r_e	Radius of electromagnets connection.
r_o	Radius of rubber feet.
k_s	Leaf spring stiffness.
k_h	Rubber foot horizontal stiffness.
k_v	Rubber foot vertical stiffness.
b_h	Rubber foot horizontal damping coefficient.
b_v	Rubber foot vertical damping coefficient.
μ	Friction coefficient between the part and the track.
w	Vibration frequency.

r_p	Track radius.
ϕ	Track angle at the beginning.
Y_1	Base vertical displacement.
Y_2	Bowl vertical displacement.
λ_1	Twisting of the base.
λ_2	Twisting of the bowl.
d	Deflection of the leaf spring.
F_d	Electromagnets force on the bowl.
F_a	Leaf spring axial force.
F_b	Bending force.
F_v	Support force provided by the rubber feet.
F_h	Force to counteract twisting provided by the rubber feet.
m_p	Part mass.
g	Gravitational acceleration.
N	Track surface normal.
y_v	Track vertical displacement.
y_p	Track parallel displacement.
t_1	Detach time.
t_2	Rise time.
v_v	Part vertical velocity.
Cg	Center of gravity.
MDFT	Modified dynamic feeding test.
MDBT	Modified dynamic bowl test.
CSA	Centroid solid angle.

CHAPTER 1

INTRODUCTION

The vibratory bowl feeder is the preferred choice for many machine builders as well as companies in industry such as automotive, pharmaceutical, cosmetics, electronics, fasteners and plastics, to sort and orient parts before automated assembly.

The most important factor to consider when selecting a parts feeder is the type of parts to be fed. Bowl sizes and types are determined through a variety of factors such as: part size and configuration, part abrasiveness, condition of the part when handled, required feed rate and bowl direction.

The design of industrial parts feeders is a long, trial and error process that can take months. To design a part feeder the engineer needs to have in mind some significant problems with the parts. Some of those problems are the complexity of the parts and the feeder, the number of the parts, and the absence of good impact friction models in the literature.

This investigation consisted on the development of a model that predicts the influence or the effect of the vibration amplitude in the orientation efficiency. For that reason, the model was based on the identified parameters, such as part's geometry and part's orientation at the end of the bowl feeder, to optimize the design and performance of the vibratory bowl feeder.

The experiments were conducted using different parts in the bowl feeder test-bed to estimate the probabilities that the parts have when resting in all possible aspects while moving through a surface in movement. The set of those probabilities is called the Dynamic Probability Profile. With those experiments, any deviation between the Dynamic Probability Profile and the Static Probability Profile obtained from static models and static experiments were compared.

1.1 Problem Description

The industries have the necessity of mathematical models to predict the probabilities of natural resting aspects of parts from their geometries on a surface in motion. For this, using the experimental station design by Rincón (Rincón, 2001), a study using five parts with different geometries to study the dynamic probabilities of natural resting in the vibratory bowl feeder was developed.

1.2 Objectives

1. To study the relationship between geometric features in complex parts and their Dynamic Probability Profiles (DPP).

   To achieve the goal, experiments were conducted on which complex parts were allowed to travel on a vibratory bowl feeder track. Five parts were studied during the experiments, the part's names are latch, stab & contact, handle, magnet and arc chute. The number of parts resting on each aspect will be used to estimate each aspect's probability. The set of all the probabilities is the Dynamic Probability Profile.

The geometric features under study are the area ratio and the height ratio. The area ratio is the total surface area of the part divided by the area of the aspect i, (A_{total}/ A_i). The height ratio is the total height of the part divided by the height of the aspect i, (h_{total}/ h_i).

2. To compare the area ratio and the height ratio with the theoretical models predicting the static probability profile of these parts. The models used in this study were the Centroid Solid Angle (CSA) and the Stability Method.
3. To study the impact of the vibration amplitude in the orientation efficiency of the bowl feeder for the parts studied.

1.3 Summary

In automated assembly lines the parts must be correctly oriented to facilitate the process of the product assembly. The studies of the probabilities of the natural resting behavior of the parts in vibratory bowl feeders provide good information to improve the feeder efficiency and the orientation mechanism for the vibratory bowl feeder.

Chapter 2 presents brief information of previous work in vibratory bowl feeder research related to the development of the parts models in a static surface plus some experiments and studies of the vibratory bowl feeder dynamics. Chapter 3 shows the experimental workstation used to realize the Modified Dynamic Feeding Test and Modified Dynamic Bowl Test, and also the experimental parameters. Chapter 4 presents a theoretical analysis of probabilities for the natural resting behavior of five parts. Chapter 5 shows the experimental results and their analysis. Chapter 6 explains the obtained conclusions and future works recommendations.

CHAPTER 2

PREVIOUS WORKS

Some researchers have studied the natural resting tendency of different shape parts. In the work of Ngoi, Lim, Lye and Lee, several methods to analyze the natural resting aspect of a component were used. Each method has a hypothesis to describe the purpose of the method and also they compare each one of them with the Boothroyd's Energy Barrier Method. These methods are: centroid solid angle, displacement centre of gravity and dynamic models. Those methods are described next.

2.1 The Energy Barrier Method

Boothroyd described the development of the energy barrier method, which could analyze all types of geometries. The analysis was extended to other regular prisms such as triangular and hexagonal prisms by circumscribing a cylinder round the prisms. The results obtained for the cylindrical prism could be used to predict the probability profile of these regular prisms. The energy barrier method is based on the following assumptions and hypothesis:

- Surfaces can be hard or soft. A surface is soft if, when a part is dropped on it, the horizontal component of the impact force is significant and this causes the part to roll across the surface changing rapidly from one resting aspect to

another. A surface is hard if, when a part dropped on it, the horizontal component of the impact force has an insignificant effect.

- The parts are dropped from a height such that the part has sufficient energy after impact to undergo at least a change of resting aspect.

The use of the energy barrier method to analyze the probability profile of parts on soft surfaces is based on the hypothesis that, the probability for a part to come to rest in a particular natural resting aspect is a function of two factors: the energy tending to prevent a change of aspect and the amount of energy possessed by a part when it begins to fall into that natural resting aspect.

The energy barrier for a change in aspect of a part is represented by the area E_{ab} formed by the projection of the change of center of mass height in aspect b during a change of aspect from aspect a to b. This is illustrated for a squared-sectioned prism in figure 2.1. Aspect a refers to the part resting on the end (square face) and aspect b refers to the part resting on the side. Let E_{ab} represent the area of change in aspect from end a to side b and E_{ab} represent the area of energy barrier for a change in aspect from side b to end a. According to Boothroyd, the energy barrier areas are constructed as shown in Figure 2.1. The expressions for the areas are:

$$E_{ab} = x^2\left(\alpha_2 p^2 + q - \alpha_1 q^2 - \frac{y}{x}\right) \tag{2.1}$$

$$E_{ba} = x^2\left[\alpha_2 p^2 + q - \frac{\pi}{2} - 1\right] \tag{2.2}$$

Where,

x represents the horizontal distance between the center of mass and the part sides,

y represents the vertical distance between the center of mass and the part base (in the case of a square section x = y),

$$p = \left[2 + \left(\frac{y}{x} \right)^2 \right]^{\frac{1}{2}}, \tag{2.3}$$

$$q = \left[1 + \left(\frac{y}{x} \right)^2 \right]^{\frac{1}{2}}, \tag{2.4}$$

$$\alpha_1 = \arcsin\left(\frac{1}{q} \right) \tag{2.5}$$

$$\alpha_2 = \arcsin\left(\frac{1}{p} \right) \tag{2.6}$$

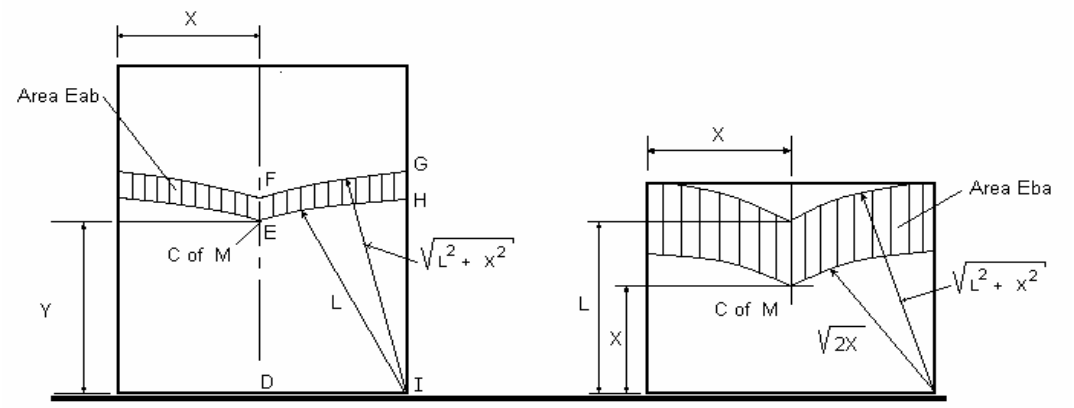

Figure 2.1. Energy barrier for a squared prism (obtained from Boothroyd et al, 1992).

Taking in consideration the number of each possible part aspects, the probability for aspect is given by: (Boothroyd et al, 1992)

$$P_a = \frac{2E_{ab}}{2E_{ab} + 4E_{ba}} \tag{2.7}$$

And for aspect b

$$P_b = 1 - P_a \tag{2.8}$$

The energy barrier method effectively analyzes simple shaped parts with constant cross-section and having two resting aspects. However, for complex parts the method becomes computationally intensive and requires a clear visualization of the energy barrier of the given part; hence, making the method less attractive. (Boothroyd et al, 1992)

2.2 Centroid Solid Angle Method

A solid angle is defined as being of one steradian unit subtended by portion of a spherical surface whose area is equal to the square of the radius of the sphere.

The centroid solid angle construction is presented in the Figure 2.2,

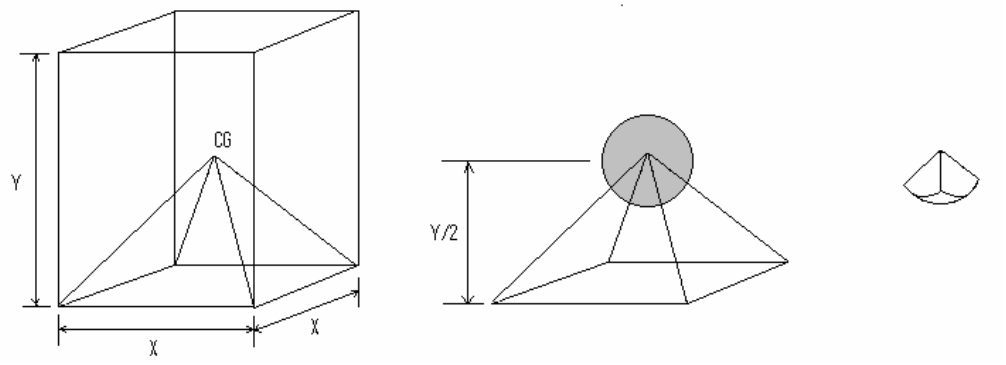

(a) (b) (c)

Figure 2.2. Centroid solid angle construction (a) surface area (b) solid sphere with its center at the apex (c) enveloped volume (obtained from Ngoi et al, 1995a).

The centroid solid angle may be computed by the equation,

$$Centroid \quad Solid \quad Angle = \frac{Surface \quad Area}{R^2} \tag{2.9}$$

where the Surface Area and the radio R are shown in the Figure 2.3.

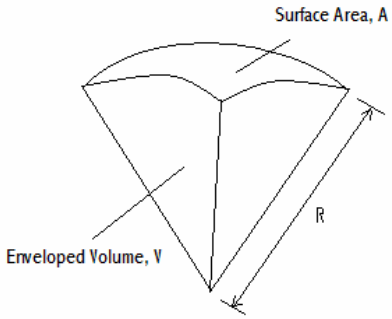

Figure 2.3. Centroid solid angle (obtained from Ngoi et al, 1995a).

The centroid solid angle method makes the same assumptions on the classifications of surfaces as the energy barrier method, and that the probability that a part would rest in a particular resting aspect when dropped on a soft surface is proportional to the centroid solid angle. This method is based on the hypothesis that the probability for a part resting in a particular resting aspect is directly proportional to the solid angle or solid angle ratio subtended by the centroid to that surface, and inversely proportional to the height of the centroid from that resting aspect.

The generalized equation is shown next.

$$P_i = \frac{Q_i / h_i}{\sum_{j=1}^{n} (Q_j / h_j)} \tag{2.10}$$

where P_i is the probability of the aspect i, Q_i is the centroid solid angle subtended by aspect i, and h_i is the height of the centroid from aspect i.

The centroid solid angle method is based in the hypothesis that the probability of a component resting on a specific aspect is directly proportional to the magnitude of the centroid solid angle and inversely proportional to the height of its centroid from that aspect. Ngoi, Lim and Lee applied this hypothesis to prismatic parts of square, triangular, hexagonal, cylindrical and rectangular cross-section. (Ngoi et al, 1995b)

To predict the natural resting behavior of prismatic parts of irregular cross-section, Ngoi, Lim and Lee proposed a hypothesis based on the centroid solid angle. This hypothesis assumed that the probability of a part resting on a specific natural resting aspect is proportional to the height of the centroid from that surface.

The generalized equation,

$$P_i = \frac{Q_i \big/ h_i}{\sum_{j}^{n} \left(Q_j \big/ h_j \right)} \tag{2.11}$$

$$\sum_{i=1}^{n} P_i = 1 \tag{2.12}$$

where P_i is the probability of aspect i, Q_i is centroid solid angle subtended by aspect I and h_i is height of the centroid from aspect i.

This hypothesis was used to analyze a complicated geometry, symmetrical and non-symmetrical T-shaped prism. During this analysis, Lee, Ngoi and Lim compared this hypothesis with the Boothroyd's Energy Barrier Method having a consistent result with a deviation not exceeding 7%. (Ngoi et al, 1995b)

2.3 Displacement Centre of Gravity Method

This method is based on the hypothesis that the probability of a part coming to rest in a particular aspect is proportional to the centroid solid angle and inversely proportional to the height of the center of gravity from the aspect in question. This method is applied to a part with a displaced center of gravity. Lee, Lim and Ngoi used a CAD computation of the centroid solid angle to determine the enveloped volume.

The main advantage of this method is that it uses very basic, well-defined geometric properties of the component being analyzed, the location of the center of gravity and the solid angle. (Ngoi et al, 1995c)

2.4 Experimental Studies

A previous study driven by Rosario and Hernández Coronas was based on the dynamic test of the feeder and the dynamic feeding test. Both tests were based on the previous experiments carried out by Boothroyd and Ho, 1972. In this study several questions were presented with relationship to the statistical analysis of the results and the impact of diverse variables in the dynamic aspects of the piece.

One of the results of this analysis was the necessity to use more samples to obtain a better estimate. However, although more parts would provide a better estimate of the dynamic profile of the probability, it also represented a problem in terms of the logistics of the experiments. In the original experiments all the parts were counted and classified (Rosario and Hernández Coronas, 1997). In the experiment there were always some parts that were taken off the wall of the track of the feeder, these they were classified as uncertain. The main problem with this was that the profile of probability was not the quite an exact thing. On the other hand, statistically speaking, it is not appropriate to eliminate the uncertain parts because then the sample size will differ of test on approval. With this situation a correct analysis of the results will become impossible to carry out. As a solution intended, it was to use more parts, maintaining as the same sample size a group of the parts used in the rail. This way they don't take into account the uncertain parts.

A study driven by Levy was based on the analysis of the behavior of components as these are conveyed up to the bowl track. The research studied two mathematical models for computing the probability distributions of the natural resting aspects of prismatic parts. The first model employs the concept of the centroid solid angle of components, and the other is based on stability considerations. The models were applied to prismatic parts with square, cylindrical, triangular, hexagonal, rectangular, and symmetrical and asymmetrical T shape prism. The models were also applied to analyze three different terminal connectors for which empirical data was

available. Analytical results were benchmarked with the empirical data and found to agree well with the drop test results conducted by others researchers (Levy, 2000).

Also Rincon did an investigation that proposes a dynamic model that allows the analysis of the movement of the feeder and, simultaneously, it establishes a relation with the dynamics of the parts. In addition, a study of the probability of natural rest of pieces when falling in a surface in movement was made. These results were compared with the method of the centroid solid angle and the stability method, obtaining itself a good approach (Rincón, 2002).

2.5 Dynamic Models

Chua and Tay presented a mathematical model for predicting the natural resting aspect of small, regular, shaped and uniform density parts. The objective of their model is facilitating the design of effective and efficient orientation devices for vibratory bowl feeders. In their investigation they use rectangular, cylindrical and prismatic parts with regular cross-section. At the end, they view that the major factor is the geometry of the parts to determine the natural resting aspect of them. (Chua et al, 1998)

On the other hand, Maul and Brian worked with a system model and simulation of the vibratory bowl feeder. They developed a mathematical model of a bowl feeder by using state-space methods to evaluate the bowl feeder parameters. From this mathematical method a computer simulation can predict the velocity of the parts in the bowl and the part feed rate. The mathematical model was divided in two models:

bowl motion and part motion. In the bowl motion model, they assume that the bowl and base are rigid bodies and that all other components have a linear behavior. In the part motion model, it is assumed that the part is small enough to be considered a point mass when compared to the bowl, the part weighs significantly less than the bowl, and its weight does not affects the motion of the bowl. The model predicts the motion of the bowl using state space methods for a model of the feeder having six degree of freedom. The only disadvantage is that the velocities of the parts in the bowl feeder are quite sensitive to small perturbation in feeder parameters. (Maul et al, 1998)

In automatic assembly the important factor is the orientation of the part because the part has to be aligned in a desired orientation before assembly. This means that the main key to the efficient design of a vibratory bowl feeder is an understanding of the probability that given part will come naturally to rest on particular aspect (Ngoi et al, 1995d).

2.6 Summary

In this chapter some of the methods developed to study the probability of parts natural resting in a vibratory bowl feeder were discussed. These were the energy barrier, the centroid solid angle, and the displacement center of gravity. The centroid solid angle and the stability methods were successfully applied to analyze the natural resting behavior of a part family in previous works. The equations deduced by the methods to be referred later were used to compare with experimental data of this work.

CHAPTER 3

EXPERIMENTAL PROCEDURE

This chapter describes the steps followed to develop the experimental tests and how the parameters necessary to verify the dynamic model were obtained. Also, this chapter describes the experimental station design, the selection of the experiment parts, the experiment description and the test realized to verify the results.

3.1 Experimental Station Description

A workstation designed by Rincón was used to realize the experimental procedure, shown in Figure 3.2. The components of the workstation are a vibratory bowl feeder, a computational program, data acquisition equipment and sensors. (Rincón, 2001)

3.1.1 Vibratory Bowl Feeder

Vibratory bowl feeders are used in automated assembly for aligning and feeding a variety of parts and also have a lot of different application in modern industries. A typical vibratory bowl feeder is show in Figure 3.1, it consist of a metallic bowl supported on three or four sets of inclined leaf springs secured to heavy base. Vibration is applied to the bowl from an electromagnet mounted on the base. The electromagnet generates the force to drive the bowl feeder.

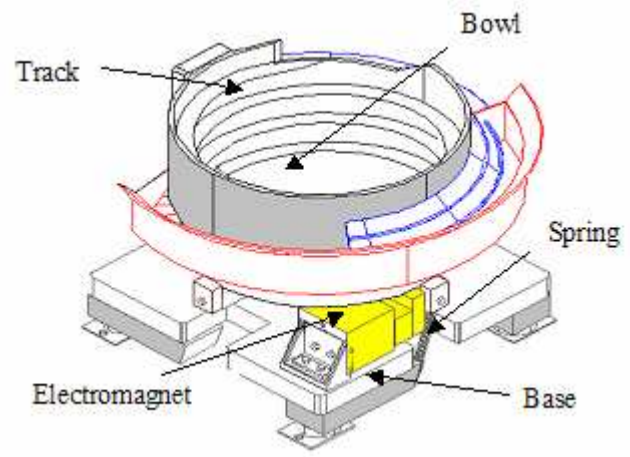

Figure 3.1. Vibratory Bowl Feeder (obtained from Rincón, 2002)

The vibratory bowl feeder used was an industrial system from Service Engineering Inc. For the experiment the feeder didn't have the orientation devices. The feeder had four leaf springs and two vertical electromagnets. The feeder had a controller from Performance Feeder Inc. Model PF-2R used to control the vibration amplitude. The feeder parameters are shown in the next table.

Table 3.1.a Vibratory Bowl Feeder Parameters (Rincón, 2002)

Parameters	Value
Base mass (M_1)	85.127 kg
Bowl mass (m_2)	65.688 kg
Base Mass Moment of Inertia (I_1)	3.56 kg.m^2
Bowl Mass Moment of Inertia (I_2)	2.51 kg.m^2

Table 3.1.b Vibratory Bowl Feeder Parameters (Rincón, 2002) cont.

Parameters	Value
Leaf Spring Angle (θ)	73.17^o
Radius of leaf spring connection at base (r_1)	0.18 m
Radius of leaf spring connection at bowl (r_2)	0.18 m
Radius of electromagnets connection (r_e)	0.14 m
Radius of rubber feet (r_o)	0.1845 m
Leaf spring stiffness (k_s)	41×10^6 Nm
Rubber foot horizontal stiffness (k_h)	35.9×10^6 Nm
Rubber foot vertical stiffness (k_v)	39.5×10^6 Nm
Rubber foot horizontal damping coefficient (b_h)	3.191298 Nm/s^2
Rubber foot vertical damping coefficient (b_v)	12.147 Nm/s^2
Friction coefficient between the part and the track (μ)	0.3
Vibration frequency (w)	120 rad/s
Track radius (rp)	0.21 m
Track angle at the beginning (ϕ)	3^o

3.1.2 Computational Programs

To rcompile the necessary data from the experiment a computer was used. The Excel program was used to save the data and the experimental results.

3.1.3 Data Acquisition Equipment

A PCI 4451 card from National Instruments was used for the data acquisition in the experiment, this card has two input and two outputs channels. Also an ICP Sensor Signal Conditioner PCB 482A22 model with four channels and a BNC connector were used for the weak signals.

3.1.4 Sensors

A triaxial accelerometer PCB 356A16 model and a force sensor PCB 208C03 model were used in the experiments.

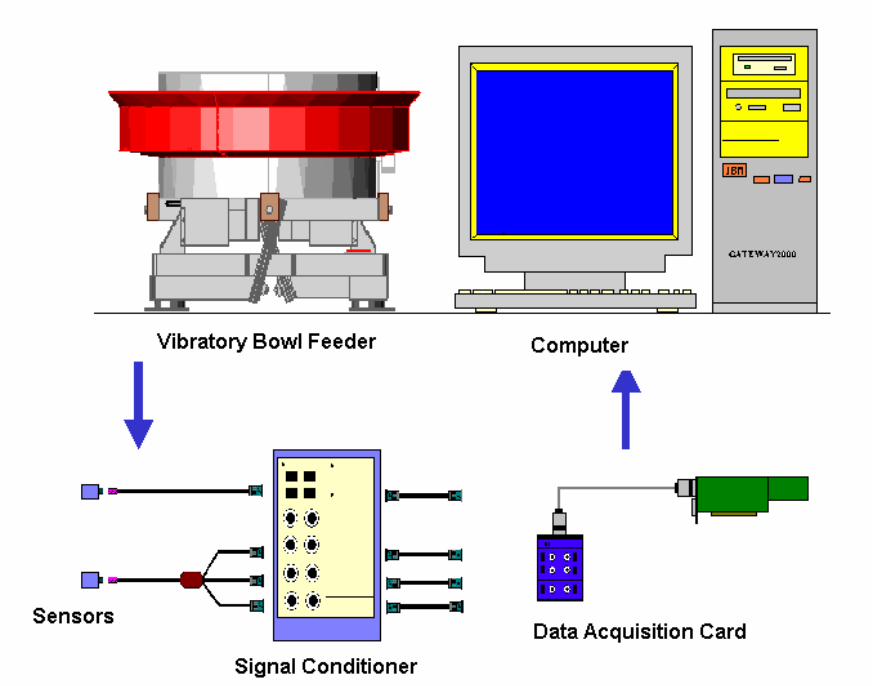

Figure 3.2. Experimental Work Station. (obtained from Rincón, 2002)

3.2 Experimental Procedure

For the experimental procedure two tests were conducted. They were: Modified dynamic feeding test (MDFT) and the Modified dynamic bowl test (MDBT), both of them described by Rosario and Hernández Corona, 1997. The Modified dynamic feeding test is useful to determine the dynamic probability profile of the parts that are supplied by the feeder when they suffer no recirculation. While the Modified dynamic feeding test allows the first parts to recirculate at least two times in the bowl. In both experiments the aspect of parts that overlaps were considered since the feeder didn't have passive mechanisms of orientation.

3.2.1 Modified dynamic feeding test

It is assumed that the dynamic feeding test provides the distribution probabilities for all possible positions that can be initially adopted by the part when initially dropped in the bowl feeder. The results of this test helps designers chose appropriate orienting devices for the feeder.

1. Select initial operating parameters
    a. Ensure that the operation parameters are such that forward conveying will occur for the part being studied and that the unrestricted feedrate allows a reasonable waiting period for the conclusion of each test trial.

   b. Select the number of times that the experiment will be repeated for each value of amplitude of vibration being tested. To obtain reasonable confidence levels in the final results, the test should be performed at least ten times.
   c. Select the spectrum of vibration amplitudes. This depends in the feeder and the parts.
   d. Select a reasonable number of parts for sound statistical analysis. A safe minimum is to use one hundred and fifty parts. However, this number depends also on how many parts will fit in the bowl track.
2. Turn on the feeder.
3. Throw the parts in the feeder.
4. Wait until 100 parts out of the total number being used enter the track.
5. Turn off the feeder.
6. Count the occurrence of the different orientations acquired by parts. Only those parts in contact with the feeder wall or track count, including the count of overlapping parts.
7. Pick up all the parts from the feeder and repeat steps 2–6 the number of times decided previously in step 1-b.

3.2.2 Modified dynamic bowl test

The modified dynamic bowl test is similar to the MDFT. The original test, used by Murch (Murch et al, 1972), is based on the assumption that when the connectors are dropped back into bottom of the bowl, they will tend to orient themselves into their natural resting position. The parts were dropped on the bowl bottom and allowed to climb up the track. The parts advanced up track and re-circulated back in the bowl. A simple piece of cardboard was attached at the top of the track so that the parts could return to bowl bottom and continue circulating.

1. Select initial operating parameters;
    a. Ensure that the operating parameters are such that forward conveying will occur for the part being studied and that the unrestricted federate allows a reasonable waiting period for the conclusion of each test trial.
    b. Select the number of times that the experiment will be repeated for each value of amplitude of vibration being tested. To obtain reasonable confidence levels in the final results, the test should be performed at least ten times.
    c. Select the range of vibration amplitudes. This depends on the feeder and the part.

   d. Select a reasonable number of parts for a sound statistical analysis. A safe minimum is to use one hundred and fifty parts. However, this number depends also on how many parts will fit in the bowl track.
   e. Select a time interval that allows the first parts to recirculate at least two times at minimum vibration amplitude. This will ensure that all the parts will recirculate at least once.
2. Turn on the feeder.
3. Throw the parts in the feeder.
4. Wait until the time interval elapses.
5. Turn off the feeder.
6. Count the occurrence of the different orientations acquired by the hundred parts. Only those parts in contact with the feeder wall or track count, including the count of overlapping parts.
7. Pick up all the parts from the feeder and repeat steps 2–6 the number of times decided previously in step 1-b.

The key step in both experiments is to use a feeder that will hold on its track a high number. In this way, even though some parts may stay in the bottom of the parts, there will be enough parts in the track for a sound statistical analysis. Following the experimental studies done by Levy, Rincón, Rosario and Hernández, three vibration

amplitude values were chosen for both tests to study the behavior of the parts in the vibratory bowl feeder, The vibration amplitude values that allow forward conveying at a reasonable feedrate are 78%, 80% and 82%.

3.2.3 Additional Procedure

To study the behavior of the part, Dr. Agustin Rullan came with a very interesting idea. It was to study the behavior of the part in a specific location of the track of the vibratory bowl feeder by taking video for approximately 10 minutes per frequency of vibration and then compare them with the other procedures. The chosen part to study the probability of the natural resting at the end of the track or the top of the feeder at 78%, 80% and 82% of the vibration amplitude was the handle part. In the appendix are the data and the results of this experiment.

3.3 Experiment Design and Parameter Selection

Chosen the modified dynamic feeding and modified dynamic bowl test, the selections of the factors was the next step. For this case the chosen factors are vibration amplitude and the parts geometry. Inside of each factor three levels were selected, low, medium and large, for that reason a procedure of a 3^3 factorial experiment was used. (Montgomery, 1997). A 100 parts was the sample size in the experiments choose based on previous works, choosing a $\alpha = 0.05$ or a 95% confidence level, with an error, e =.05, and a $Z_{.025} = 1.96$, the standard deviation was $\sigma = .255$.

3.3.1 Studied Parts

The study of the parts behavior in a surface in motion was realized with five parts with different geometries. The Figure 4.3 shows the five parts considered in the study.

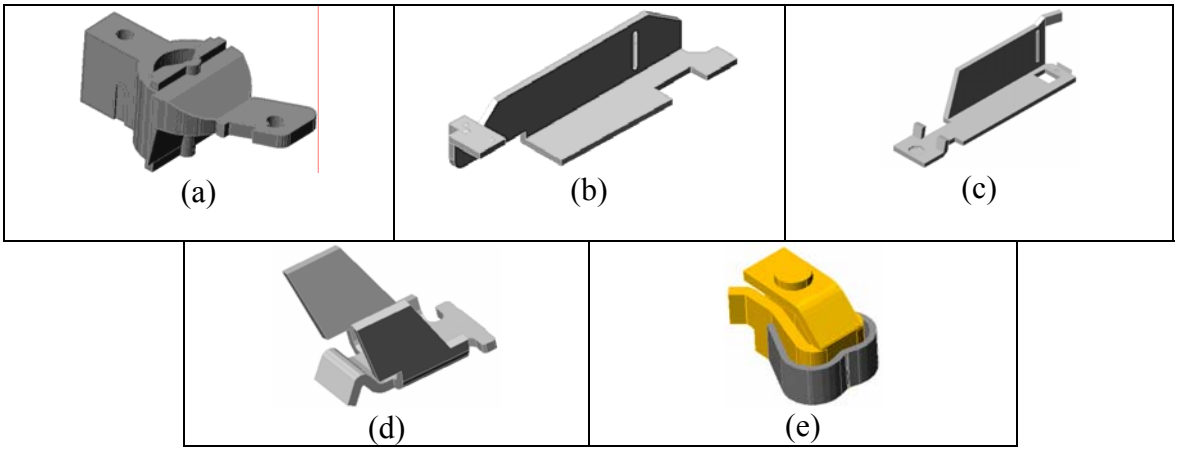

Figure 3.3. Studied parts: (a) handle, (b) magnet, (c) latch, (d) arc chute and (e) stab & contact.

In the experiments, each part have several possible natural resting positions, each one is detailed next.

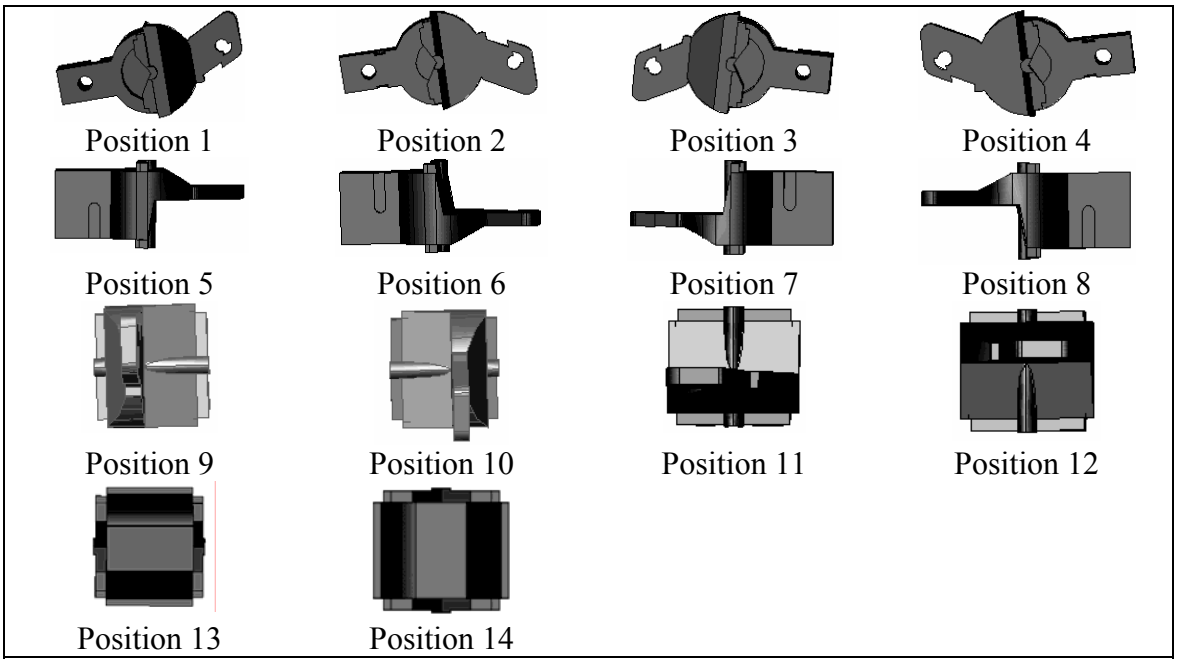

Figure 3.4. Handle Positions

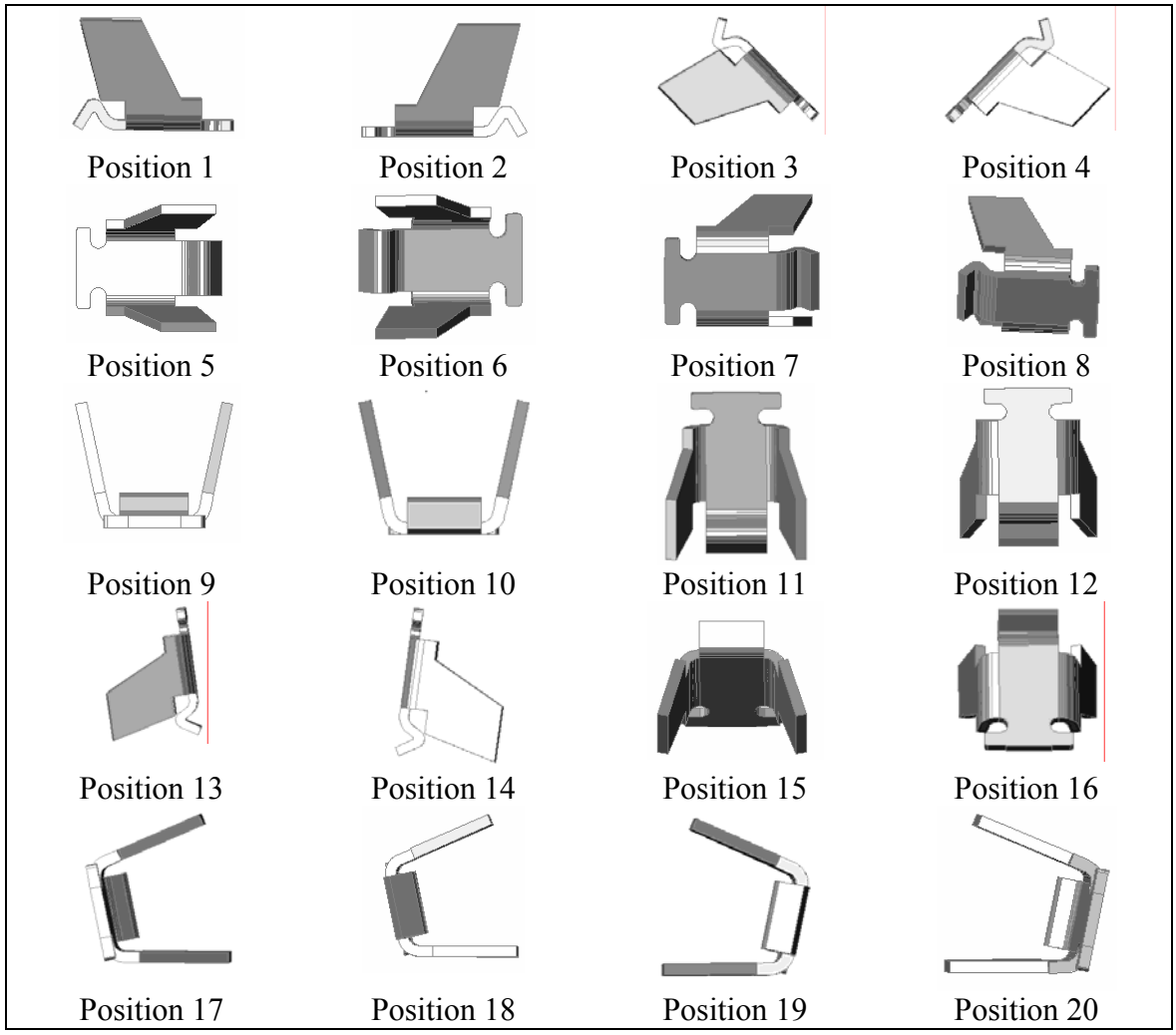

Figure 3.5. Arc Chute Positions

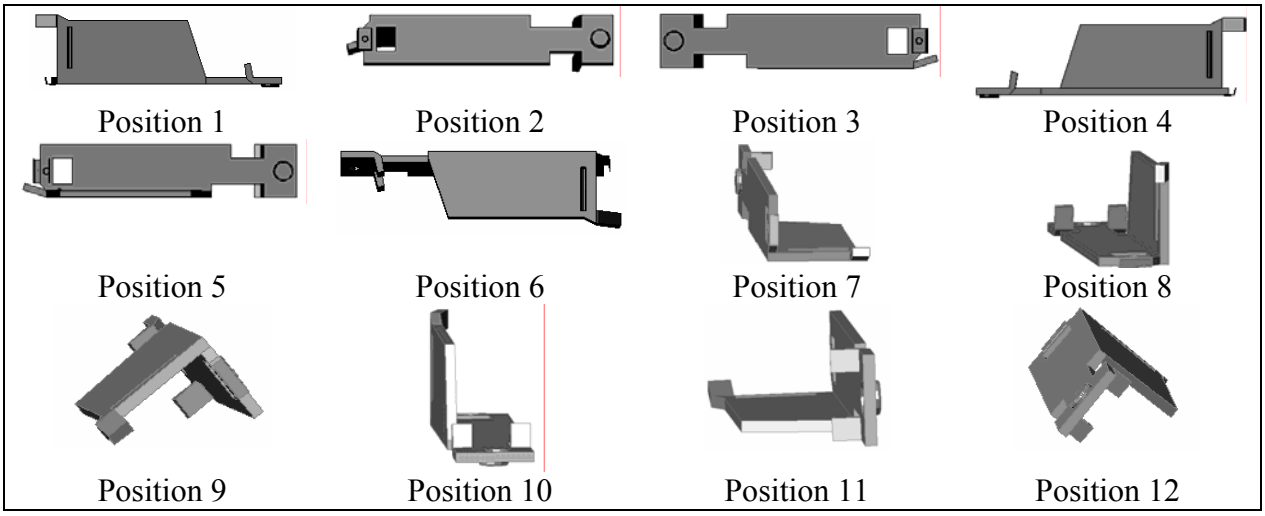

Figure 3.6. Latch Positions

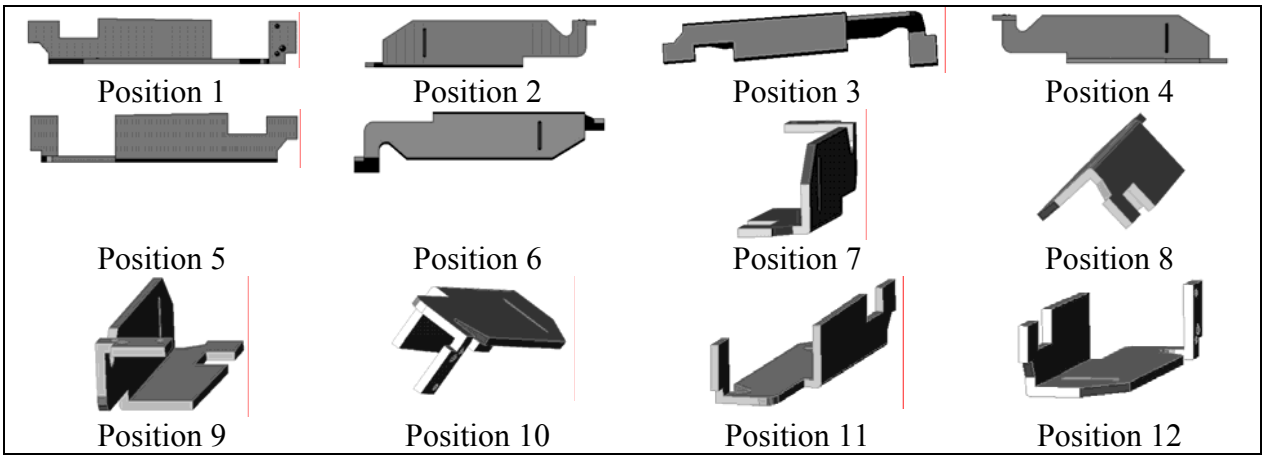

Figure 3.7. Magnet Positions

Figure 4.7. Stab & Contact Positions

3.4. Summary

In this chapter, the equipment configuration used for the experiments and the types of tests used were described. Finally, a description of the different parts and their corresponding aspects within the bowl track were provided. A significant number of different positions describe the behavior of the five parts. The vibration of the bowl feeder and the geometry of the parts influence the parts tendency towards a certain position.

CHAPTER 4

THEORETICAL ANALYSIS

4.1 Centroid Solid Angle Method

A solid angle is defined, as being of one steradian unit subtended by portion of a spherical surface area is equal to the square of the radius of the sphere. The centroid solid angle makes the assumptions that the probability hat a part would rest in a particular resting aspect when dropped on a soft surface is proportional to the centroid solid angle. (Ngoi et al, 1997 b).

This method based on the hypothesis that the probability for a part resting in a particular resting aspect is directly proportional to the solid angle ratio subtended by the centroid to that surface, and inversely proportional to the height of the centroid from that resting aspect. The generalized equation is as shown in equation 2.11.

To calculate the centroid solid angle, building a interception volume (explained in Chapter 2), with AutoCad 2000 was used. In determining the centroid solid of an angle, first virtual faces were added where relevant and the transformed prism, as show in Figure 4.1, was analyzed. A virtual face is draw if the part has contact only in corners or points that have two different faces.

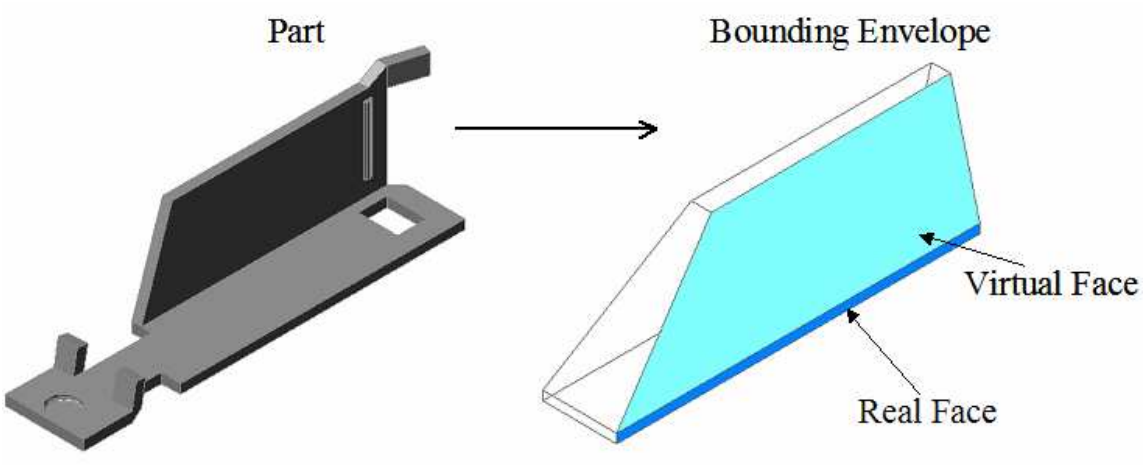

Figure 4.1. Bounding envelope for a complex part.

A pyramid, whose apex was located at the centroid, was constructed at each face after the original solid was erased. The faces of the pyramid were defined by lines drawn from the apex to each vertex of the natural resting aspect, shown in Figure 4.2. A solid sphere of an arbitrary radius, that not exceeds the part height, was constructed with its centre coincident with the apex of the pyramid. The pyramids intersect and the sphere, as shown in Figure 4.2, is the enveloped volume.

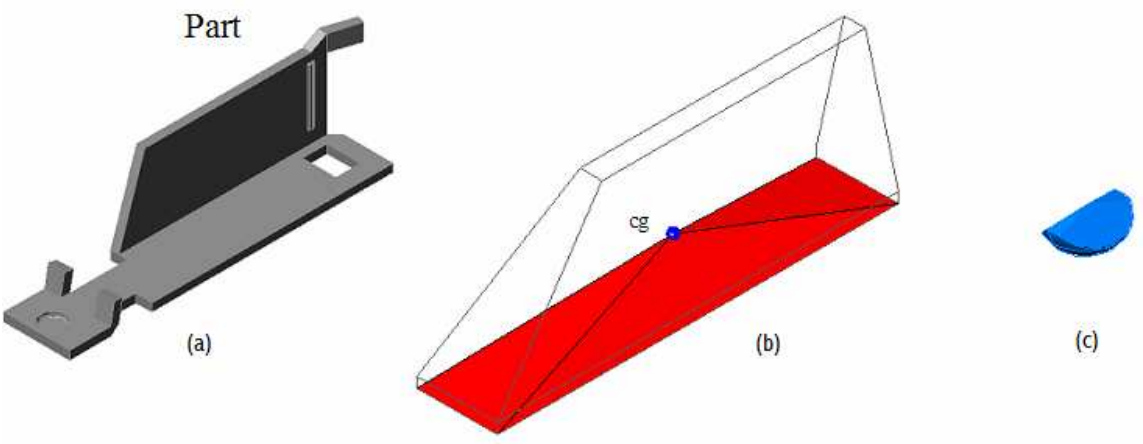

Figure 4.2. (a) Original part, (b) construction of pyramid and sphere and (c) enveloped volume.

The latch part had eight different faces in the study and eight pyramids were constructed to find the enveloped volume and the probability of the part, these aspects are shown in the Appendix A. Three of these aspects were chosen because there was the natural resting positions that the part adopts during the experiments. The formula for the latch part probabilities and the results are shown in Table 4.1, and the rest of the results for the other parts are shown in the appendix.

$$p_1 = \frac{\frac{Q_1}{h_1}}{\frac{Q_1}{h_1} + \frac{Q_2}{h_2} + \frac{Q_3}{h_3}} \tag{4.2}$$

$$p_2 = \frac{\frac{Q_2}{h_2}}{\frac{Q_1}{h_1} + \frac{Q_2}{h_2} + \frac{Q_3}{h_3}} \tag{4.3}$$

$$p_3 = \frac{\frac{Q_3}{h_3}}{\frac{Q_1}{h_1} + \frac{Q_2}{h_2} + \frac{Q_3}{h_3}} \tag{4.4}$$

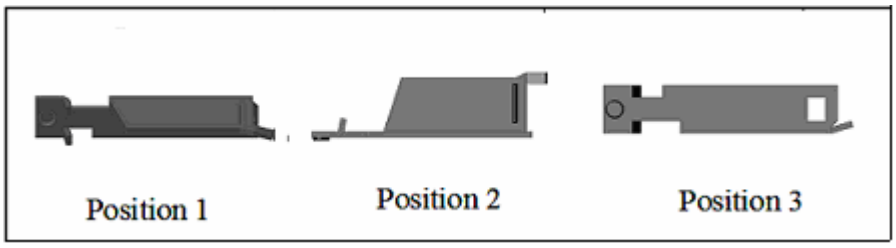

Figure 4.3. Latch Natural Resting Positions.

Table 4.1. Probability distribution: CSA method for latch part.

Position	Qi	hi	Qi/hi	Probability
1	0.1562	18.3416	0.008516	0.066318
2	0.1455	2.9298	0.049662	0.386732
3	0.1734	2.4688	0.070237	0.546951
Total	0.4751		0.128415	1

4.2 Stability Method

Stability is the state of being able to keep in position and based on logical analysis, the larger the contacting area; the more stable would be the part in the natural resting aspect. Also the lower the center of gravity of the part, the more stable would be that part in that natural resting aspect. (Chua and Tye, 1998).

Therefore, stability S is a function of the size of the contact area A and the distance $\bar{y}$ of the center of gravity from the base. In addition, S is proportional to A and inversely proportional to $\bar{y}$. The generalized equation (Chua and Tye, 1998) is presented below.

$$P_i = \frac{N_i A_i / \bar{y}_i}{\sum N_i A_i / \bar{y}_i} \qquad (4.5)$$

Where P_i is the probability for the aspect i, N is the number of surface identical to and inclusive of the contacting surface, A is the contact area, and $\bar{y}$ is the distance from base to center of gravity.

The formula for the latch part probabilities and the results are shown in the table 4.2, and the rest of the results for the other parts are shown in the appendix.

$$P_1 = \frac{\frac{A_1}{\bar{y}_1}}{\frac{A_1}{\bar{y}_1} + \frac{A_2}{\bar{y}_2} + \frac{A_3}{\bar{y}_3}} \tag{4.6}$$

$$P_2 = \frac{\frac{A_2}{\bar{y}_2}}{\frac{A_1}{\bar{y}_1} + \frac{A_2}{\bar{y}_2} + \frac{A_3}{\bar{y}_3}} \tag{4.7}$$

$$P_3 = \frac{\frac{A_3}{\bar{y}_3}}{\frac{A_1}{\bar{y}_1} + \frac{A_2}{\bar{y}_2} + \frac{A_3}{\bar{y}_3}} \tag{4.8}$$

Table 4.2. Probability distribution: Stability method for the latch part.

Position	Ai	hi	Ai/hi	Probability
1	367.6144	18.3416	20.04266	0.074223
2	314.4	2.9298	107.3111	0.397398
3	352.2499	2.4688	142.6806	0.528379
Total	1034.264		270.0344	1

4.3 Probability Data Comparison

To test if the model given by the null hypothesis fits the data the Pearson's x^2 test for goodness of fit was used for it. A useful measure for the overall discrepancy between the observed and expected frequency is given by the equation 4.9. For this test the rejection region is that when $x^2 \geq x^2_{\propto}$ where $x^2_{\propto}$ is the upper $\propto$ point of the x^2 distribution with degree of freedom = k – 1 = (number of cell) – 1. (Johnson et al, 1992)

$$x^2 = \sum_{i=1}^{k} \frac{(n_i - np_{io})^2}{np_{io}} = \sum_{cells} \frac{(O-E)^2}{E} \qquad (4.9)$$

where,

O = Observed frequency

E = Expected frequency under H_o

H_o = Cell probability

n_k = respective cell frequency

p_k = cell probability

Referring to the latch data, take $\propto = .05$, the computations for the x^2 statistic are shown in the table 4.3, the comparisons for the other parts' positions are included in the Appendix D. Using the table of percentage points of x^2 distribution, $x^2_{.05} = 5.99$ with d.f = 2. Because the observed $x^2 = 463.05$ is larger than $x^2_{.05}$ value, the null hypothesis is rejected at $\propto = .05$.

Table 4.3. The x^2 Test for Goodness of Fit for Latch Part Data for MDBT Method versus CSA at 78%

MDBT vs CSA at 78% Amplitude				
Positions	1	2	3	Total
Observed frequency (O)	230	236	534	1000
Probability under Ho	0.066318	0.386732	0.546951	1
Expected frequency (E)	66.31759	386.7318	546.9506	1000
$\frac{(O-E)^2}{E}$	403.9944	58.74894	0.306641	463.05
				d.f.=2

Some parameters that were studied were the part's height ratio (h_{total}/ h_i) and area ratio (A_{total}/ A_i). These parameter were compared with the results of both methods, MDBT and MDFT methods, and the results for the latch part are shown in the table 4.3 and 4.4, and the rest of the results for the other parts are shown in the appendix. The figures 4.4 to 4.7 show the comparison of the probability distribution of latch' aspects compared with the height ratio and area ratio, respectively. Comparisons for the other parts' positions are included in the appendix A and C.

Table 4.4. Comparison of the Experimental Probabilities data with the height ratio (h_{total}/ h_i) per latch's aspects.

Positions	MDBT			MDFT			H total/Hi
	78%	80%	82%	78%	80%	82%	
1	0.23	0.277	0.306	0.195	0.2	0.242	0.597
2	0.236	0.225	0.208	0.31	0.335	0.307	3.735
3	0.534	0.498	0.486	0.495	0.465	0.451	4.432

Table 4.5. Comparison of the Experimental Probabilities data with the area ratio (A_{total}/ A_i) per latch's aspects.

Positions	MDBT			MDFT			A total/ Ai
	78%	80%	82%	78%	80%	82%	
1	0.23	0.277	0.306	0.195	0.2	0.242	3.483
2	0.236	0.225	0.208	0.31	0.335	0.307	4.073
3	0.534	0.498	0.486	0.495	0.465	0.451	3.635

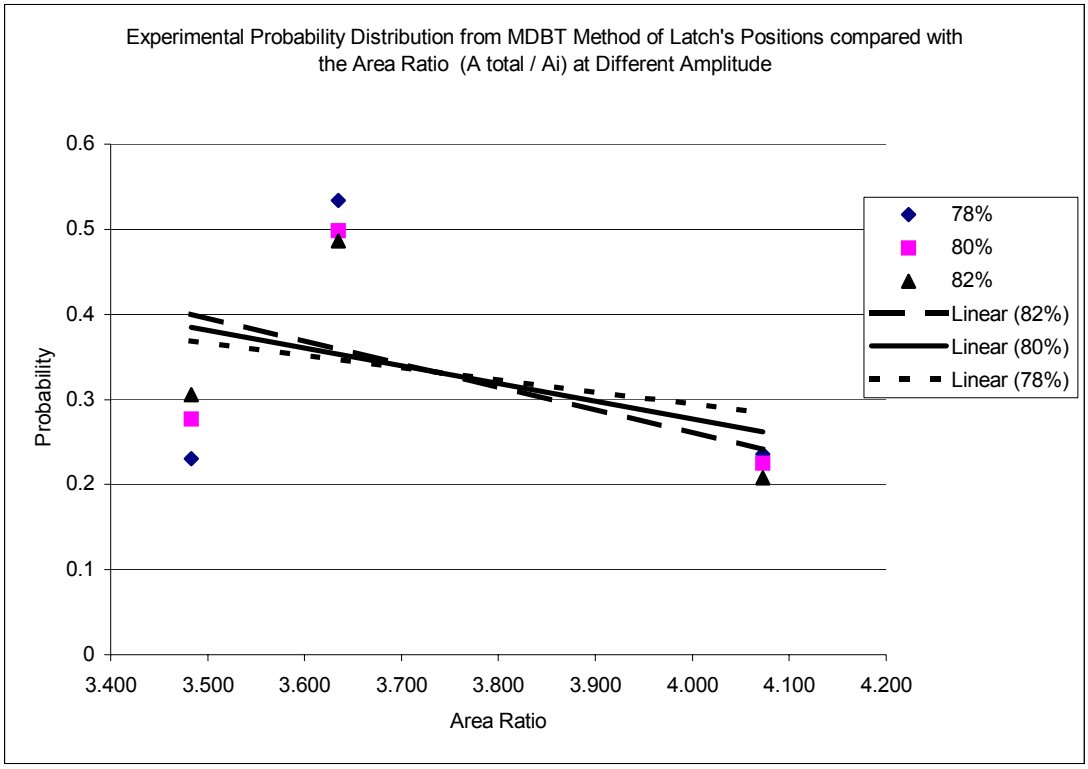

Figure 4.4. Experimental Probability distribution from MDBT method of the latch's aspects compared with the area ratio (A_{total}/ A_i).

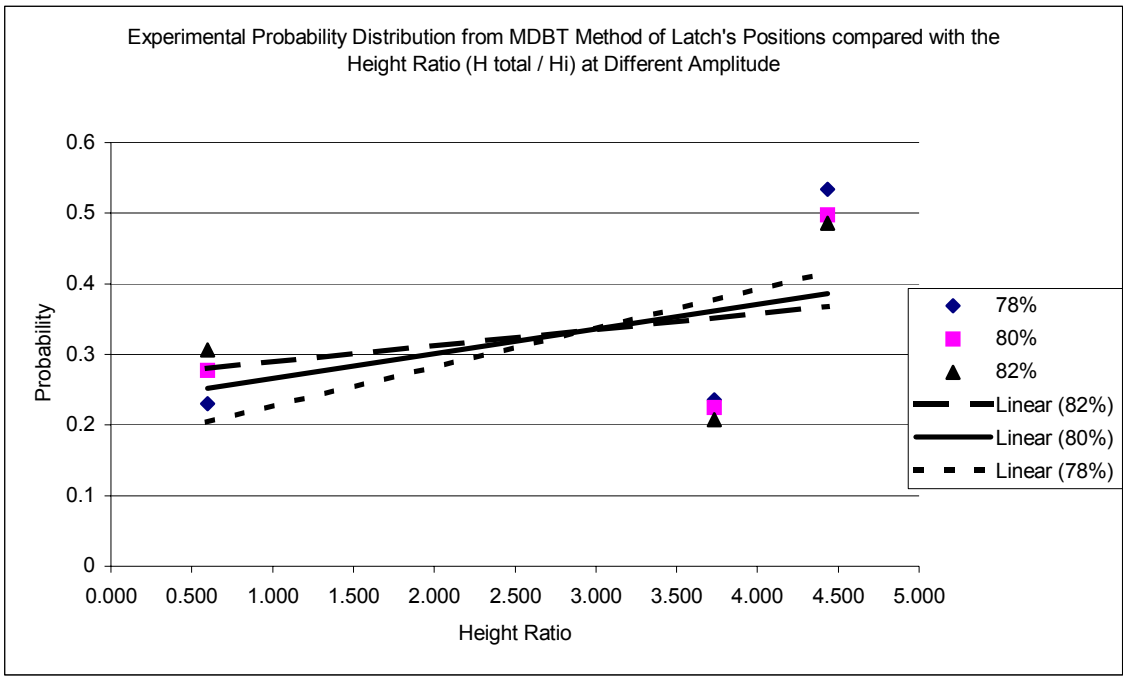

Figure 4.5. Experimental Probability distribution from MDBT method of the latch's aspects compared with the height ratio (h_{total}/ h_i).

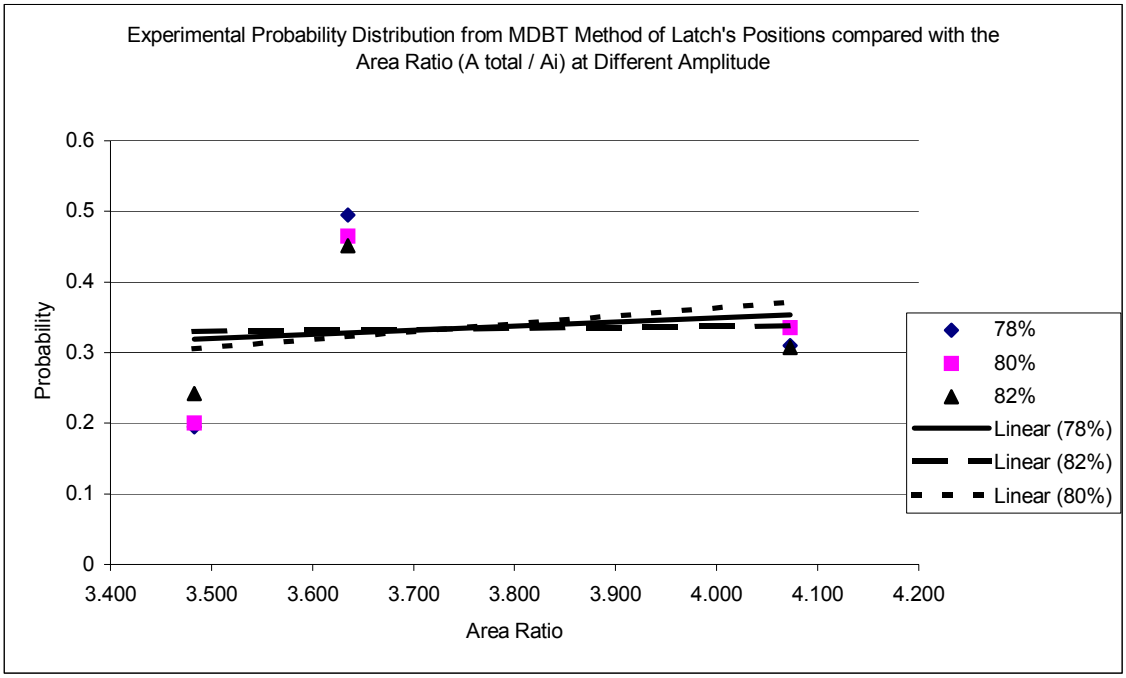

Figure 4.6. Experimental Probability distribution from MDFT method of the latch's aspects compared with the area ratio (A_{total}/ A_i).

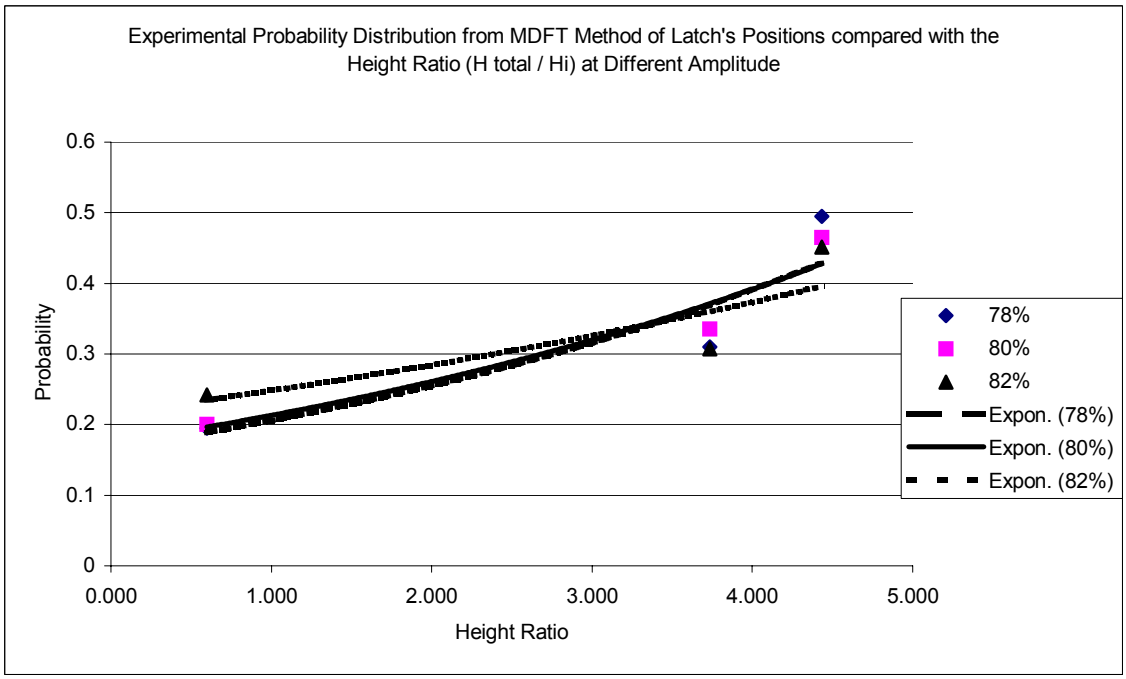

Figure 4.7. Experimental Probability distribution from MDFT method of the latch's aspects compared with the height ratio (h_{total}/ h_i).

The hypothesis is that there exists a proportional correlation between the probability and the two chosen parameters as follow:

$$P \propto \frac{h_{total}}{h_i} \tag{4.10}$$

$$P \propto \frac{A_i}{A_{total}} \tag{4.11}$$

Comparing the experimental probability data with the two chosen parameters, the area ratio and the height ratio, as the probability increases the height ratio increases and the area ratio decreases for some of the parts. This can be observed from the regression graph shown that the probability is directly proportional with the height ratio, having a positive slope, and indirectly proportional to area ratio, having a negative slope.

4.4 Summary

In this chapter a theoretical analysis of the probability of natural resting aspect for latch part was realized using the centroid solid angle and the stability method. These methods were applied to parts in a static surface; the realized experiments considered a dynamic surface and these results are explained in detail in the Chapter 5. Using the Pearson's x^2 test for goodness of fit to measure for the overall discrepancy between the observed and expected data for all the studied parts conclude that the null hypothesis was rejected because the $x^2 \geq x^2_{\propto}$ at $\propto = .05$. This means that doesn't exist a statistical correlation between the analytic methods, the centroid solid angle, stability methods, and the experimental results for parts with complex geometry. Analyzing the data of the height ratio (h_{total}/h_i) per aspect for each part it is clear that, as the ratio increases the probability for a part to rest in a more stable aspect is higher. And also analyzing the data of the area ratio (A_{total}/ A_i) per aspect for each part, as the ratio decrease the probability for a part to rest in a more stable aspect is higher for some of the parts. A regression relation between the both methods, MDFT and MDBT, and the parameters chosen, area ratio and height ratio, for each part demonstrate the proportionality between them. The area ratio and the height ratio are good parameters to predict the stability of the part's aspects.

CHAPTER 5

EXPERIMENTAL RESULTS

This chapter includes the results obtained from the modified dynamic feeding and the modified dynamic bowl tests and a comparison of the experimental results with the centroid solid angle and stability methods.

5.1 Parts' Behavior while moving through a surface in movement

For the study, the centroid solid angle and the stability methods were compared with the experimental results. The arc chute, handle, stab & contact, magnet and latch were the parts used to define the probability profile in the vibratory bowl feeder (Figure 3.3). Figures 5.1 - 5.5 show the probability profiles obtained for each part at vibration amplitude of 78%. Comparisons for vibration amplitudes of 80% and 82% are included in the appendix C. The figures show that the stable aspect in the experimental surface is even more stable in a dynamic surface and the less stable aspects in a dynamic surface.

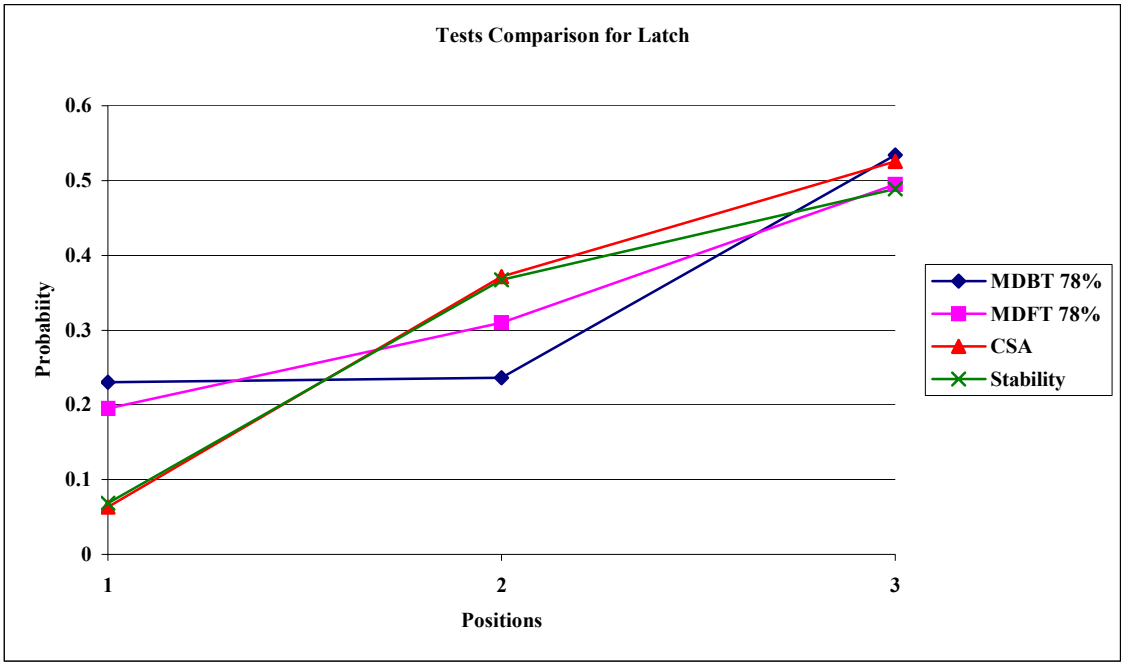

Figure 5.1. Latch probability profile (amplitude = 78%).

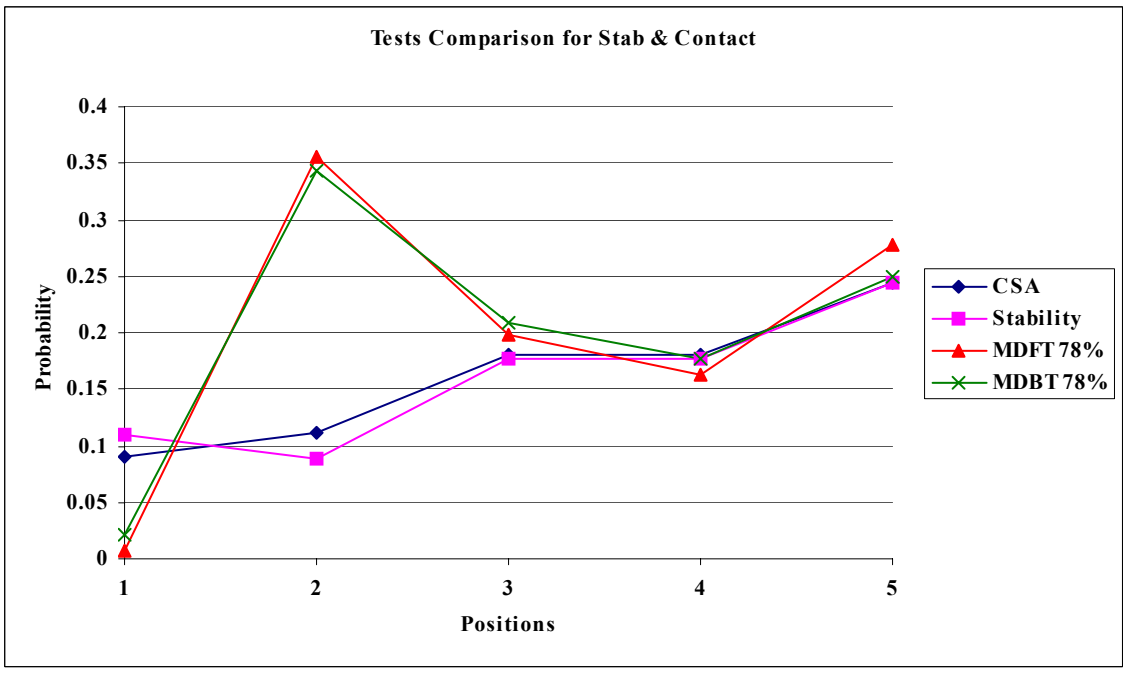

Figure 5.2. Stab & contact probability profile (amplitude = 78%).

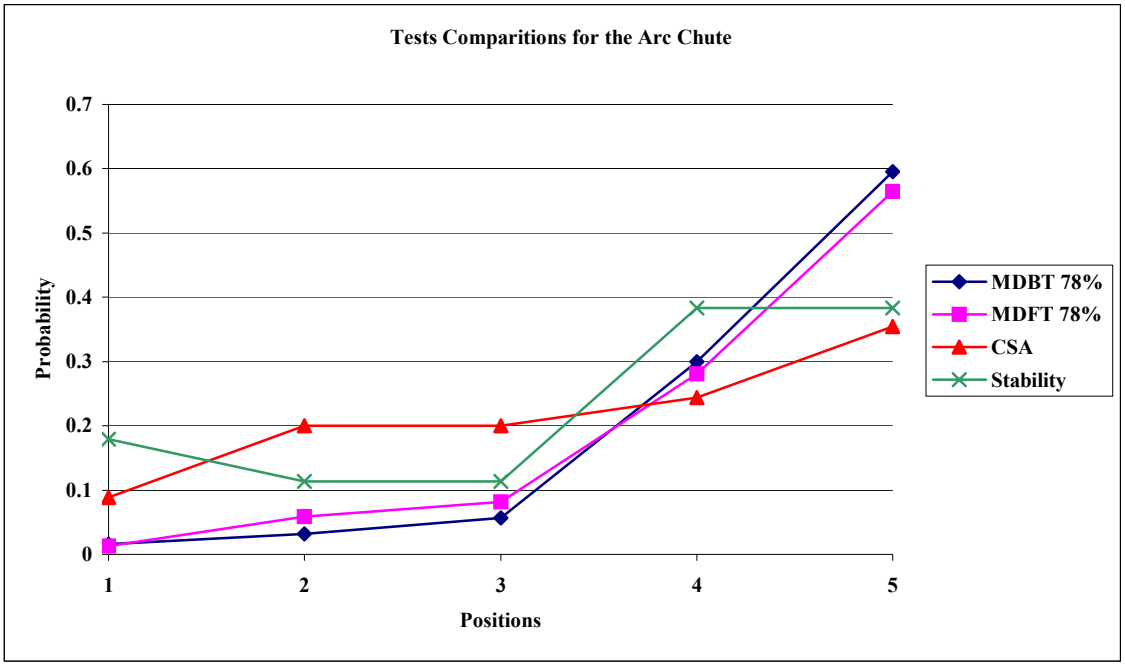

Figure 5.3. Arc chute probability profile (amplitude = 78%).

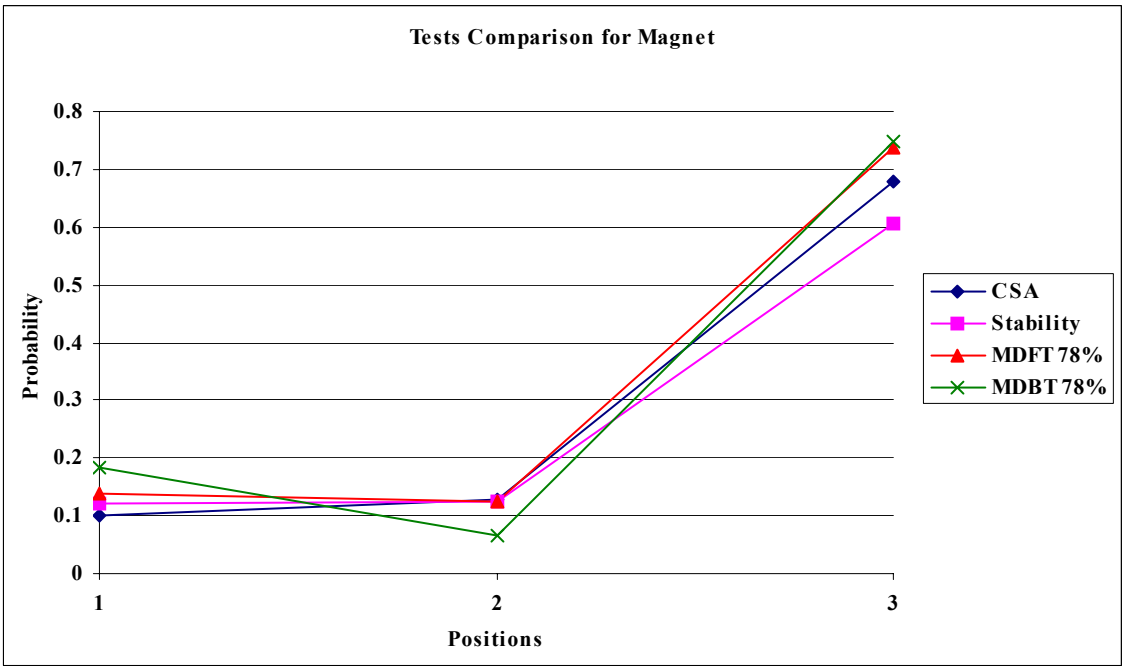

Figure 5.4. Magnet probability profile (amplitude = 78%).

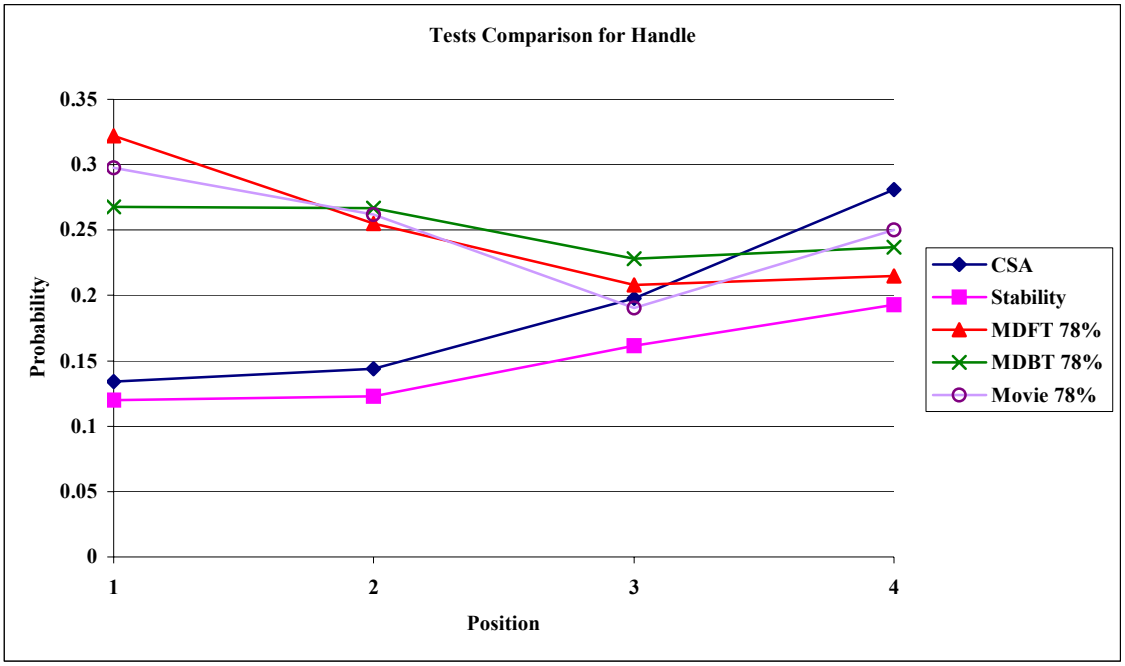

Figure 5.5. Handle probability profile (amplitude = 78%).

Figures 5.6 – 5.15 show the experimental probability profile for the different vibration amplitudes. These figures show that no matter the vibration amplitude the part had, the tendency is to take the more stable aspect. In general, from the results it was observed that the parts followed the same tendencies and an amplitude variation only improve the mores stable aspects and suppress the unstable ones.

In case of the handler part, a discrepancy (or a less correlation) was shown on this phenomenon as could be seen in Figures 5.14 and 5.15. Also in Figure 5.16- 5.17 show a graph of difference to see the impact of the vibration in the handle behavior.

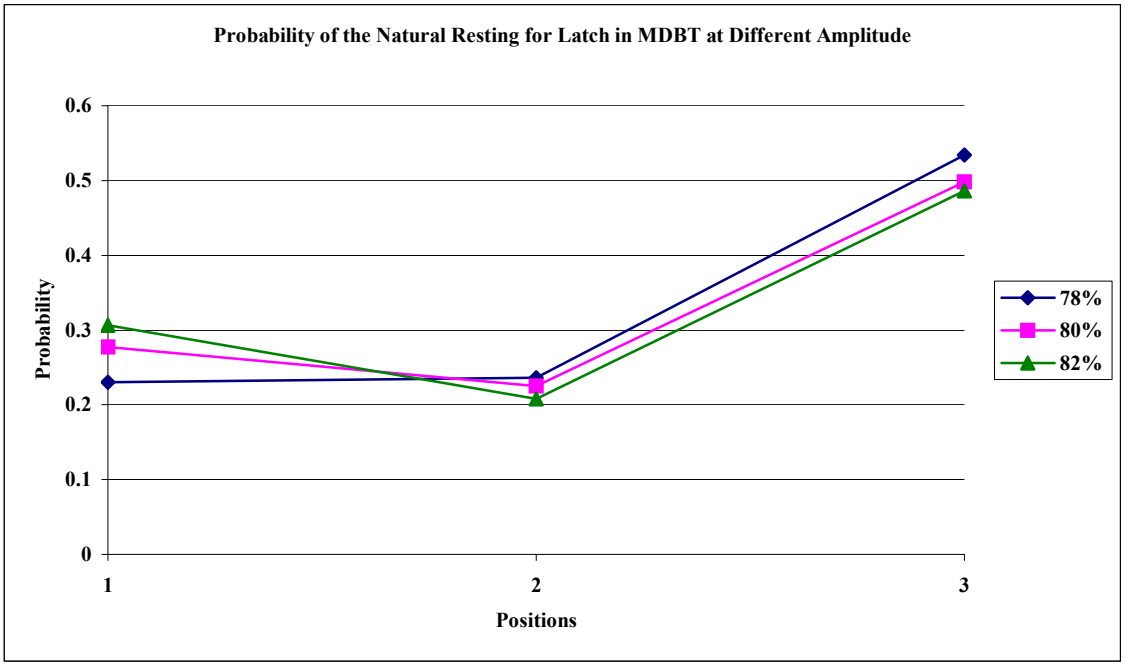

Figure 5.6. Experimental results for the latch in MDBT.

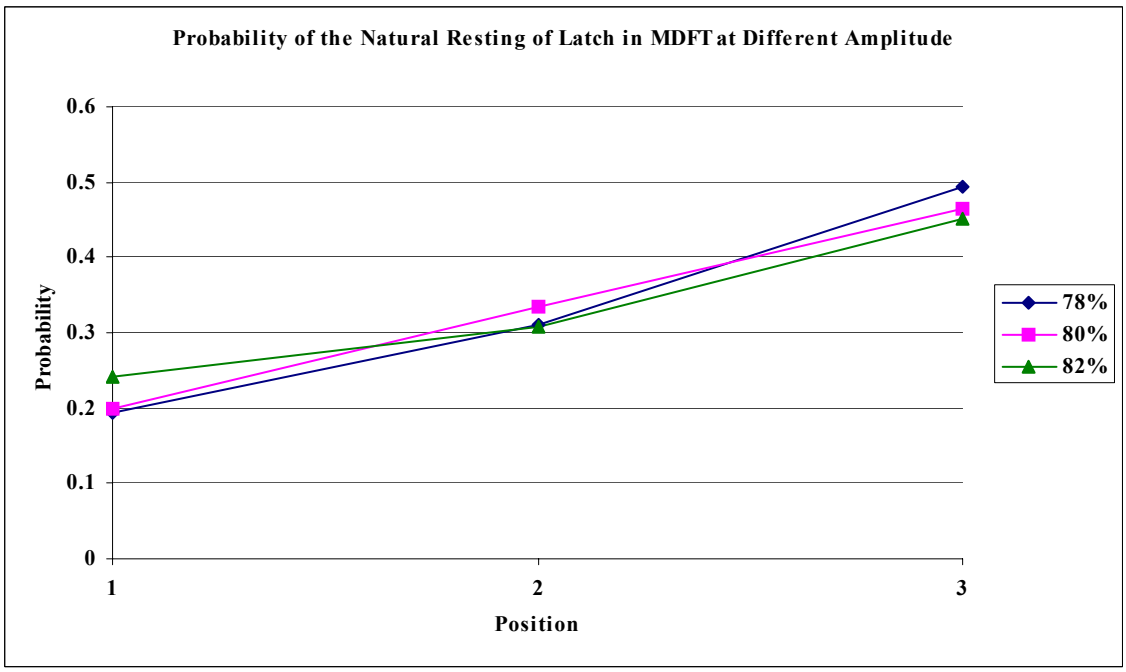

Figure 5.7. Experimental results for the latch in MDFT.

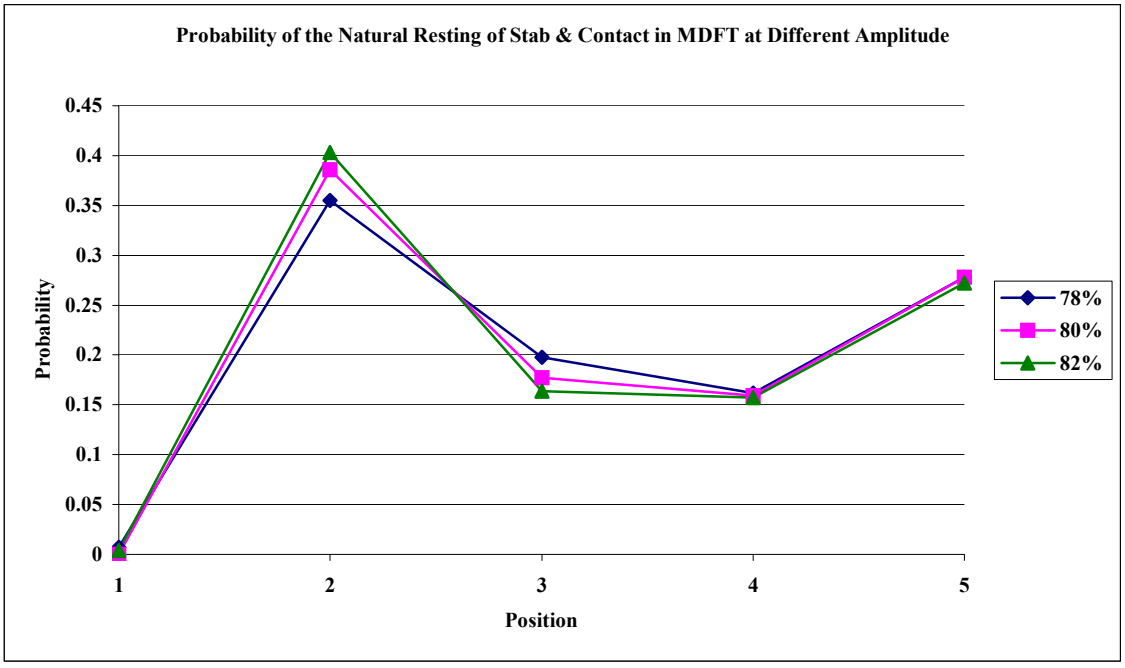

Figure 5.8. Experimental results for the stab & contact in MDFT.

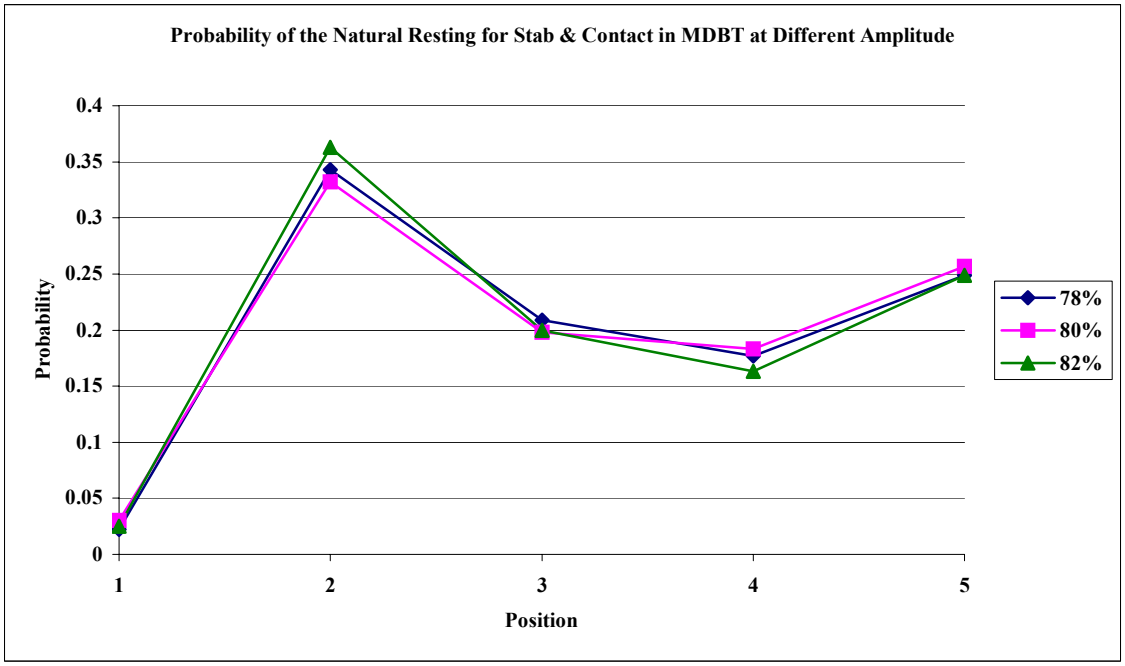

Figure 5.9. Experimental results for the stab & contact in MDBT.

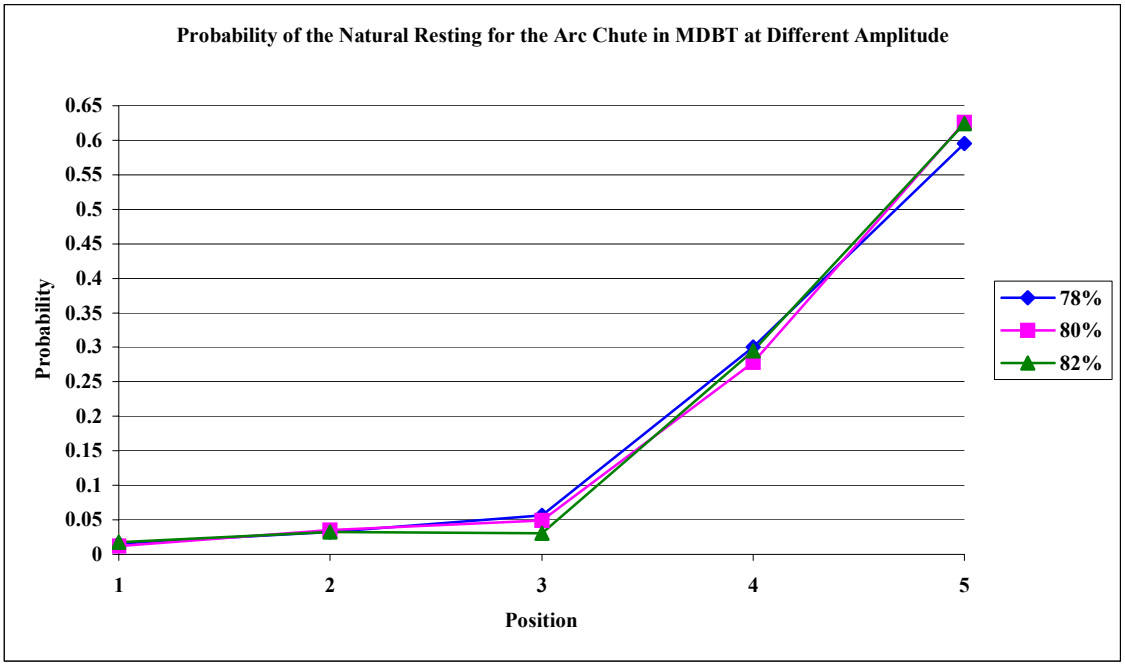

Figure 5.10. Experimental results for the arc chute in MDBT.

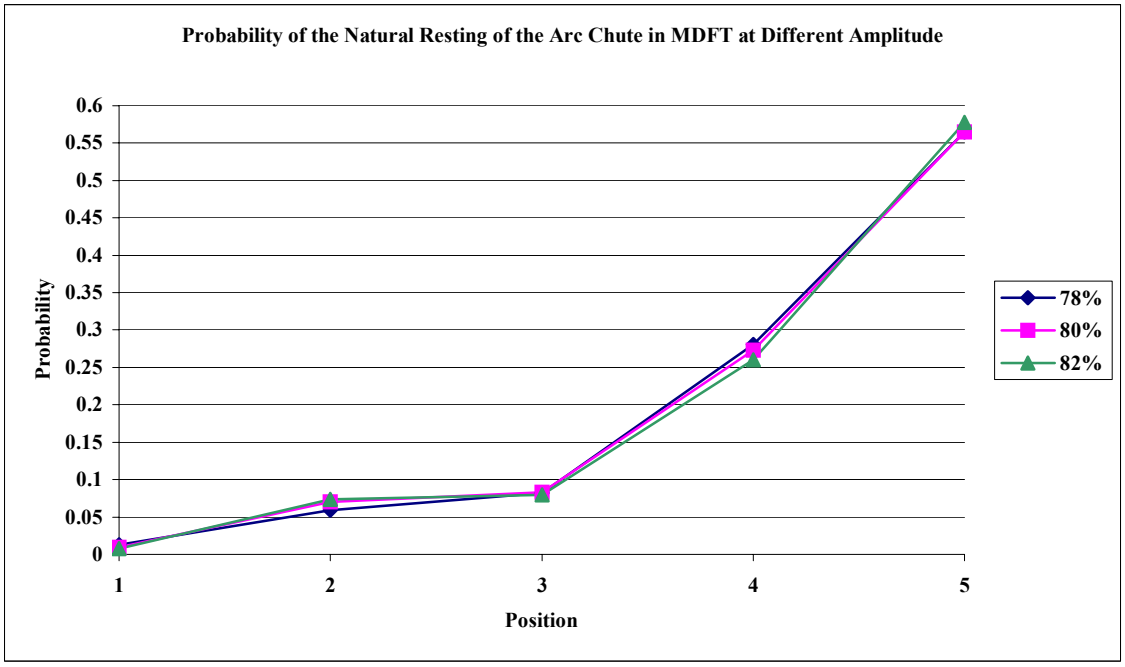

Figure 5.11. Experimental results for the arc chute in MDFT.

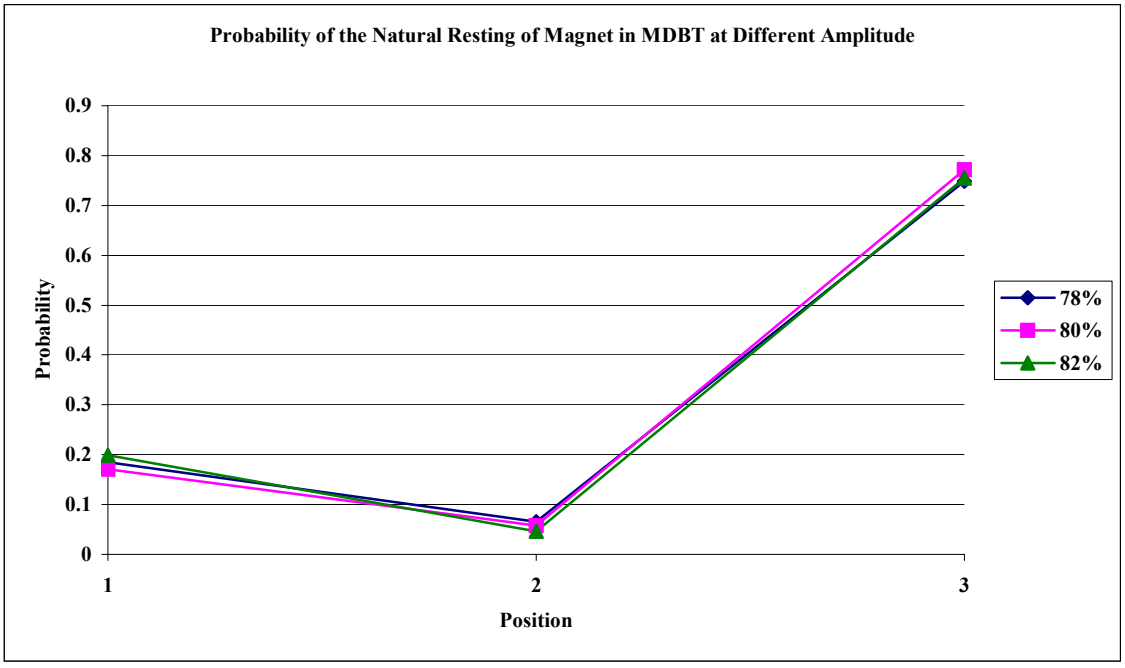

Figure 5.12. Experimental results for the magnet in MDBT.

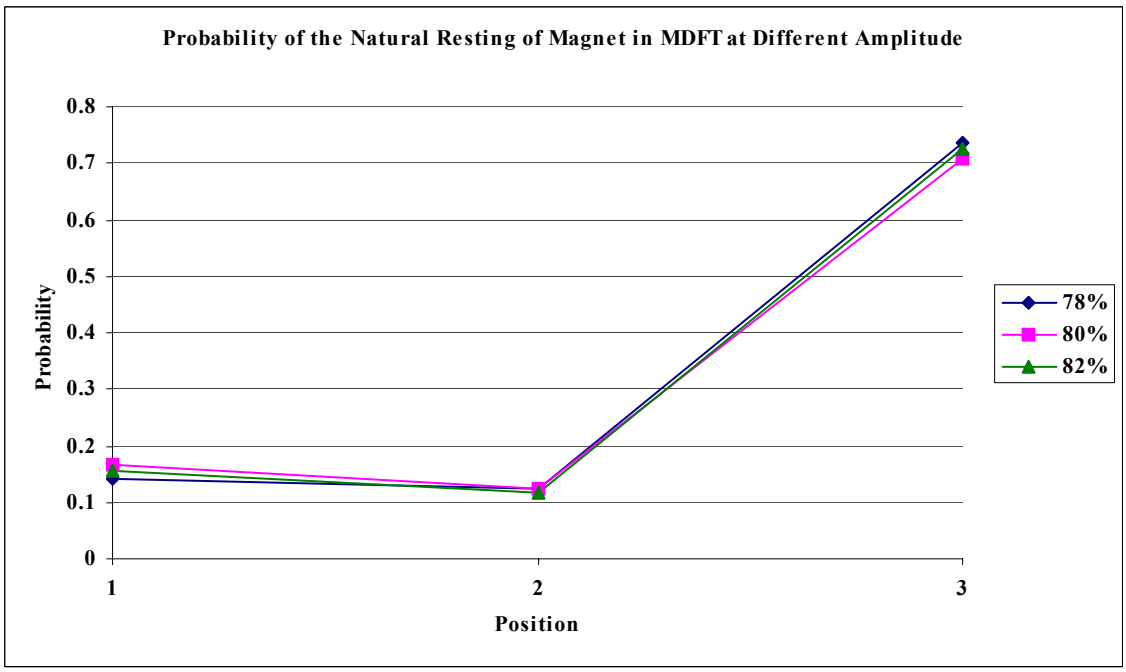

Figure 5.13. Experimental results for the magnet in MDFT.

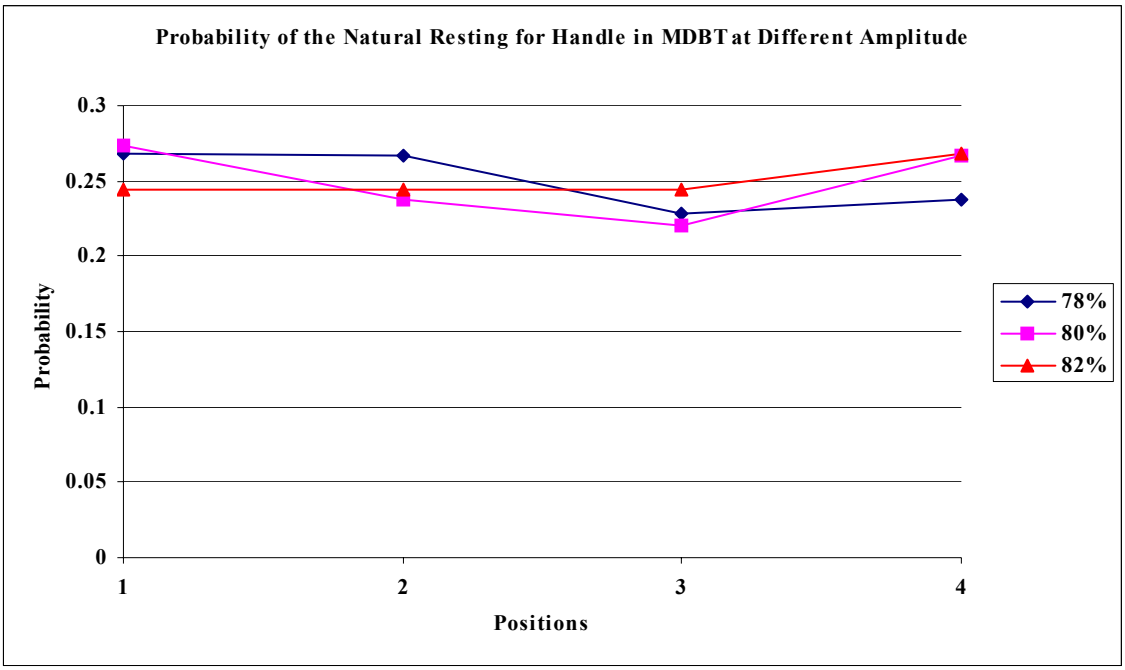

Figure 5.14. Experimental results for the handle in MDBT.

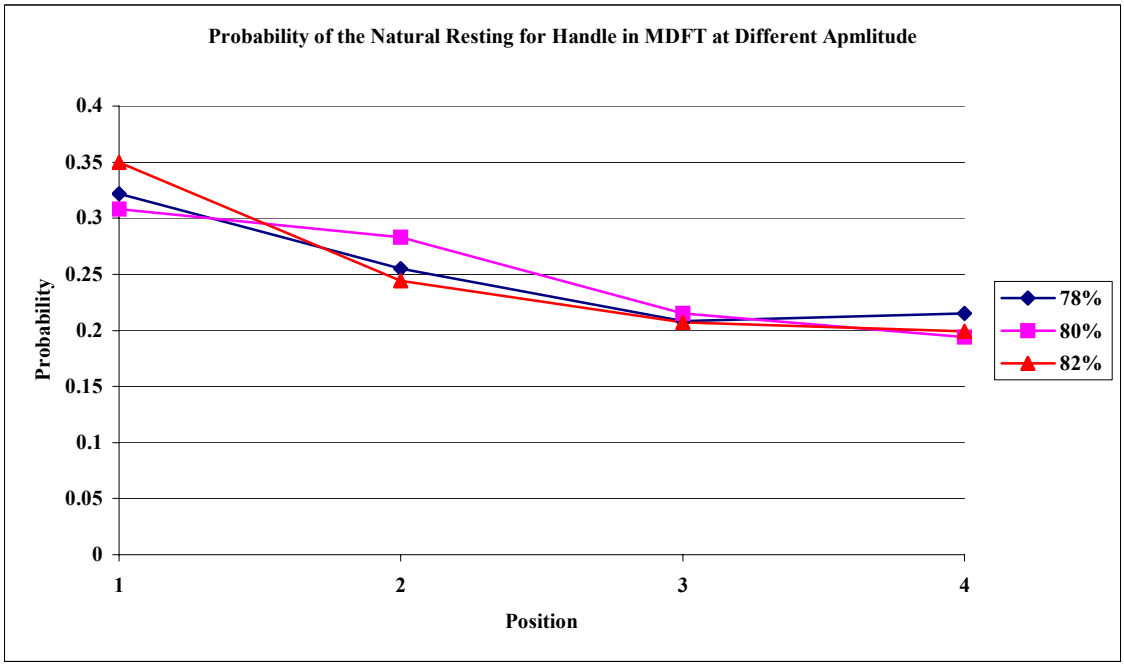

Figure 5.15. Experimental results for the handle in MDFT.

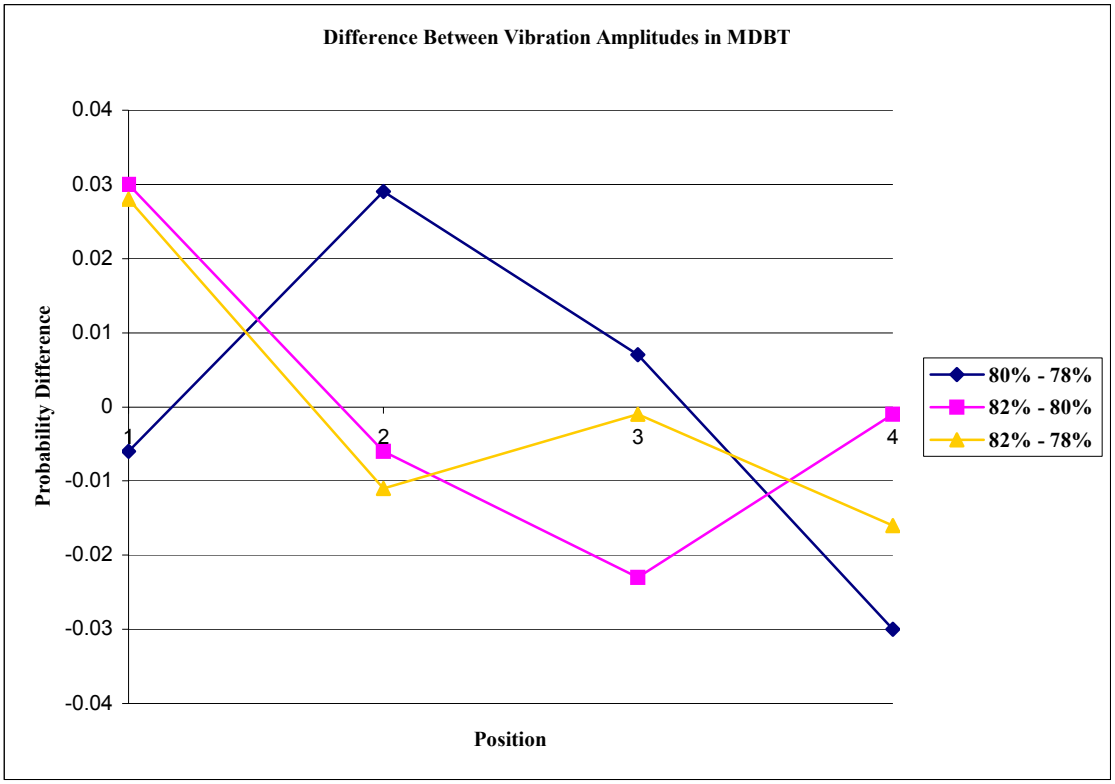

Figure 5.16. Handle vibration amplitude differences in MDBT

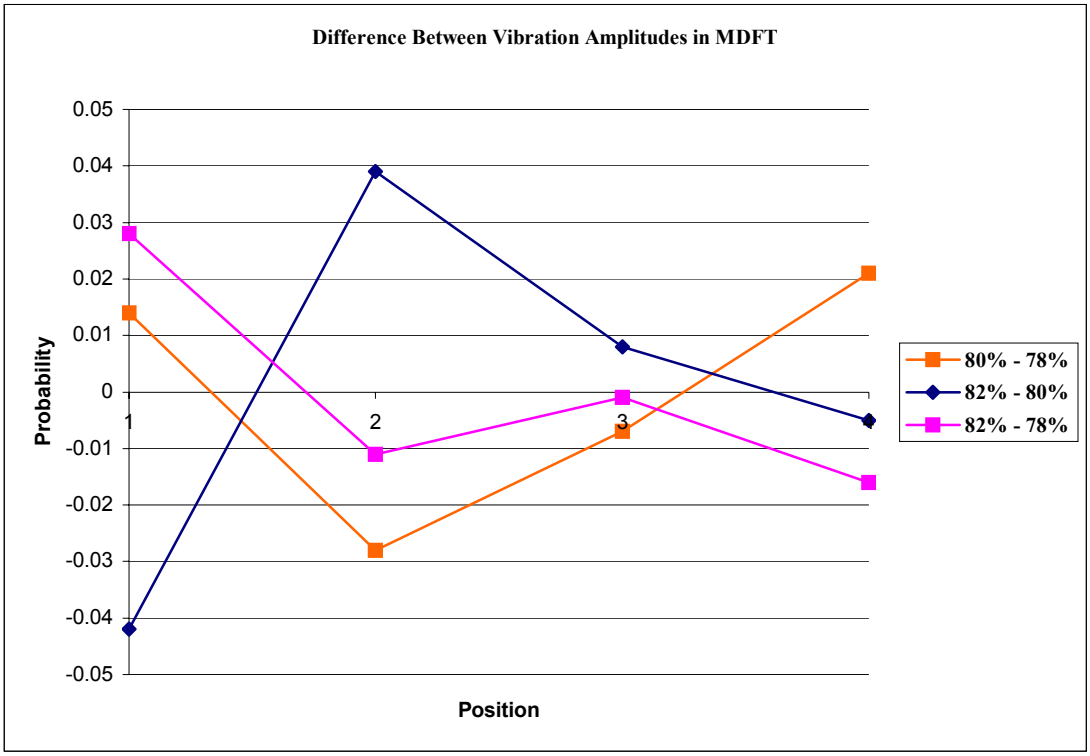

Figure 5.17. Handle vibration amplitude differences in MDFT

5.2 Summary

This chapter presented the results obtained of the data collected from the two modified dynamic tests realized with the parts handle, magnet, stab &contact, arc chute and latch, at different vibration amplitudes. The centroid solid angle and stability methods aren't statistical approximations for the probability profiles of most parts. These results were compared with the centroid solid angle and stability methods. The figures showed that the stable aspect in the experimental surface is even more stable in a dynamic surface and the less stable aspects are almost or totally null in a dynamic surface. Also the figures showed that, no matter the vibration amplitude, the part had the tendency to take the more stable aspects.

CHAPTER 6

CONCLUSIONS AND RECOMMENDATIONS

6.1 Conclusions

- The centroid solid angle and stability method predict that the parts take the more stable aspect or position while moving through a surface in movement, when the two methods were compared with the MDFT and MDBT results, doesn't exist a statistical correlation between the analytic methods, the centroid solid angle, stability methods, and the experimental results for parts with complex geometry.
- The shape of the parts impacts the vibration amplitude resulting in a small probability profile. This was observed in figures 5.6 to 5.15.
- The experimental probability for a part resting on a stable aspect is directly proportional to the height ratio (h_{total}/ h_i). This was observed in figure 4.5 and 4.7.
- The experimental probability for a part resting on a stable aspect is indirectly proportional to the area ratio (A_{total}/ A_i) for some of the parts. This was observed in figure 4.4.
- The vibration amplitude doesn't have any significant effect over the orientation efficiency of the bowl feeder for the parts studied. This was observed in figure 5.6 to 5.15

6.2 Recommendations

The research provides good data that can help with the study of the behavior of the vibratory bowl feeder. The results show similar tendencies between experimental and theoretical results.

For future work it is recommended to study the behavior of the parts on a specific location of the track of the vibratory bowl feeder by taking video. This will help study the behavior of the parts when the vibratory bowl feeder is turned on. And also continue the development of theoric model for parts with complex geometry.

Another future activity will be improving the sensor system to calibrate the feeder and to develop a user manual explaining the system's function, how to operate it and help with the troubleshooting.

BIBLIOGRAPHY

Boothroyd, Geoffrey. 1992, "Assembly Automation and Product Design", Marcel Dekker Inc.

Chua P. S. K. and Tay M. L. 1998, "Modelling the Natural Resting Aspect of Small Regular Shaped Parts", Transactions of the ASME, Vol. 120, pp. 540-546

Levy, J. C. 2001. "Study of the Probabilities of the Natural Resting Aspects of Small Parts in a Bowl Feeder" Thesis M.S. University of Puerto Rico, Mayagüez

Maul Gary and Thomas Brian. 1998, "A Systems Model and Simulation of the Vibratory Bowl Feeder", The Ohio State University, pp. 309-314.

Murch, L.E., 1972. "Parts Behavior in Vibratory Feeders, Hanbook of Feeding and Orienting Techniques for Small Parts", University of Massachusetts at Amherst, 20p.

Montgomery, D. 1997, "Design and Analysis of Experiments". John Wiley & Song, Inc. New York.

Ngoi, B.K.A., Lee, S.S.G., Lim, L.E.N. 1995a, "Analyzing the Natural Resting Aspects of a Component by its Centroid Solid Angle", Journal of Electronic Manufacturing, Vol. 53 No 3, pp. 193-197.

Ngoi, B.K.A., Lee, S.S.G., Lim, L.E.N. 1995b, "Analyzing the Probabilities of the Natural Resting Aspects of a Component with a Displaced Center of Gravity", International Journal of Production Research, Vol. 33 No 9, pp. 2387-2394.

Ngoi, B.K.A., Lee, S.S.G., Lim, L.E.N., Lye, S.W. 1995c. "Analyzing the Natural Resting Aspects of a Component for Automated Assembly". Journal of Engineering Manufacture, Vol. 209, pp. 125-135.

Ngoi, B.K.A., Lee, S.S.G., Lim, L.E.N. 1995d, "Analyzing the Natural Resting Aspects of a complex Part", International Journal of Production Research, Vol. 33 No 11, pp. 3163-3172

Ngoi, B.K.A., Lee, S.S.G., Lim, L.E.N, Lye, S.W. 1997. "Determining the Probabilities of the Natural Resting Aspects of Parts from Their Geometries". Assembly Automation, Vol. 17 No 2, pp. 137-142.

Rao, S., 1990, Mechanical Vibrations, Addison-Wesley Publishing Company, Inc. New York.

Rincón, A. 2002. "Estudio del Comportamiento de Piezas Complejas en un Alimentador Vibratorio" M.S. Thesis, University of Puerto Rico, Mayagüez, P.R.

Rosario, L.M. y Hernández Coronas, J.D, 1997. Study of the Behavior of Certain Connector in a Vibratory Bowl Feeder, Proceedings of the 1997 ASME Design Engineering Technical Conferences, 2nd Design for Manufacturing Conference, September 14-17, Sacramento, CA.

Johnson, R.A. and Bhattacharyya, G.K. 1992. Statistics: Principles and Methods. John Wiley & Sons, Inc. 2nd Edition, Canada. pp. 512 – 513 and pp. 633.

APPENDIX A

PROBABILITY PROFILE OF THE PARTS USING THE CENTROID SOLID ANGLE AND STABILITY METHODS

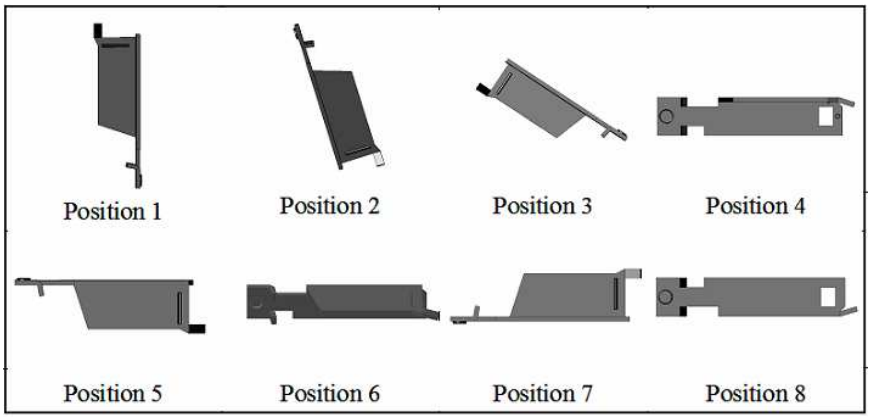

Figure A.1. Latch Different Positions

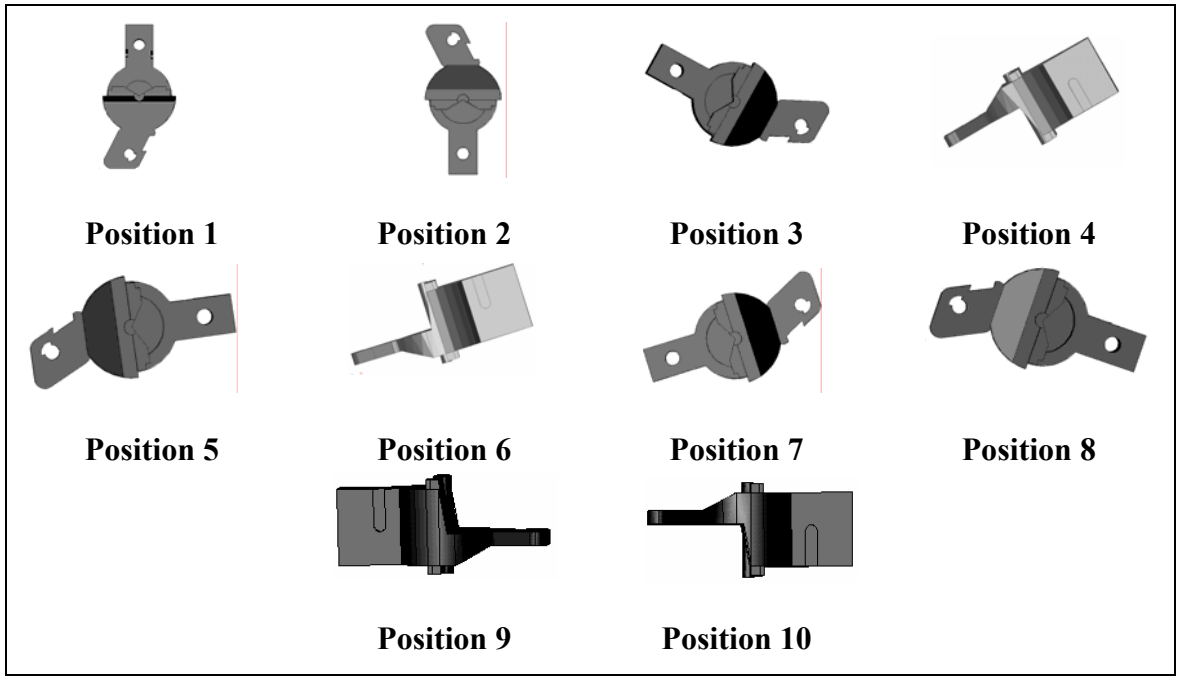

Figure A.2. Handle Different Positions

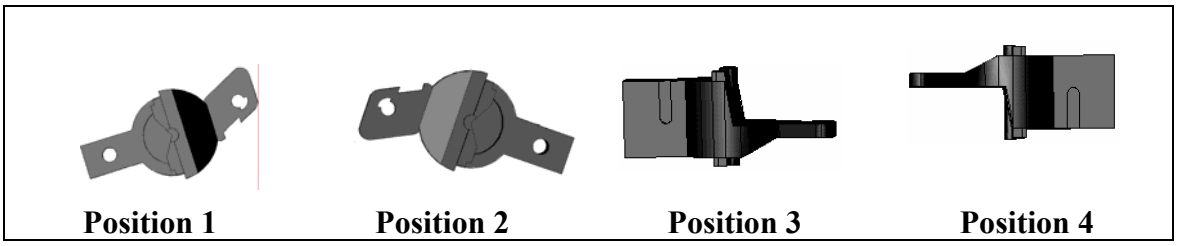

Figure A.3. Handle Natural Resting Aspects

Table A.1. Probability distribution: CSA method for handle part.

Position	Q_i	h_i	Q_i/h_i	Probability
1	0.9716	10.1185	0.09602	0.17726
2	1.0188	9.8938	0.10297	0.19009
3	0.979	6.9139	0.1416	0.2614
4	1.1636	5.7861	0.2011	0.37125
Total	4.133		0.5417	1

Table A.2. Probability distribution: stability method method for handle part.

Position	A_i	h_i	A_i / h_i	Probability
1	236.0141	10.1185	23.325	0.20116
2	236.0141	9.8938	23.8547	0.20573
3	216.6358	6.9139	31.3334	0.27022
4	216.6358	5.7861	37.4407	0.32289
Total			115.954	1

Table A.3. Experimental Comparison of the Probabilities Data with the Height Ratio (h_{total}/ h_i) per Handle's Aspects.

Positions	MDBT			MDFT			H total/Hi
	78%	80%	82%	78%	80%	82%	
1	0.268	0.274	0.244	0.322	0.308	0.35	1.255
2	0.267	0.238	0.244	0.255	0.283	0.244	1.284
3	0.228	0.221	0.244	0.208	0.215	0.207	1.837
4	0.237	0.267	0.268	0.215	0.194	0.199	2.195

Table A.4. Experimental Comparison of the Probabilities Data with the Area Ratio (A_{total}/ A_i) per Handle's Aspects.

Positions	MDBT			MDFT			A total/ Ai
	78%	80%	82%	78%	80%	82%	
1	0.268	0.274	0.244	0.322	0.308	0.35	7.626
2	0.267	0.238	0.244	0.255	0.283	0.244	7.626
3	0.228	0.221	0.244	0.208	0.215	0.207	8.308
4	0.237	0.267	0.268	0.215	0.194	0.199	8.308

Table A.5. Probability Profile for Part Handle Using the Movie Data.

Position	Frequency			Probability		
	78%	80%	82%	78%	80%	82%
1	50	85	116	0.29762	0.286195	0.26009
2	44	72	97	0.2619	0.242424	0.217489
3	32	72	123	0.19048	0.242424	0.275785
4	42	68	110	0.25	0.228956	0.246637
Total	168	297	446	1	1	1

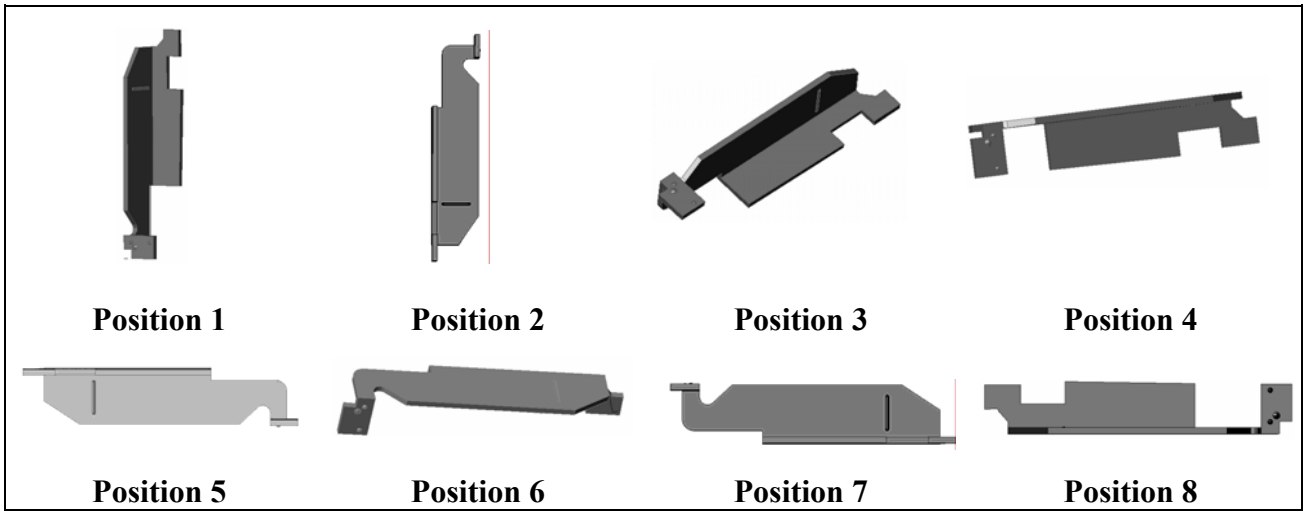

Figure A.4. Magnet Different Positions

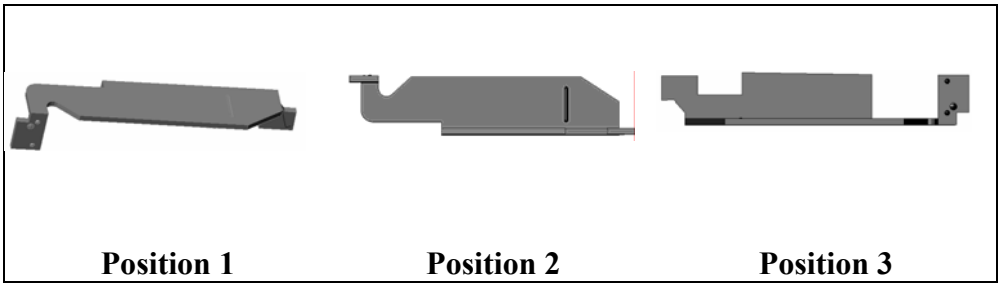

Figure A.5. Magnet Natural Resting Aspects

Table A.6. Probability distribution: CSA method for magnet part.

Position	Qi	hi	Qi/hi	Probability
1	6.2092	7.1172	0.87242	0.1105473
2	8.058	7.1518	1.12671	0.1427689
3	12.0064	2.0375	5.89271	0.7466839
Total	26.2736			1

Table A.7. Probability distribution: stability method for magnet part.

Position	Ai	Hi	Ai / Hi	Probability
1	303.844	7.1172	42.6914	0.142
2	314.243	7.1518	43.939	0.14615
3	436.05	2.0375	214.012	0.71185
Total	1054.14		300.643	1

Table A.8. Experimental Comparison of the Probabilities Data with the Height Ratio (h_{total}/ h_i) per Magnet's Aspects.

Positions	**MDBT**			**MDFT**			**H total/Hi**
	78%	80%	82%	78%	80%	82%	
1	0.185	0.171	0.199	0.14	0.166	0.157	1.335
2	0.066	0.058	0.046	0.124	0.125	0.117	1.328
3	0.749	0.771	0.755	0.736	0.709	0.726	4.663

Table A.9. Experimental Comparison of the Probabilities Data with the Area Ratio (A_{total}/ A_i) per Magnet's Aspects.

Positions	**MDBT**			**MDFT**			**A total/ Ai**
	78%	80%	82%	78%	80%	82%	
1	0.185	0.171	0.199	0.14	0.166	0.157	5.230
2	0.066	0.058	0.046	0.124	0.125	0.117	5.057
3	0.749	0.771	0.755	0.736	0.709	0.726	3.644

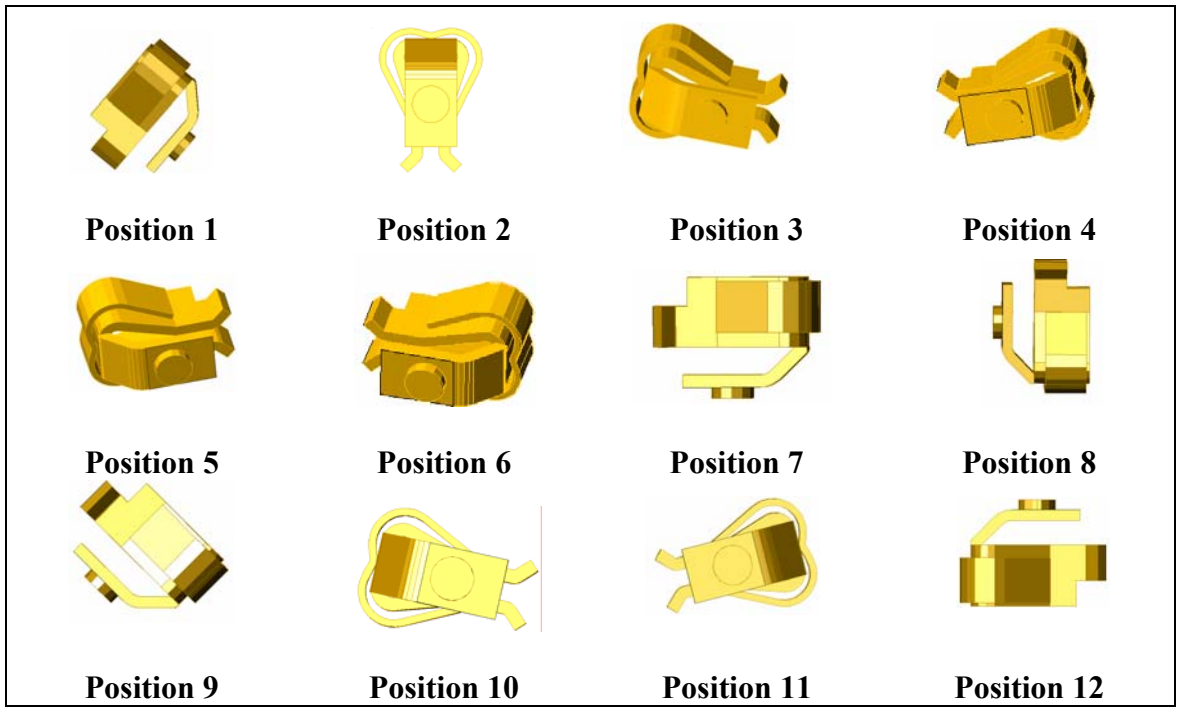

Figure A.6. Stab& Contact Different Positions

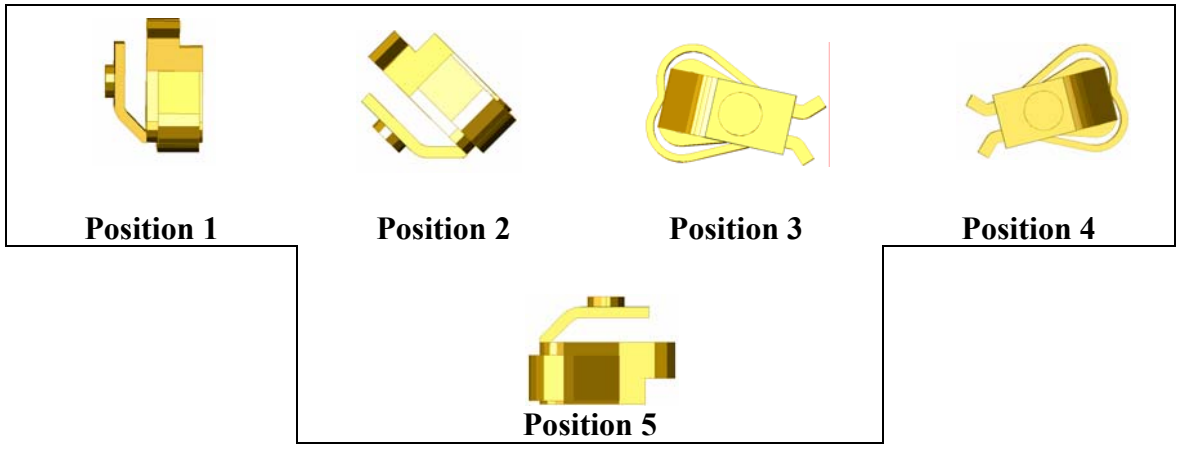

Figure A.7. Stab& Contact Natural Resting Aspects

Table A.10. Probability distribution: CSA method for stab & contact part.

Position	Qi	hi	Htotal/hi	Qi/hi	Probability
1	4.8558	6.1015	1.701795	0.795837089	0.11257
2	5.4327	5.5837	1.859609	0.972957	0.13763
3	7.6345	4.8286	2.150416	1.581100112	0.22365
4	7.638	4.8286	2.150416	1.58182496	0.22376
5	9.6106	4.4958	2.3096	2.137684061	0.30239
Total	35.1716			8.764900185	1

Table A.11. Probability distribution: stability method for stab & contact part.

Position	Ai	Hi	Ai / Hi	Probability
1	77.3735	6.1015	12.6811	0.13769
2	57.1305	5.5837	10.2317	0.1111
3	98.6665	4.8286	20.4338	0.22187
4	98.6665	4.8286	20.4338	0.22187
5	127.308	4.4958	28.3171	0.30747
Total			92.0974	1

Table A.12. Experimental Comparison of the Probabilities Data with the Height Ratio (h_{total}/ h_i) per Stab & Contact's Aspects.

Positions	**MDBT**			**MDFT**			**H total/Hi**
	78%	80%	82%	78%	80%	82%	
1	0.022	0.03	0.025	0.007	0	0.004	1.702
2	0.343	0.332	0.363	0.355	0.386	0.403	1.860
3	0.209	0.198	0.2	0.198	0.177	0.164	2.150
4	0.177	0.183	0.163	0.162	0.159	0.157	2.150
5	0.249	0.257	0.249	0.278	0.278	0.272	2.310

Table A.13. Comparison of the Probabilities Data with the Area Ratio (A_{total}/ A_i) per Stab & Contact's Aspects.

Positions	MDBT			MDFT			A total/ Ai
	78%	80%	82%	78%	80%	82%	
1	0.022	0.03	0.025	0.007	0	0.004	8.300
2	0.343	0.332	0.363	0.355	0.386	0.403	11.241
3	0.209	0.198	0.2	0.198	0.177	0.164	6.509
4	0.177	0.183	0.163	0.162	0.159	0.157	6.509
5	0.249	0.257	0.249	0.278	0.278	0.272	5.044

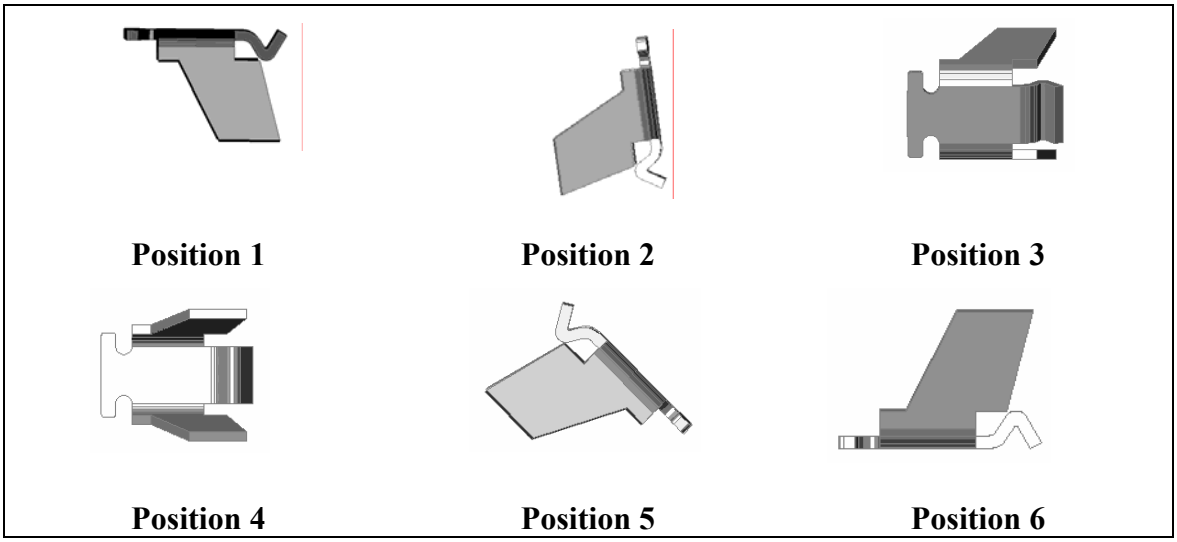

Figure A.8. Arc Chute Different Positions

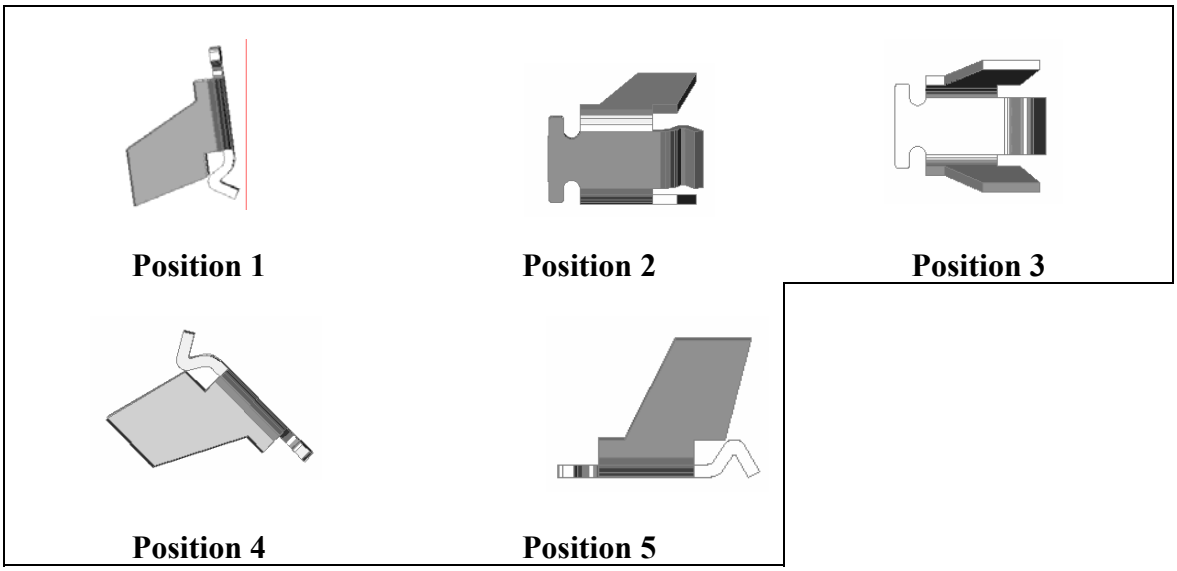

Figure A.9. Arc Chute Natural Resting Aspects

Table A.14. Probability distribution: CSA method for arc chute part.

Position	Qi	hi	Htotal/hi	Qi/hi	Probability
1	18.0756	10.1419	1.113144	1.78227	0.08134
2	29.8701	7.4007	1.52545	4.03612	0.18421
3	29.8703	7.4007	1.52545	4.03615	0.18421
4	36.3687	7.4007	1.52545	4.91422	0.22429
5	37.2037	5.2094	2.167121	7.14165	0.32595
Total	133.313			21.9104	1

Table A.15. Probability distribution: stability method for arc chute part.

Position	Ai	Hi	Ai / Hi	Probability
1	100.321	10.1419	9.8917	0.15211
2	46.3172	7.4007	6.25849	0.09624
3	46.3172	7.4007	6.25849	0.09624
4	158.885	7.4007	21.469	0.33014
5	110.186	5.2094	21.1514	0.32526
Total	462.027		65.029	1

Table A.16. Comparison of the Probabilities Data with the Height Ratio (h_{total}/ h_i) per Arc Chute's Aspects.

Positions	MDBT			MDFT			H total/Hi
	78%	80%	82%	78%	80%	82%	
1	0.022	0.012	0.018	0.013	0.009	0.008	1.113
2	0.343	0.035	0.032	0.059	0.07	0.074	1.525
3	0.209	0.049	0.031	0.082	0.083	0.08	1.525
4	0.177	0.278	0.295	0.281	0.273	0.26	1.525
5	0.249	0.626	0.624	0.565	0.565	0.578	2.167

Table A.17. Comparison of the Probabilities Data with the Area Ratio (A_{total}/ A_i) per Arc Chute's Aspects.

Positions	MDBT			MDFT			A total/ Ai
	78%	80%	82%	78%	80%	82%	
1	0.022	0.012	0.018	0.013	0.009	0.008	5.495
2	0.343	0.035	0.032	0.059	0.07	0.074	11.902
3	0.209	0.049	0.031	0.082	0.083	0.08	11.902
4	0.177	0.278	0.295	0.281	0.273	0.26	3.470
5	0.249	0.626	0.624	0.565	0.565	0.578	5.003

APPENDIX B

EXPERIMENTAL DATA

B.1 Modified Dynamic Feeding Test

Table B.1 Experimental data for part handle at 78% amplitude.

Position	E1	E2	E3	E4	E5	E6	E7	E8	E9	E10	Total
1	8	11	17	7	9	11	6	8	11	11	99
2	7	12	3	10	11	12	10	9	11	10	95
3	15	10	15	11	10	9	8	11	10	12	111
4	18	18	12	27	23	15	21	15	24	16	189
5	3	9	12	5	13	11	8	13	4	9	87
6	16	13	13	10	6	16	15	13	10	18	130
7	14	2	14	11	8	6	6	6	6	3	76
8	8	12	7	13	10	8	17	15	16	11	117
9	1	2	5	2	3	5	2	4	3	7	34
10	7	7	2	1	5	4	6	4	5	3	44
11	1	2	0	1	2	0	1	0	0	0	7
12	2	0	0	0	0	1	0	1	0	0	4
13	0	2	0	1	0	1	0	1	0	0	5
14	0	0	0	1	0	1	0	0	0	0	2
Total	100	100	100	100	100	100	100	100	100	100	1000

Table B.2 Experimental data for part handle at 80% amplitude

Position	E1	E2	E3	E4	E5	E6	E7	E8	E9	E10	Total
1	15	13	9	9	14	4	7	10	12	12	105
2	11	14	17	10	7	15	8	6	8	11	107
3	13	7	13	18	17	17	17	17	16	11	146
4	13	19	18	18	15	11	15	20	19	17	165
5	7	4	11	6	6	10	16	9	3	7	79
6	12	15	13	6	8	10	17	10	14	7	112
7	8	6	6	10	6	12	4	8	4	12	76
8	12	9	7	14	16	12	12	13	18	15	128
9	3	6	3	5	9	3	1	1	3	4	38
10	3	4	2	3	1	3	3	4	2	4	29
11	0	2	0	0	0	1	0	2	1	0	6
12	2	1	1	1	1	2	0	0	0	0	8
13	1	0	0	0	0	0	0	0	0	0	1
14	0	0	0	0	0	0	0	0	0	0	0
Total	100	100	100	100	100	100	100	100	100	100	1000

Table B.3 Experimental data for part handle at 82% amplitude

Position	E1	E2	E3	E4	E5	E6	E7	E8	E9	E10	
1	17	6	8	11	14	15	14	8	10	10	113
2	9	12	10	12	3	4	6	13	12	8	89
3	4	19	15	11	12	11	10	12	12	16	122
4	19	20	17	19	24	19	21	22	24	16	201
5	10	5	6	5	9	10	3	9	5	7	69
6	11	13	17	13	7	13	14	8	14	12	122
7	7	5	10	6	5	8	13	6	4	8	72
8	17	10	8	13	18	14	15	12	5	15	127
9	2	4	4	4	3	3	2	4	5	5	36
10	4	5	3	4	2	2	2	0	4	3	29
11	0	1	0	0	0	1	0	2	1	0	5
12	0	0	1	2	3	0	0	2	3	0	11
13	0	0	1	0	0	0	0	2	1	0	4
14	0	0	0	0	0	0	0	0	0	0	0
	100	100	100	100	100	100	100	100	100	100	1000

Table B.4 Experimental data for part magnet at 78% amplitude

Position	E1	E2	E3	E4	E5	E6	E7	E8	E9	E10	Total
1	49	42	45	33	46	44	38	45	35	43	420
2	4	7	1	5	2	3	6	4	7	2	41
3	9	5	6	7	5	6	9	6	9	8	70
4	2	8	9	11	7	10	7	8	9	10	81
5	27	34	29	39	35	34	30	30	28	29	315
6	9	3	8	5	4	2	10	4	10	7	62
7	0	0	0	0	0	0	0	0	0	0	0
8	0	0	0	0	0	0	0	0	0	1	1
9	0	0	0	0	0	1	0	0	1	0	2
10	0	1	2	0	1	0	0	2	1	0	7
11	0	0	0	0	0	0	0	1	0	0	1
12	0	0	0	0	0	0	0	0	0	0	0
Total	100	100	100	100	100	100	100	100	100	100	1000

Table B.5 Experimental data for part magnet at 80% amplitude

Position	E1	E2	E3	E4	E5	E6	E7	E8	E9	E10	Total
1	39	40	32	40	43	39	46	40	41	43	403
2	6	4	3	4	2	5	3	1	2	4	34
3	7	8	8	8	10	5	11	8	8	7	80
4	11	11	9	9	7	11	6	11	6	9	90
5	26	30	39	36	27	33	27	28	30	27	303
6	9	7	8	3	10	6	6	10	11	10	80
7	0	0	0	0	0	0	0	0	0	0	0
8	0	0	1	0	1	0	1	0	0	0	3
9	0	0	0	0	0	0	0	1	0	0	1
10	1	0	0	0	0	0	0	1	1	0	3
11	0	0	0	0	0	0	0	0	0	0	0
12	1	0	0	0	0	1	0	0	1	0	3
Total	100	100	100	100	100	100	100	100	100	100	1000

Table B.6 Experimental data for part magnet at 82% amplitude

Position	E1	E2	E3	E4	E5	E6	E7	E8	E9	E10	Total
1	36	39	42	48	45	41	39	34	30	36	390
2	2	2	4	5	3	3	5	6	3	4	37
3	11	13	6	4	9	9	9	9	10	7	87
4	10	5	8	8	9	6	7	7	8	10	78
5	36	29	30	31	26	33	32	36	42	36	331
6	5	11	7	3	3	8	8	8	7	6	66
7	0	0	0	0	1	0	0	0	0	0	1
8	0	0	1	0	0	0	0	0	0	0	1
9	0	0	0	0	1	0	0	0	0	0	1
10	0	0	1	0	1	0	0	0	0	1	3
11	0	1	1	0	2	0	0	0	0	0	4
12	0	0	0	1	0	0	0	0	0	0	1
Total	100	100	100	100	100	100	100	100	100	100	1000

Table B.7 Experimental data for part latch at 78% amplitude

Position	E1	E2	E3	E4	E5	E6	E7	E8	E9	E10	Total
1	10	11	12	16	17	13	7	18	16	19	139
2	12	11	8	5	9	9	9	10	7	7	87
3	29	21	14	17	18	23	25	24	24	24	219
4	14	16	20	24	21	14	20	19	13	9	170
5	24	21	38	29	23	33	31	21	30	23	273
6	10	17	8	9	11	8	8	8	10	18	107
7	1	1	0	0	0	0	0	0	0	0	2
8	0	0	0	0	0	0	0	0	0	0	0
9	0	0	0	0	0	0	0	0	0	0	0
10	0	1	0	0	0	0	0	0	0	0	1
11	0	1	0	0	0	0	0	0	0	0	1
12	0	0	0	0	1	0	0	0	0	0	1
Total	100	100	100	100	100	100	100	100	100	100	1000

Table B.8 Experimental data for part latch at 80% amplitude

Position	E1	E2	E3	E4	E5	E6	E7	E8	E9	E10	Total
1	17	15	22	13	15	16	13	15	12	12	150
2	11	4	7	13	14	9	11	12	8	10	99
3	18	19	20	18	18	22	23	23	23	19	203
4	19	17	15	22	18	17	11	14	27	23	183
5	22	35	26	23	30	25	30	23	21	26	261
6	13	9	10	10	5	10	10	11	9	10	97
7	0	0	0	0	0	0	1	0	0	0	1
8	0	0	0	0	0	0	0	0	0	0	0
9	0	0	0	0	0	0	0	0	0	0	0
10	0	0	0	1	0	0	0	1	0	0	2
11	0	0	0	0	0	0	0	0	0	0	0
12	0	1	0	0	0	1	1	1	0	0	4
Total	100	100	100	100	100	100	100	100	100	100	1000

Table B.9 Experimental data for part latch at 82% amplitude

Position	E1	E2	E3	E4	E5	E6	E7	E8	E9	E10	Total
1	14	17	15	9	12	6	22	9	12	12	128
2	7	10	14	17	13	8	7	15	9	10	110
3	25	19	22	19	23	19	21	12	17	13	190
4	19	20	14	14	13	20	18	23	17	20	178
5	22	27	20	29	29	28	17	24	29	33	258
6	13	7	15	12	10	18	11	16	16	12	130
7	0	0	0	0	0	1	0	0	0	0	1
8	0	0	0	0	0	0	0	0	0	0	0
9	0	0	0	0	0	0	2	0	0	0	2
10	0	0	0	0	0	0	0	1	0	0	1
11	0	0	0	0	0	0	2	0	0	0	2
12	0	0	0	0	0	0	0	0	0	0	0
Total	100	100	100	100	100	100	100	100	100	100	1000

Table B.10 Experimental data for part arc chute at 78% amplitude

Position	E1	E2	E3	E4	E5	E6	E7	E8	E9	E10	Total
1	28	16	25	24	19	20	20	18	27	22	219
2	14	25	20	10	22	19	23	21	16	17	187
3	11	9	13	15	12	14	12	8	11	8	113
4	11	11	7	12	11	10	7	6	5	5	85
5	4	4	2	7	1	2	2	7	6	4	39
6	2	6	2	4	3	1	1	1	4	3	27
7	1	1	2	4	1	1	3	4	4	4	25
8	5	6	8	2	3	4	2	3	1	4	38
9	6	8	6	8	11	9	11	12	13	14	98
10	8	3	7	2	9	5	8	5	7	7	61
11	2	1	0	2	0	1	0	1	0	0	7
12	0	0	0	0	0	0	0	1	0	0	1
13	0	0	1	0	1	0	0	1	0	1	4
14	0	0	0	0	0	0	0	1	0	0	1
15	4	6	4	5	3	2	2	5	3	5	39
16	4	2	3	3	3	9	7	5	3	5	44
17	0	1	0	1	0	0	0	0	0	1	3
18	0	0	0	0	0	2	0	1	0	0	3
19	0	1	0	0	0	0	1	0	0	0	2
20	0	0	0	1	1	1	1	0	0	0	4
Total	100	100	100	100	100	100	100	100	100	100	1000

Table B.11 Experimental data for part arc chute at 80% amplitude

Position	E1	E2	E3	E4	E5	E6	E7	E8	E9	E10	Total
1	21	22	26	24	15	25	17	24	29	18	221
2	22	14	18	17	15	20	21	15	18	22	182
3	12	16	8	12	13	15	13	11	12	11	123
4	6	11	10	11	8	9	6	6	7	10	84
5	3	2	2	4	8	1	2	6	4	5	37
6	2	6	5	2	1	3	3	5	2	3	32
7	4	8	3	3	2	3	4	3	2	3	35
8	2	5	3	3	10	2	4	1	6	1	37
9	11	7	8	7	11	5	11	11	8	8	87
10	5	4	5	12	5	8	10	7	7	12	75
11	0	0	1	1	1	0	0	1	0	0	4
12	1	0	0	0	1	0	0	0	0	0	2
13	0	0	1	0	0	0	0	1	0	0	2
14	0	0	0	0	1	0	0	0	0	0	1
15	6	2	3	2	5	4	4	1	3	2	32
16	3	2	6	2	2	3	3	7	2	4	34
17	1	0	0	0	2	0	1	1	0	1	6
18	0	0	1	0	0	0	0	0	0	0	1
19	1	1	0	0	0	1	0	0	0	0	3
20	0	0	0	0	0	1	1	0	0	0	2
Total	100	100	100	100	100	100	100	100	100	100	1000

Table B.12 Experimental data for part arc chute at 82% amplitude

Position	E1	E2	E3	E4	E5	E6	E7	E8	E9	E10	Total
1	27	29	20	18	27	23	26	22	19	23	234
2	12	22	26	26	15	25	16	15	23	23	203
3	13	12	11	12	10	14	13	14	14	17	130
4	8	11	9	9	9	6	9	9	8	5	83
5	4	4	6	3	6	2	5	2	4	4	40
6	6	4	9	3	3	2	2	7	3	1	40
7	4	1	1	5	5	5	3	2	6	1	33
8	3	5	2	5	3	5	4	3	0	4	34
9	8	2	3	4	9	9	5	6	5	7	58
10	5	7	6	8	7	3	13	13	10	11	83
11	0	0	0	0	2	0	0	1	0	1	4
12	0	0	0	0	1	0	0	0	0	0	1
13	1	0	0	1	0	0	0	0	1	0	3
14	0	0	0	0	0	0	0	0	0	0	0
15	1	1	3	5	1	2	3	4	2	2	24
16	6	2	3	0	2	3	1	2	3	1	23
17	1	0	1	1	0	1	0	0	1	0	5
18	0	0	0	0	0	0	0	0	0	0	0
19	1	0	0	0	0	0	0	0	0	0	1
20	0	0	0	0	0	0	0	0	1	0	1
Total	100	100	100	100	100	100	100	100	100	100	1000

Table B.13 Experimental data for part stab & contact at 78% amplitude

Position	E1	E2	E3	E4	E5	E6	E7	E8	E9	E10	Total
1	3	3	6	7	9	10	6	5	4	8	61
2	12	12	14	10	9	10	7	8	7	10	99
3	7	8	11	7	7	7	14	10	13	8	92
4	2	2	4	2	3	3	2	3	3	2	26
5	14	10	4	8	9	11	12	9	7	6	90
6	16	10	12	16	13	13	10	9	13	13	125
7	4	2	2	0	1	2	4	1	2	3	21
8	12	7	13	14	8	13	11	11	16	14	119
9	0	0	0	0	0	0	0	0	0	0	0
10	0	0	0	0	0	0	0	0	0	0	0
11	0	0	0	0	0	0	0	0	0	0	0
12	0	0	0	0	0	0	0	0	0	1	1
13	7	11	8	8	10	3	5	12	6	9	79
14	6	6	4	3	7	11	3	3	4	4	51
15	5	6	6	7	8	9	12	5	13	14	85
16	5	14	7	3	8	4	10	11	7	5	74
17	3	4	2	5	4	2	2	7	2	1	32
18	4	5	4	8	4	2	2	3	3	2	37
19	0	0	0	0	0	0	0	0	0	0	0
20	0	0	2	0	0	0	0	0	0	0	2
21	0	0	1	1	0	0	0	2	0	0	4
22	0	0	0	1	0	0	0	1	0	0	2
23	0	0	0	0	0	0	0	0	0	0	0
Total	100	100	100	100	100	100	100	100	100	100	1000

Table B.14 Experimental data for part stab & contact at 80% amplitude

Position	E1	E2	E3	E4	E5	E6	E7	E8	E9	E10	Total
1	10	5	2	8	5	6	8	6	3	9	62
2	6	9	11	7	9	4	5	5	11	12	79
3	9	13	13	15	13	11	10	8	10	6	108
4	2	2	4	3	5	3	2	2	1	5	29
5	8	6	7	13	12	12	11	13	7	10	99
6	16	23	17	14	10	20	9	16	11	13	149
7	4	1	3	1	2	3	5	2	4	2	27
8	16	11	8	12	10	9	13	11	11	10	111
9	0	0	0	0	0	0	0	0	0	0	0
10	0	0	0	0	0	0	0	0	0	0	0
11	0	0	0	0	0	0	0	0	0	0	0
12	0	0	0	0	0	0	0	0	0	0	0
13	6	9	8	3	9	8	4	8	10	8	73
14	7	5	2	6	3	3	6	7	4	4	47
15	6	9	8	7	5	7	10	9	8	4	73
16	3	3	13	6	10	8	7	8	12	8	78
17	4	2	1	2	3	3	5	2	4	5	31
18	3	2	3	3	4	3	5	3	4	4	34
19	0	0	0	0	0	0	0	0	0	0	0
20	0	0	0	0	0	0	0	0	0	0	0
21	0	0	0	0	0	0	0	0	0	0	0
22	0	0	0	0	0	0	0	0	0	0	0
23	0	0	0	0	0	0	0	0	0	0	0
Total	100	100	100	100	100	100	100	100	100	100	1000

Table B.15 Experimental data for part stab & contact at 82% amplitude

Position	E1	E2	E3	E4	E5	E6	E7	E8	E9	E10	Total
1	10	5	7	2	7	5	2	6	4	5	53
2	12	11	9	10	10	11	3	12	9	10	97
3	9	8	10	0	15	7	10	13	8	10	90
4	1	3	1	1	6	2	6	6	4	2	32
5	8	11	6	14	8	8	12	10	5	12	94
6	11	8	10	19	10	13	14	8	13	12	118
7	5	8	5	9	6	2	8	7	6	6	62
8	9	12	17	14	9	17	18	12	10	11	129
9	0	0	0	0	0	0	0	0	0	0	0
10	0	0	0	0	0	0	0	0	0	0	0
11	0	0	0	0	0	0	0	0	0	0	0
12	0	0	0	0	0	0	0	0	0	0	0
13	6	6	4	6	4	8	5	6	7	5	57
14	8	6	5	4	6	8	4	0	5	2	48
15	8	9	10	10	3	5	9	8	7	7	76
16	8	7	10	6	8	5	4	5	12	9	74
17	2	2	2	3	3	4	1	3	3	8	31
18	3	3	4	2	4	5	3	4	6	1	35
19	0	0	0	0	0	0	0	0	0	0	0
20	0	0	0	0	0	0	0	0	0	0	0
21	0	0	0	0	0	0	1	0	1	0	2
22	0	1	0	0	1	0	0	0	0	0	2
23	0	0	0	0	0	0	0	0	0	0	0
Total	100	100	100	100	100	100	100	100	100	100	1000

B.2 Modified Dynamic Bowl Test

Table B.16 Experimental data for part handle at 78% amplitude.

POSITION	E1	E2	E3	E4	E5	E6	E7	E8	E9	E10	Total
1	5	6	9	9	9	11	11	6	4	6	76
2	5	13	10	14	12	12	11	15	7	13	112
3	13	14	16	18	9	10	13	14	17	11	135
4	17	14	16	13	16	19	13	11	24	21	164
5	9	7	4	5	6	3	6	5	7	9	61
6	14	15	12	8	13	15	16	14	8	13	128
7	9	7	7	9	15	11	11	16	6	8	99
8	17	18	15	18	13	16	15	13	20	13	158
9	7	1	7	2	0	2	2	1	3	3	28
10	2	3	3	3	3	1	0	0	2	1	18
11	0	2	1	0	2	0	0	3	1	1	10
12	2	0	0	1	2	0	2	0	1	1	9
13	0	0	0	0	0	0	0	2	0	0	2
14	0	0	0	0	0	0	0	0	0	0	0
Total	100	100	100	100	100	100	100	100	100	100	1000

Table B.17 Experimental data for part handle at 80% amplitude

POSITION	E1	E2	E3	E4	E5	E6	E7	E8	E9	E10	Total
1	12	15	11	5	7	5	7	9	4	11	86
2	4	11	8	10	13	9	8	7	8	15	93
3	15	13	13	9	17	17	12	9	11	15	131
4	14	17	16	22	9	11	20	20	25	15	169
5	7	3	7	5	4	9	3	8	4	2	52
6	15	13	22	15	17	19	16	14	22	12	165
7	9	12	4	10	11	8	11	16	5	13	99
8	15	15	16	17	19	18	18	16	14	13	161
9	5	1	1	4	1	3	1	0	2	1	19
10	0	0	2	2	2	1	2	0	3	2	14
11	2	0	0	0	0	0	0	0	1	0	3
12	2	0	0	1	0	0	2	1	1	1	8
13	0	0	0	0	0	0	0	0	0	0	0
14	0	0	0	0	0	0	0	0	0	0	0
Total	100	100	100	100	100	100	100	100	100	100	1000

Table B.18 Experimental data for part handle at 82% amplitude

POSITION	E1	E2	E3	E4	E5	E6	E7	E8	E9	E10	Total
1	5	9	7	8	5	10	8	6	8	13	79
2	13	11	11	12	7	12	9	8	7	12	102
3	15	9	13	10	9	14	16	12	14	12	124
4	17	12	15	14	18	10	12	18	20	15	151
5	6	11	5	6	8	12	7	2	6	8	71
6	14	17	15	14	15	11	17	15	21	11	150
7	9	13	15	14	7	11	10	13	7	10	109
8	18	13	16	17	28	13	16	19	11	15	166
9	0	1	0	1	0	2	2	4	2	2	14
10	1	2	2	2	3	3	3	1	1	0	18
11	1	2	1	1	0	0	0	1	2	1	9
12	1	0	0	1	0	2	0	1	1	1	7
13	0	0	0	0	0	0	0	0	0	0	0
14	0	0	0	0	0	0	0	0	0	0	0
Total	100	100	100	100	100	100	100	100	100	100	1000

Table B.19 Experimental data for part magnet at 78% amplitude

POSITION	E1	E2	E3	E4	E5	E6	E7	E8	E9	E10	Total
1	43	38	45	41	45	37	40	43	37	39	408
2	3	2	3	1	2	0	4	0	1	2	18
3	5	11	5	7	9	9	12	8	11	8	85
4	7	5	3	6	4	4	3	3	5	7	47
5	31	32	34	36	29	38	32	37	35	31	335
6	8	12	9	9	9	10	7	9	10	11	94
7	0	0	0	0	0	0	0	0	0	0	0
8	0	0	0	0	0	0	0	0	0	0	0
9	0	0	0	0	0	1	0	0	0	0	1
10	1	0	1	0	1	0	1	0	1	1	6
11	1	0	0	0	1	1	1	0	0	1	5
12	1	0	0	0	0	0	0	0	0	0	1
Total	100	100	100	100	100	100	100	100	100	100	1000

Table B.20 Experimental data for part magnet at 80% amplitude

POSITION	E1	E2	E3	E4	E5	E6	E7	E8	E9	E10	Total
1	40	45	43	39	44	45	38	40	49	47	430
2	5	3	3	1	0	2	0	2	0	1	17
3	5	6	15	9	8	7	8	8	3	8	77
4	3	5	4	9	4	2	0	3	5	6	41
5	39	31	28	32	33	30	40	37	34	30	334
6	5	8	7	10	9	13	13	7	9	8	89
7	0	0	0	0	0	0	0	0	0	0	0
8	0	0	0	0	0	0	0	0	0	0	0
9	0	0	0	0	0	0	0	0	0	0	0
10	1	2	0	0	1	0	0	1	0	0	5
11	2	0	0	0	1	1	1	1	0	0	6
12	0	0	0	0	0	0	0	1	0	0	1
Total	100	100	100	100	100	100	100	100	100	100	1000

Table B.21 Experimental data for part magnet at 82% amplitude

POSITION	E1	E2	E3	E4	E5	E6	E7	E8	E9	E10	Total
1	41	31	47	46	46	43	44	46	42	37	423
2	1	2	1	3	0	2	0	0	2	2	13
3	5	11	5	8	6	7	12	5	9	8	76
4	5	5	3	4	4	4	1	3	1	3	33
5	31	38	29	30	29	32	30	37	35	35	326
6	16	13	14	9	13	10	11	9	10	11	116
7	0	0	0	0	0	0	0	0	0	0	0
8	0	0	0	0	0	0	1	0	0	1	2
9	0	0	0	0	0	0	0	0	0	0	0
10	1	0	1	0	2	0	0	0	1	0	5
11	0	0	0	0	0	1	1	0	0	3	5
12	0	0	0	0	0	1	0	0	0	0	1
Total	100	100	100	100	100	100	100	100	100	100	1000

Table B.22 Experimental data for part latch at 78% amplitude

POSITION	E1	E2	E3	E4	E5	E6	E7	E8	E9	E10	Total
1	11	6	5	8	8	5	3	2	5	9	62
2	7	11	8	12	6	6	14	14	9	11	98
3	29	22	25	27	23	30	25	20	23	29	253
4	14	21	19	16	19	10	16	17	22	18	172
5	21	20	28	22	31	33	29	32	31	21	268
6	13	17	13	14	11	12	12	14	6	10	122
7	0	1	1	0	1	1	0	1	1	1	7
8	0	0	0	0	0	2	0	0	0	0	2
9	0	1	0	0	0	0	0	0	0	0	1
10	0	0	0	0	0	0	0	0	0	0	0
11	2	1	0	0	0	1	0	0	2	0	6
12	3	0	1	1	1	0	1	0	1	1	9
Total	100	100	100	100	100	100	100	100	100	100	1000

Table B.23 Experimental data for part latch at 80% amplitude

POSITION	E1	E2	E3	E4	E5	E6	E7	E8	E9	E10	Total
1	9	7	5	10	5	12	7	7	7	5	74
2	10	11	9	13	10	9	14	9	15	19	119
3	21	30	31	25	27	20	22	28	23	26	253
4	20	15	11	15	12	21	13	9	18	17	151
5	30	21	24	22	25	20	26	25	22	21	236
6	10	15	20	11	20	14	16	22	15	12	155
7	0	0	0	3	0	3	0	0	0	0	6
8	0	0	0	0	0	0	0	0	0	0	0
9	0	0	0	0	1	0	0	0	0	0	1
10	0	0	0	0	0	0	0	0	0	0	0
11	0	1	0	0	0	1	1	0	0	0	3
12	0	0	0	1	0	0	1	0	0	0	2
Total	100	100	100	100	100	100	100	100	100	100	1000

Table B.24 Experimental data for part latch at 82% amplitude

POSITION	E1	E2	E3	E4	E5	E6	E7	E8	E9	E10	Total
1	15	3	3	6	7	4	6	7	4	8	63
2	18	15	8	13	19	12	12	17	17	15	146
3	23	27	25	20	22	28	19	20	25	22	231
4	12	16	20	23	13	9	10	11	15	16	145
5	19	25	22	26	24	32	28	33	24	20	253
6	13	14	22	11	15	15	25	12	15	17	159
7	0	0	0	1	0	0	0	0	0	1	2
8	0	0	0	0	0	0	0	0	0	0	0
9	0	0	0	0	0	0	0	0	0	1	1
10	0	0	0	0	0	0	0	0	0	0	0
11	0	0	0	0	0	0	0	0	0	0	0
12	0	0	0	0	0	0	0	0	0	0	0
Total	100	100	100	100	100	100	100	100	100	100	1000

Table B.25 Experimental data for part arc chute at 78% amplitude

POSITION	E1	E2	E3	E4	E5	E6	E7	E8	E9	E10	Total
1	16	21	28	20	21	20	24	27	28	19	224
2	22	19	10	23	19	23	16	21	16	16	185
3	3	11	14	15	12	11	11	9	9	11	106
4	7	5	7	7	11	8	7	7	9	5	73
5	3	1	1	3	5	5	1	1	0	2	22
6	3	5	1	0	1	2	0	1	1	1	15
7	1	2	0	0	3	0	1	1	1	2	11
8	3	4	1	2	4	4	4	1	4	2	29
9	11	10	7	9	5	8	11	11	7	5	84
10	9	10	17	8	9	8	6	10	8	17	102
11	0	0	1	1	0	0	0	1	0	0	3
12	0	0	0	1	1	1	1	0	0	0	4
13	0	2	1	0	0	0	0	0	0	0	3
14	0	0	1	1	0	0	2	0	0	1	5
15	11	4	5	5	5	6	7	1	3	5	52
16	9	2	5	2	2	4	8	9	14	14	69
17	1	0	0	1	0	0	0	0	0	0	2
18	0	1	1	1	0	0	0	0	0	0	3
19	0	1	0	1	2	0	1	0	0	0	5
20	1	2	0	0	0	0	0	0	0	0	3
Total	100	100	100	100	100	100	100	100	100	100	1000

Table B.26 Experimental data for part arc chute at 80% amplitude

POSITION	E1	E2	E3	E4	E5	E6	E7	E8	E9	E10	Total
1	25	27	23	20	22	27	22	23	25	28	242
2	20	19	18	16	20	21	24	15	22	23	198
3	8	7	12	14	9	12	11	11	7	7	98
4	6	5	6	9	3	8	6	9	4	4	60
5	4	1	2	1	1	2	2	1	1	1	16
6	2	1	1	1	1	4	0	4	1	1	16
7	1	3	1	0	2	1	0	5	3	2	18
8	1	3	3	2	3	2	2	4	3	1	24
9	3	10	8	14	12	7	8	7	5	6	80
10	14	14	7	6	8	8	12	13	11	13	106
11	0	0	0	0	0	1	0	0	0	1	2
12	1	1	2	0	0	1	0	0	1	0	6
13	1	0	1	0	0	0	0	0	0	0	2
14	1	0	0	0	0	1	0	0	0	0	2
15	4	4	8	7	8	3	9	4	5	5	57
16	8	5	7	7	11	2	4	3	10	6	63
17	0	0	1	1	0	0	0	1	0	1	4
18	0	0	0	0	0	0	0	0	1	0	1
19	1	0	0	2	0	0	0	0	1	1	5
20	0	0	0	0	0	0	0	0	0	0	0
Total	100	100	100	100	100	100	100	100	100	100	1000

Table B.27 Experimental data for part arc chute at 82% amplitude

POSITION	E1	E2	E3	E4	E5	E6	E7	E8	E9	E10	Total
1	25	18	29	24	31	26	18	17	27	20	235
2	17	26	26	29	13	11	22	30	19	23	216
3	10	11	8	9	9	12	11	10	15	12	107
4	5	6	10	6	5	5	2	7	8	9	63
5	1	3	0	0	1	1	3	0	2	4	15
6	2	0	1	1	1	1	2	0	1	2	11
7	3	1	1	3	1	0	2	1	2	3	17
8	1	0	2	0	2	0	2	2	2	1	12
9	8	7	5	8	6	9	8	8	5	8	72
10	7	14	10	6	9	12	9	14	15	5	101
11	0	1	1	0	0	1	1	0	0	1	5
12	0	0	0	1	0	0	2	1	0	0	4
13	0	0	0	1	1	2	1	0	0	1	6
14	1	0	0	0	0	0	0	0	1	1	3
15	11	4	0	3	7	9	5	6	1	4	50
16	8	8	7	9	12	10	11	4	1	5	75
17	0	0	0	0	0	1	0	0	0	0	1
18	1	1	0	0	0	0	1	0	0	1	4
19	0	0	0	0	2	0	0	0	1	0	3
20	0	0	0	0	0	0	0	0	0	0	0
Total	100	100	100	100	100	100	100	100	100	100	1000

Table B.28 Experimental data for part stab & contact at 78% amplitude

POSITION	E1	E2	E3	E4	E5	E6	E7	E8	E9	E10	Total
1	10	6	6	8	7	6	5	5	9	8	70
2	7	5	10	7	9	11	7	9	7	5	77
3	8	11	4	7	8	10	12	11	2	8	81
4	2	1	4	3	4	2	1	1	1	2	21
5	12	16	7	11	10	15	11	9	13	14	118
6	11	6	5	9	5	6	7	9	10	5	73
7	3	8	5	7	6	4	8	2	6	2	51
8	12	10	8	10	9	8	15	12	7	10	101
9	0	0	0	0	0	0	0	0	0	0	0
10	0	0	0	0	0	0	0	0	0	0	0
11	0	0	0	0	0	0	0	0	0	0	0
12	0	0	0	0	0	0	0	0	0	0	0
13	5	10	11	15	8	13	5	12	10	10	99
14	2	7	8	3	4	4	3	3	7	4	45
15	6	5	5	3	10	3	3	2	6	5	48
16	7	3	4	8	8	7	5	9	10	9	70
17	8	7	6	4	5	3	8	10	2	9	62
18	5	4	11	4	3	6	9	4	7	7	60
19	0	0	2	0	0	0	0	0	0	0	2
20	0	0	0	0	0	0	0	0	0	0	0
21	2	1	2	1	3	1	0	1	3	1	15
22	0	0	0	0	1	1	1	1	0	1	5
23	0	0	2	0	0	0	0	0	0	0	2
Total	100	100	100	100	100	100	100	100	100	100	1000

Table B.29 Experimental data for part stab & contact at 80% amplitude

POSITION	E1	E2	E3	E4	E5	E6	E7	E8	E9	E10	Total
1	8	5	9	10	15	5	8	5	8	11	84
2	7	9	7	2	8	3	7	11	10	7	71
3	5	13	2	8	10	9	12	11	10	9	89
4	0	1	0	2	1	2	2	1	2	2	13
5	8	9	13	14	10	12	11	16	11	11	115
6	9	11	10	5	10	12	6	6	15	3	87
7	4	2	6	2	4	3	5	10	3	3	42
8	16	12	7	10	8	6	8	8	7	6	88
9	0	0	0	0	0	0	0	0	0	0	0
10	0	0	0	0	0	0	0	0	0	0	0
11	0	0	0	0	0	0	1	0	0	0	1
12	0	0	0	0	0	0	0	1	0	1	2
13	14	8	7	10	4	12	6	6	8	11	86
14	3	3	7	5	6	4	8	4	5	6	51
15	3	2	6	5	9	7	6	3	11	4	56
16	9	9	10	5	4	7	11	5	8	11	79
17	5	10	2	13	6	9	4	3	0	5	57
18	7	4	7	7	2	4	3	6	2	8	50
19	0	0	0	0	0	1	0	1	0	0	2
20	0	0	0	0	0	0	0	0	0	0	0
21	1	1	5	1	1	2	2	1	0	1	15
22	1	1	2	1	2	2	0	2	0	1	12
23	0	0	0	0	0	0	0	0	0	0	0
Total	100	100	100	100	100	100	100	100	100	100	1000

Table B.30 Experimental data for part stab & contact at 82% amplitude

POSITION	E1	E2	E3	E4	E5	E6	E7	E8	E9	E10	Total
1	7	9	8	10	4	13	8	7	7	4	77
2	11	7	7	9	7	8	4	10	5	10	78
3	5	8	5	10	13	7	8	12	11	6	85
4	0	0	2	0	1	1	1	0	0	4	9
5	13	11	13	12	11	4	8	4	20	9	105
6	8	7	7	19	7	7	10	8	4	10	87
7	4	4	6	5	7	8	9	7	2	3	55
8	12	7	16	5	17	15	7	15	13	9	116
9	0	1	0	0	0	0	0	0	0	0	1
10	0	0	0	0	0	0	0	0	0	0	0
11	0	0	0	0	0	0	0	0	0	0	0
12	0	0	0	0	0	0	0	0	0	0	0
13	6	15	12	10	2	7	10	9	4	15	90
14	7	12	5	0	3	3	7	4	10	6	57
15	7	4	4	5	2	4	6	7	4	5	48
16	1	1	8	5	8	4	4	7	7	7	52
17	10	2	3	4	8	6	8	4	8	3	56
18	5	7	2	5	9	7	6	3	2	6	52
19	0	0	1	0	0	0	1	0	0	0	2
20	1	0	0	0	1	4	0	0	0	0	6
21	2	2	1	1	0	2	1	2	2	2	15
22	1	3	0	0	0	0	2	1	1	1	9
23	0	0	0	0	0	0	0	0	0	0	0
Total	100	100	100	100	100	100	100	100	100	100	1000

APPENDIX C

EXPERIMENTAL RESUTLS

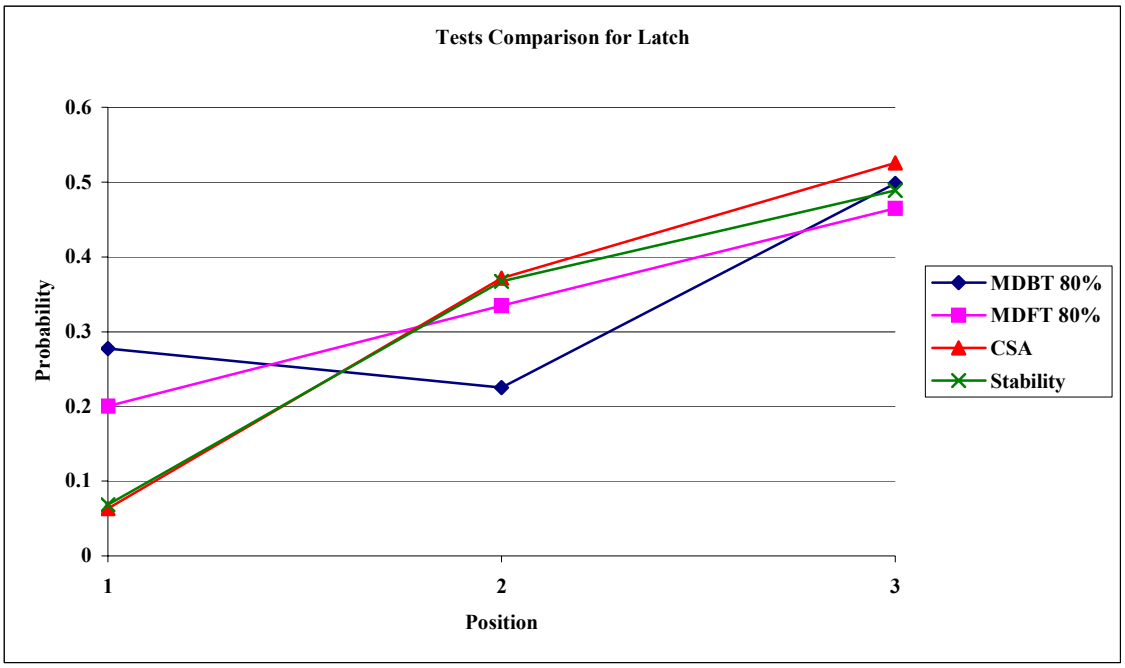

Figure C.1. Latch experimental probability profile (amplitude = 80%).

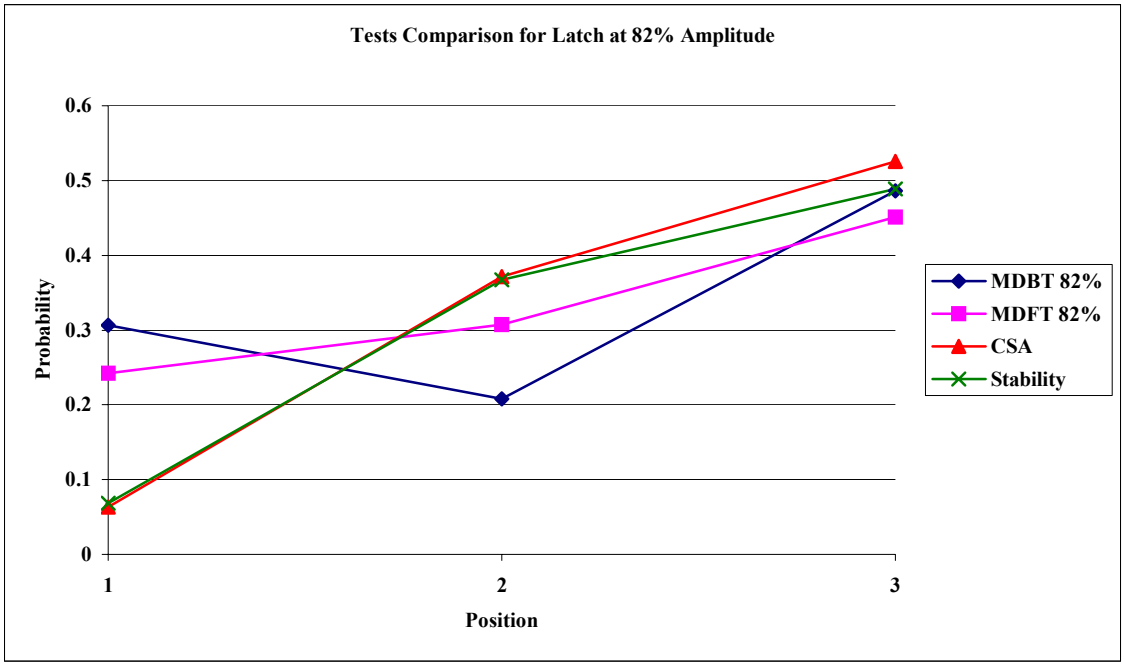

Figure C.2. Latch experimental probability profile (amplitude = 82%).

Figure C.3. Stab & contact experimental probability profile (amplitude = 80%).

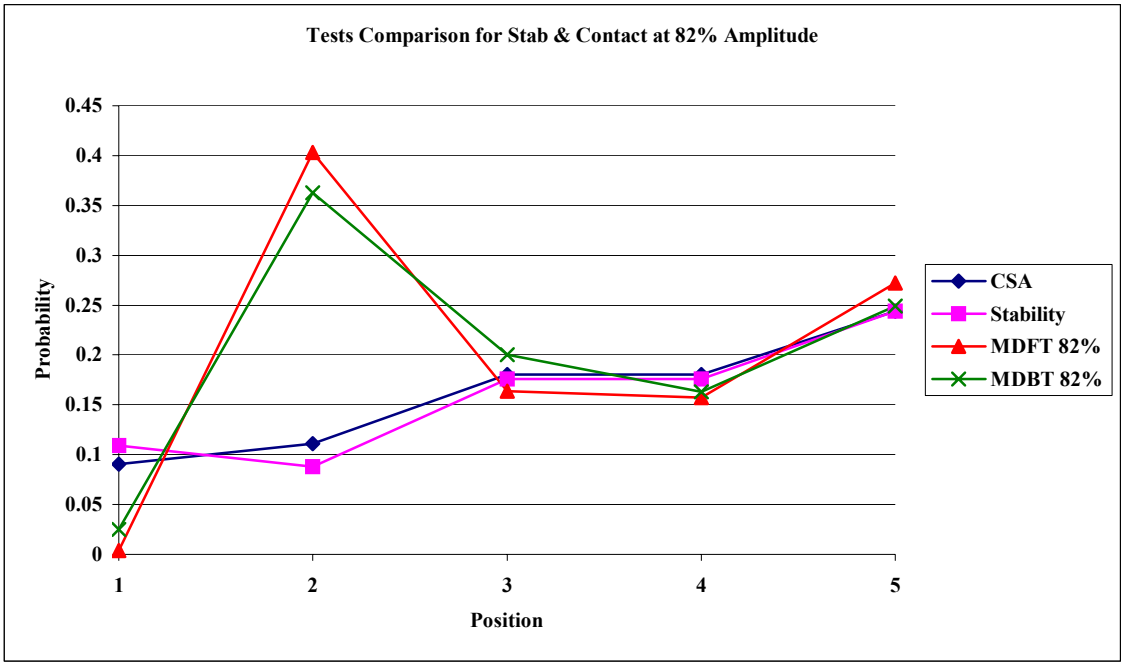

Figure C.4. Stab & contact experimental probability profile (amplitude = 82%).

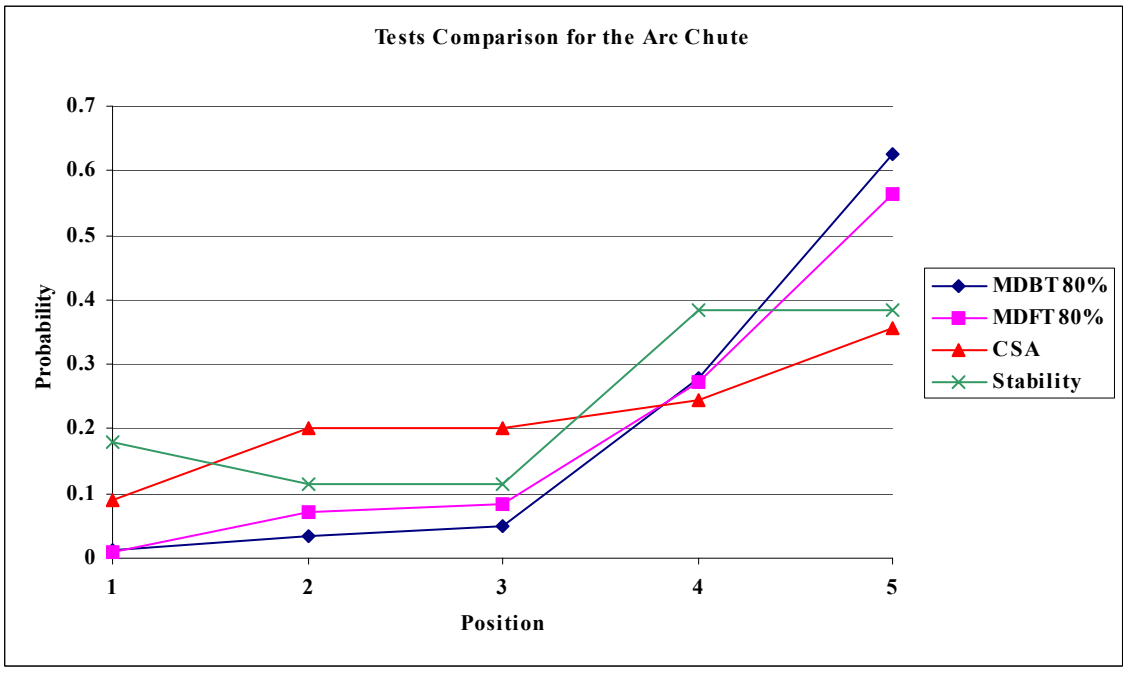

Figure C.5. Arc chute experimental probability profile (amplitude = 80%).

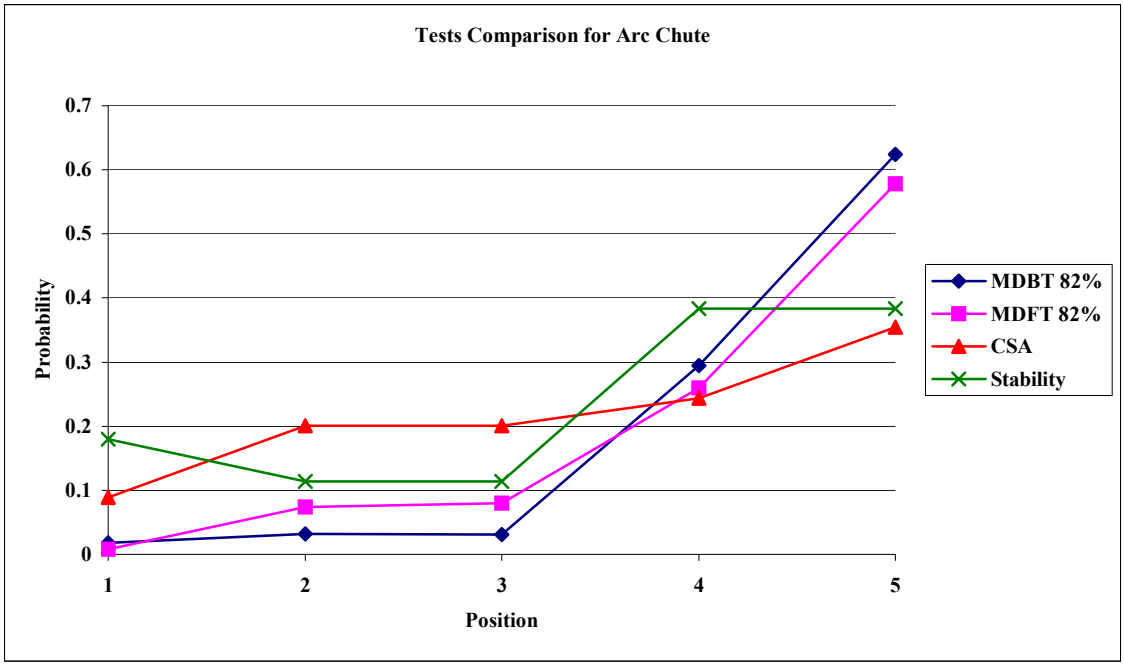

Figure C.6. Arc chute experimental probability profile (amplitude = 82%).

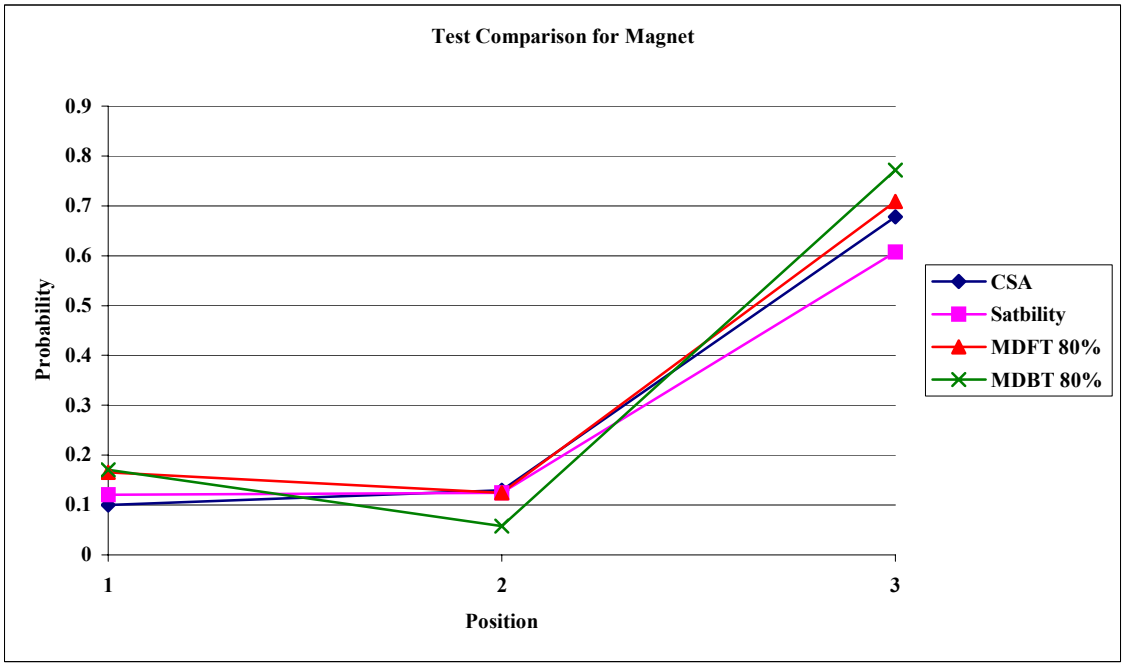

Figure C.7. Magnet experimental probability profile (amplitude = 80%).

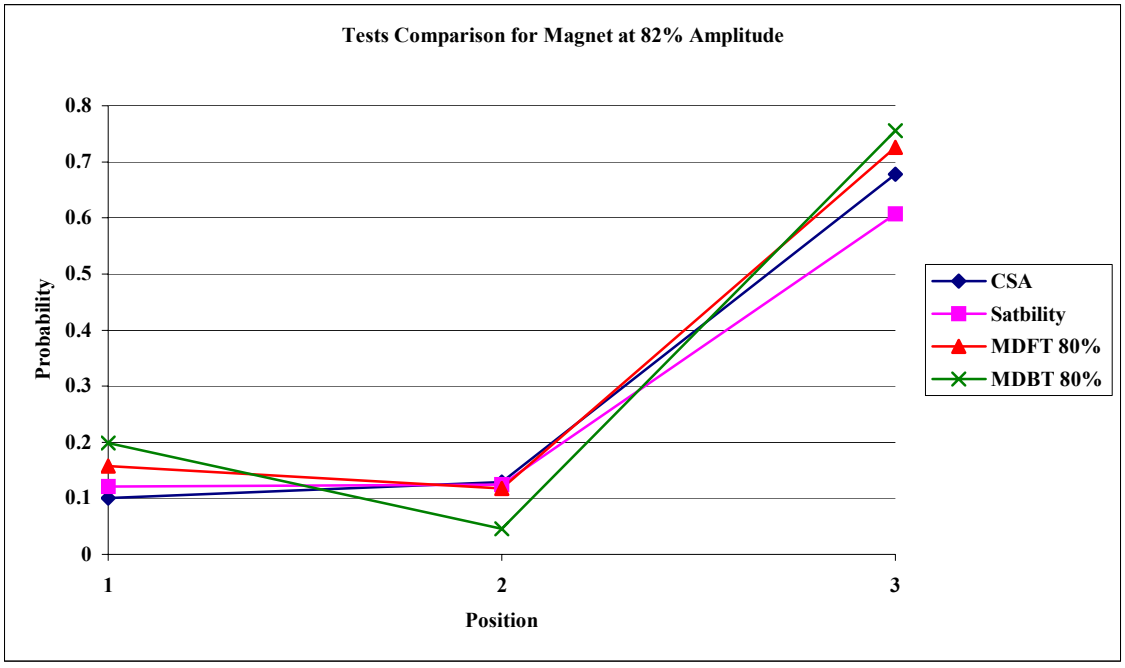

Figure C.8. Magnet experimental probability profile (amplitude = 82%).

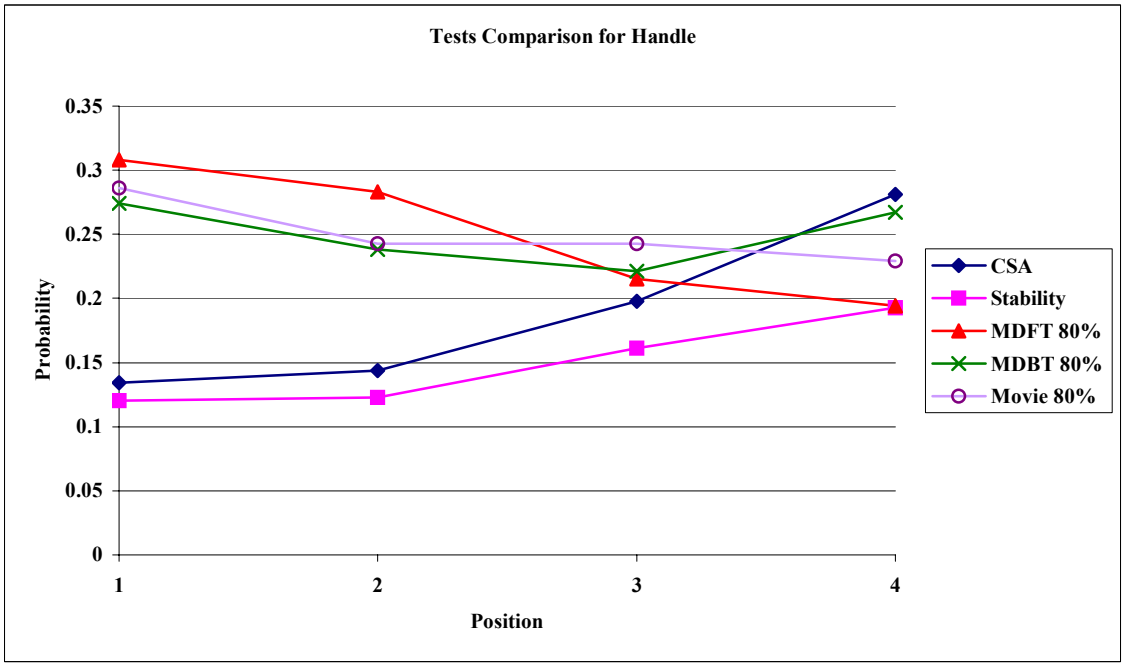

Figure C.9. Handle experimental probability profile (amplitude = 80%).

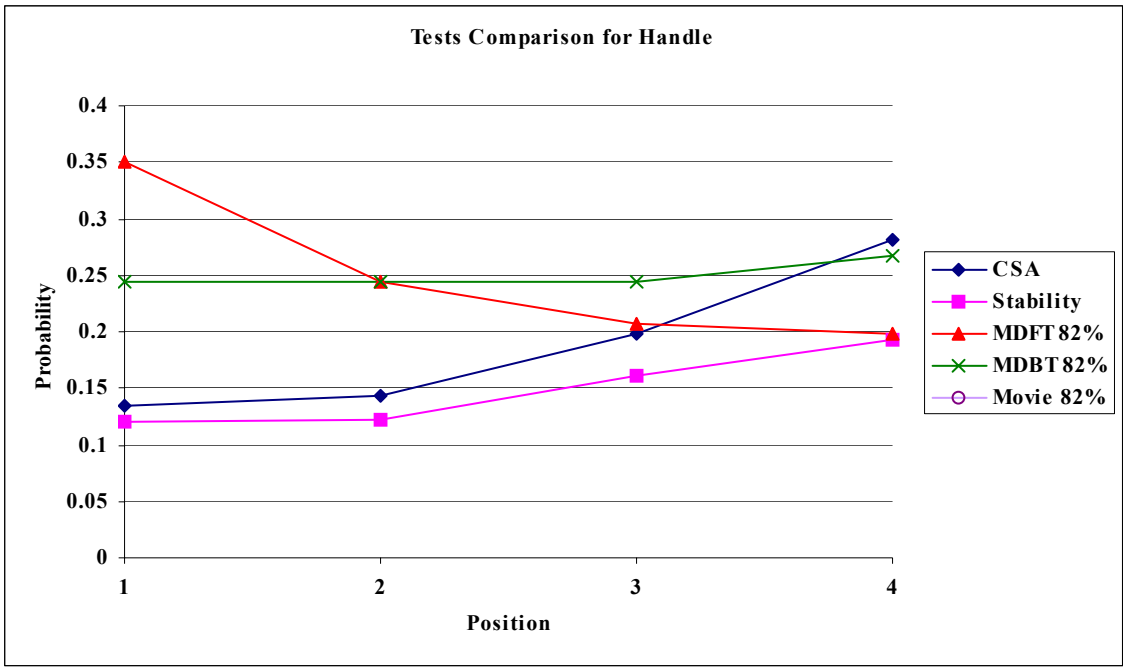

Figure C.10. Handle experimental probability profile (amplitude = 82%).

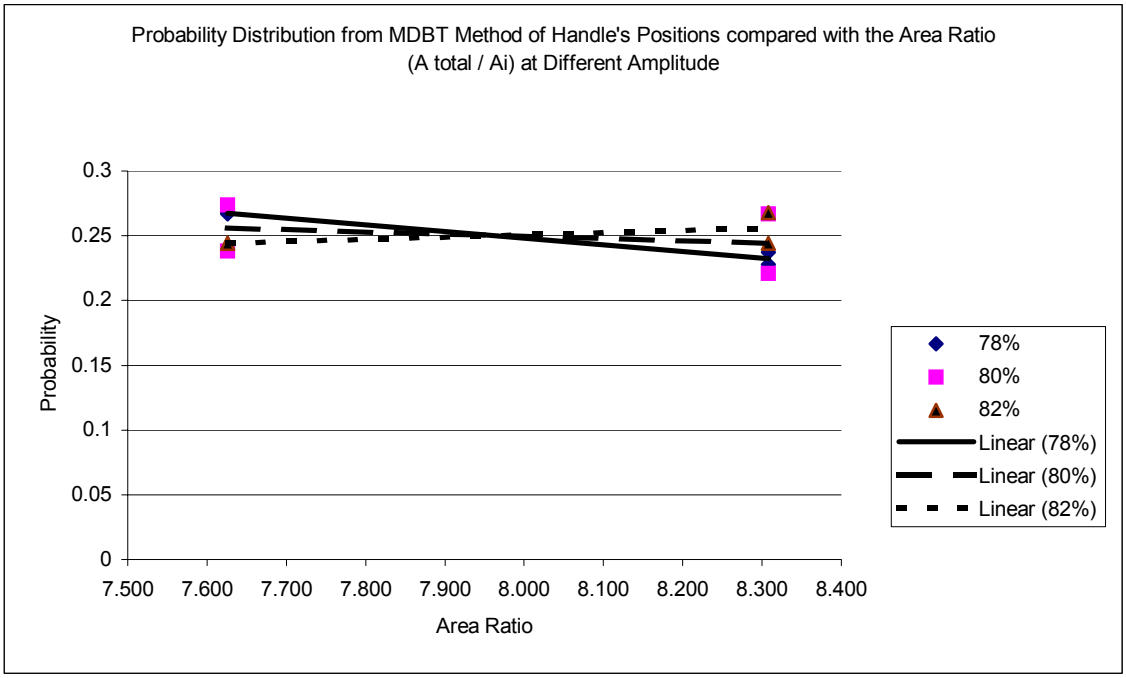

Figure C.11. Experimental Probability distribution from MDBT method of the handle's aspects compared with the area ratio (A_{total}/ A_i).

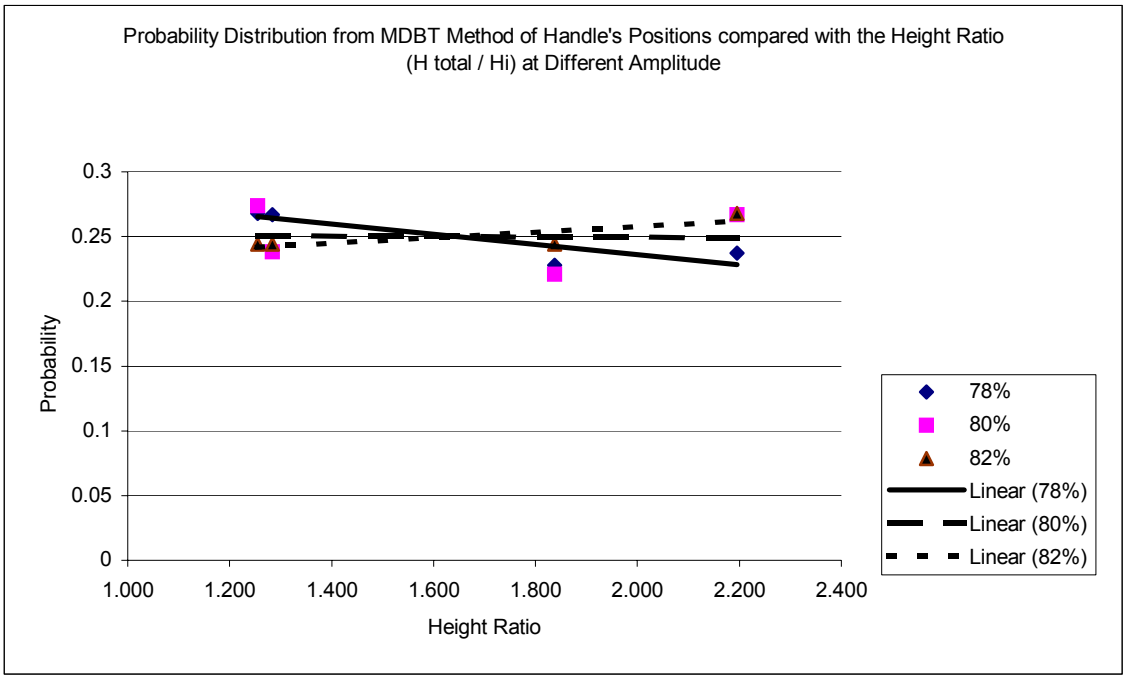

Figure C.12. Experimental Probability distribution from MDBT method of the handle's aspects compared with the height ratio (h_{total}/ h_i).

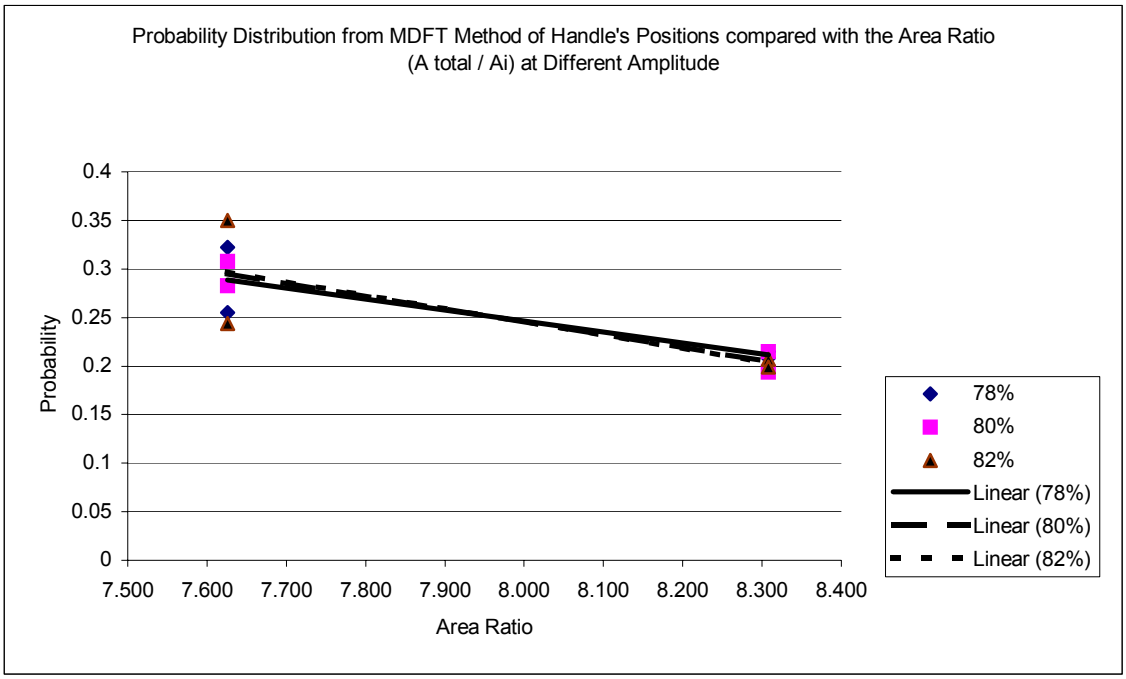

Figure C.13. Experimental Probability distribution from MDFT method of the handle's aspects compared with the area ratio (A_{total}/ A_i).

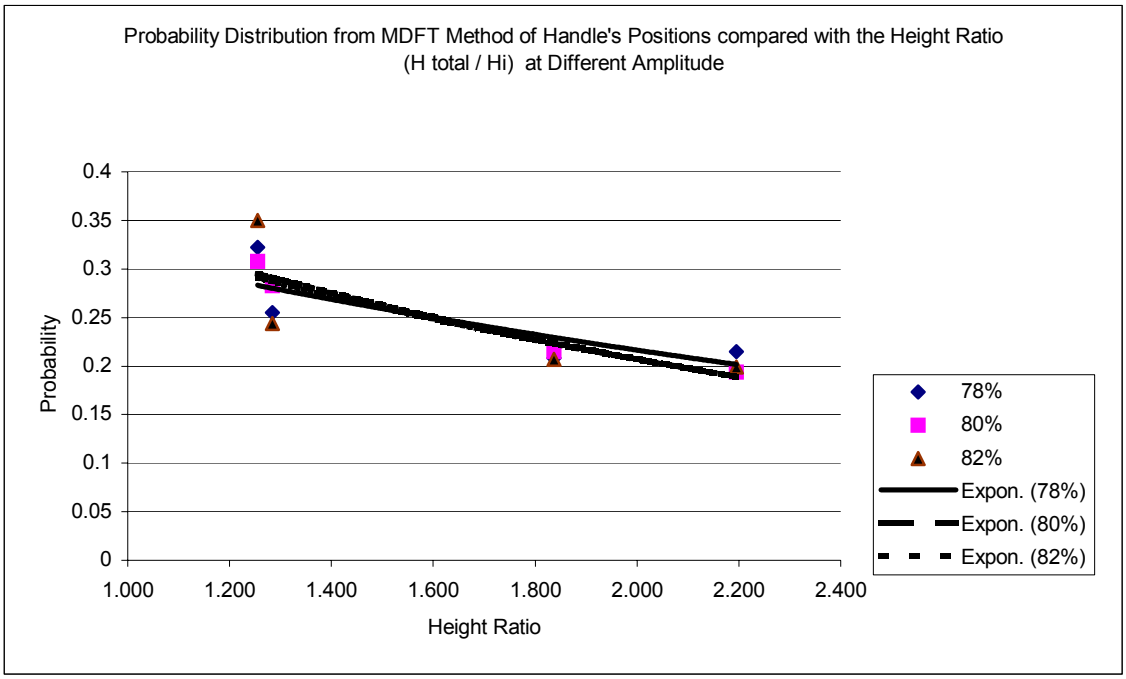

Figure C.14. Experimental Probability distribution from MDFT method of the handle's aspects compared with the height ratio (h_{total}/ h_i).

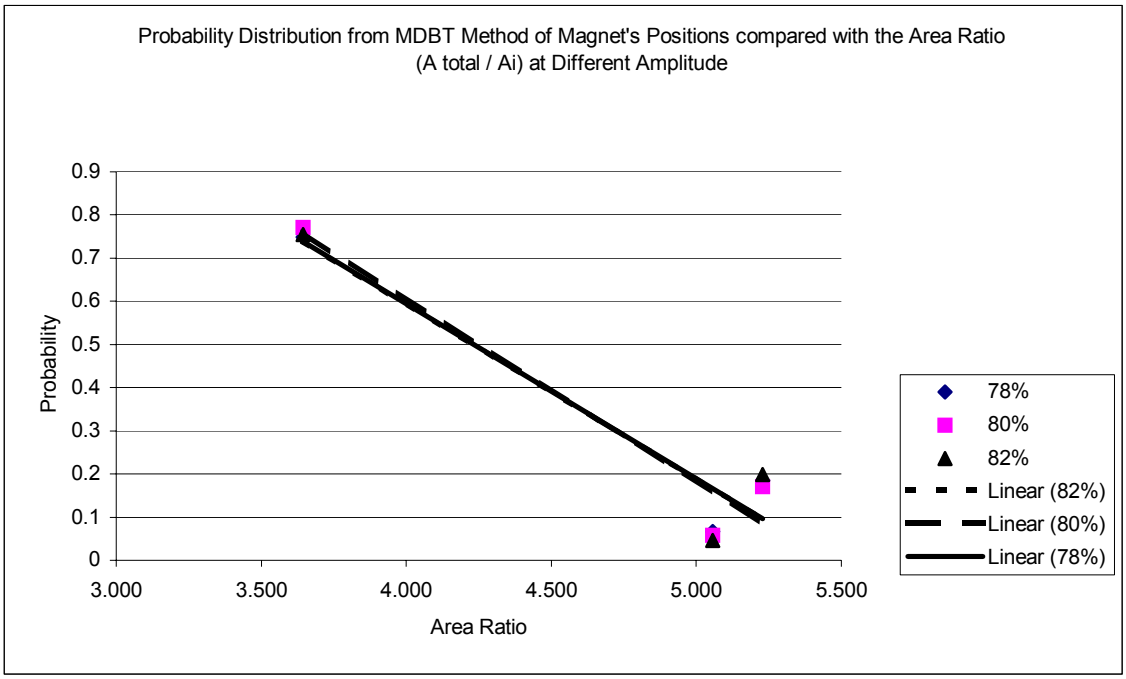

Figure C.15. Experimental Probability distribution from MDBT method of the magnet's aspects compared with the area ratio (A_{total}/ A_i).

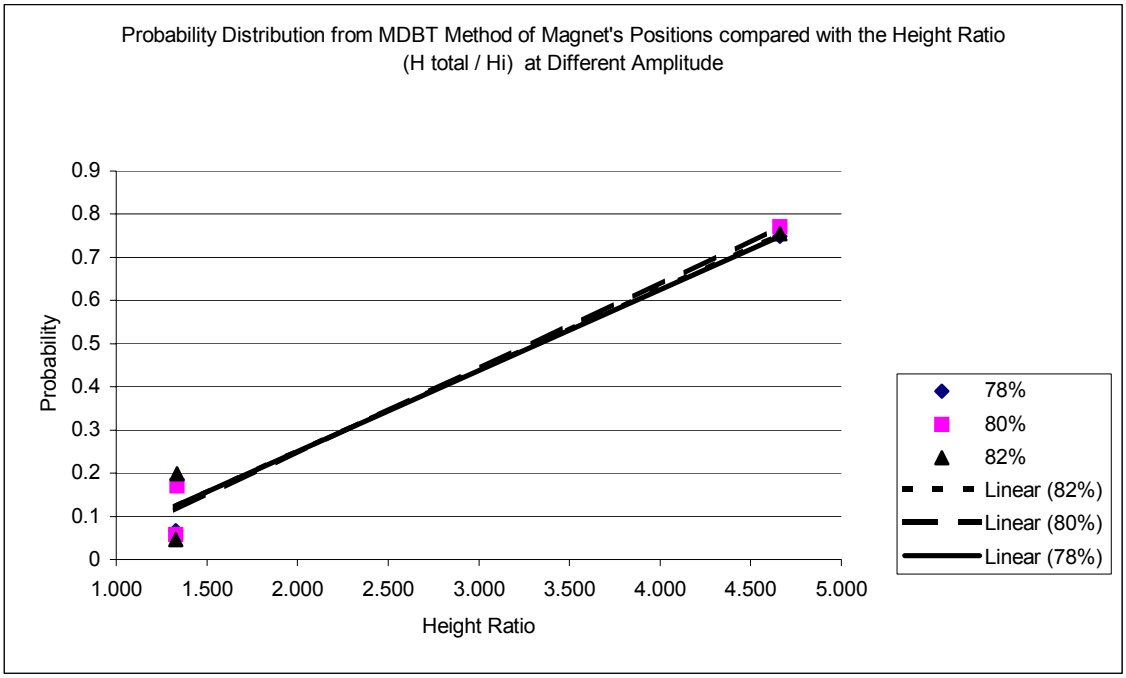

Figure C.16. Experimental Probability distribution from MDBT method of the magnet's aspects compared with the height ratio (h_{total}/ h_i).

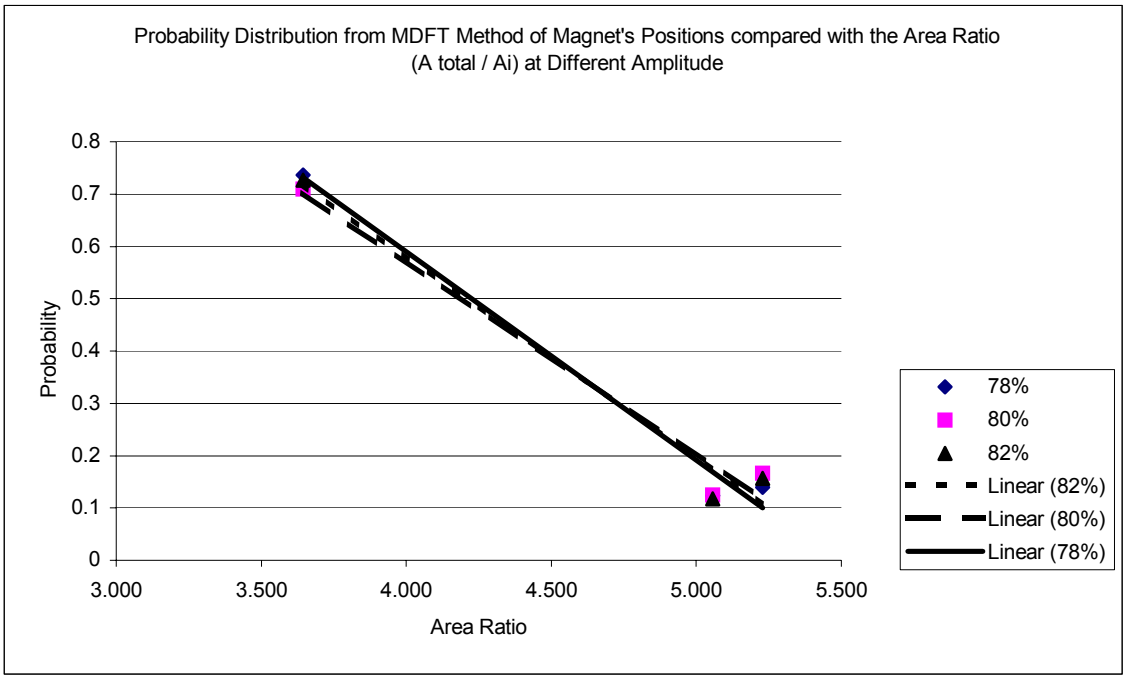

Figure C.17. Experimental Probability distribution from MDFT method of the magnet's aspects compared with the area ratio (A_{total}/ A_i).

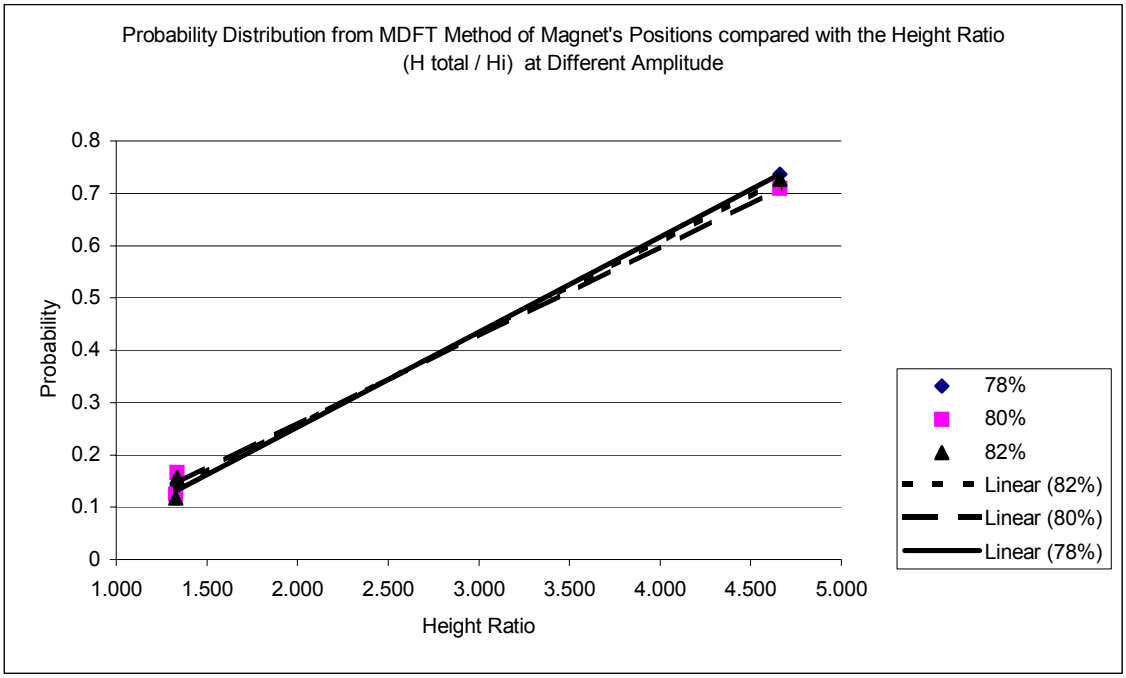

Figure C.18. Experimental Probability distribution from MDFT method of the magnet's aspects compared with the height ratio (h_{total}/ h_i).

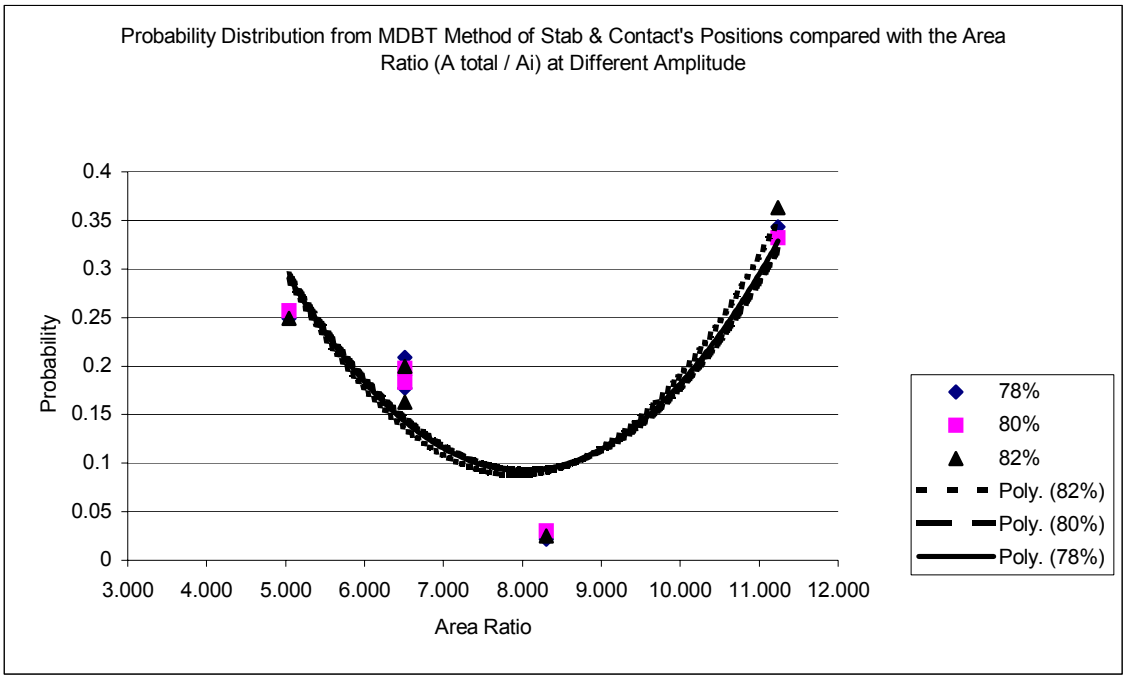

Figure C.19. Experimental Probability distribution from MDBT method of the stab &contact's aspects compared with the area ratio (A_{total}/ A_i).

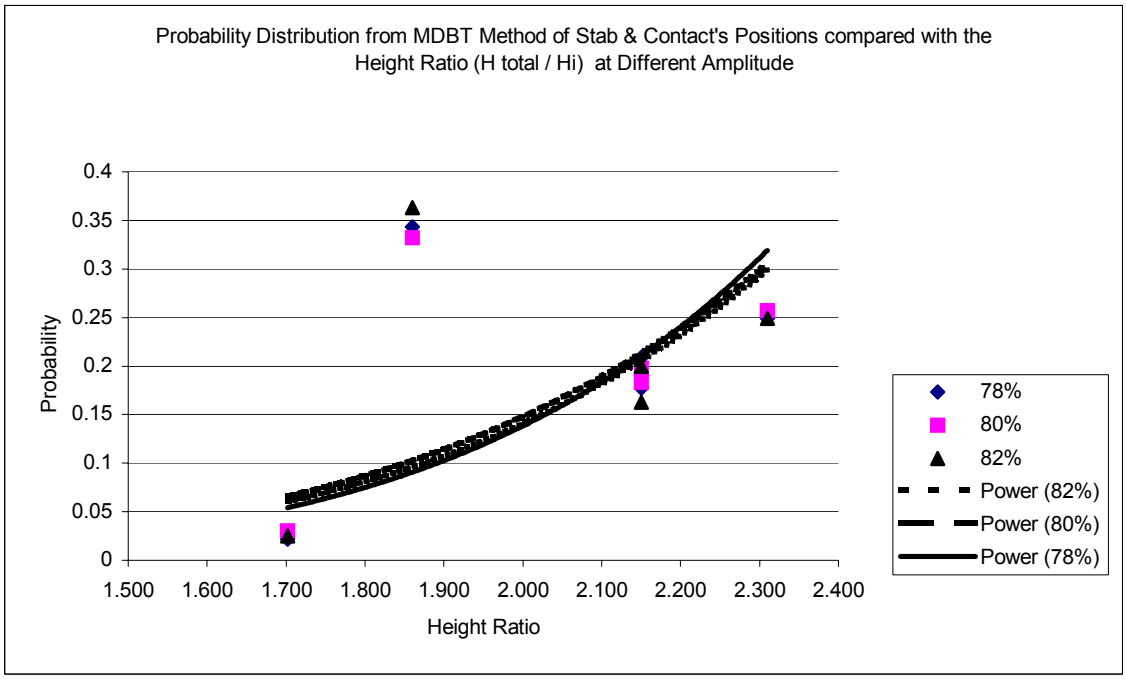

Figure C.20. Experimental Probability distribution from MDBT method of the stab & contact's aspects compared with the height ratio (h_{total}/ h_i).

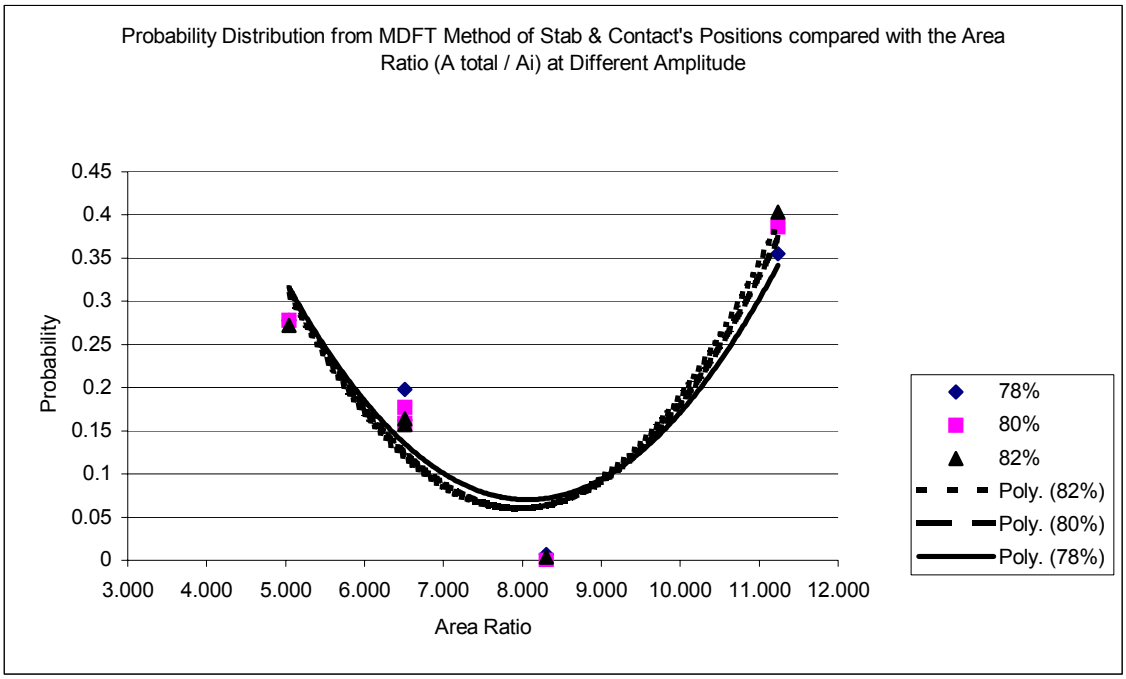

Figure C.21. Experimental Probability distribution from MDFT method of the stab & contact's aspects compared with the area ratio (A_{total}/ A_i).

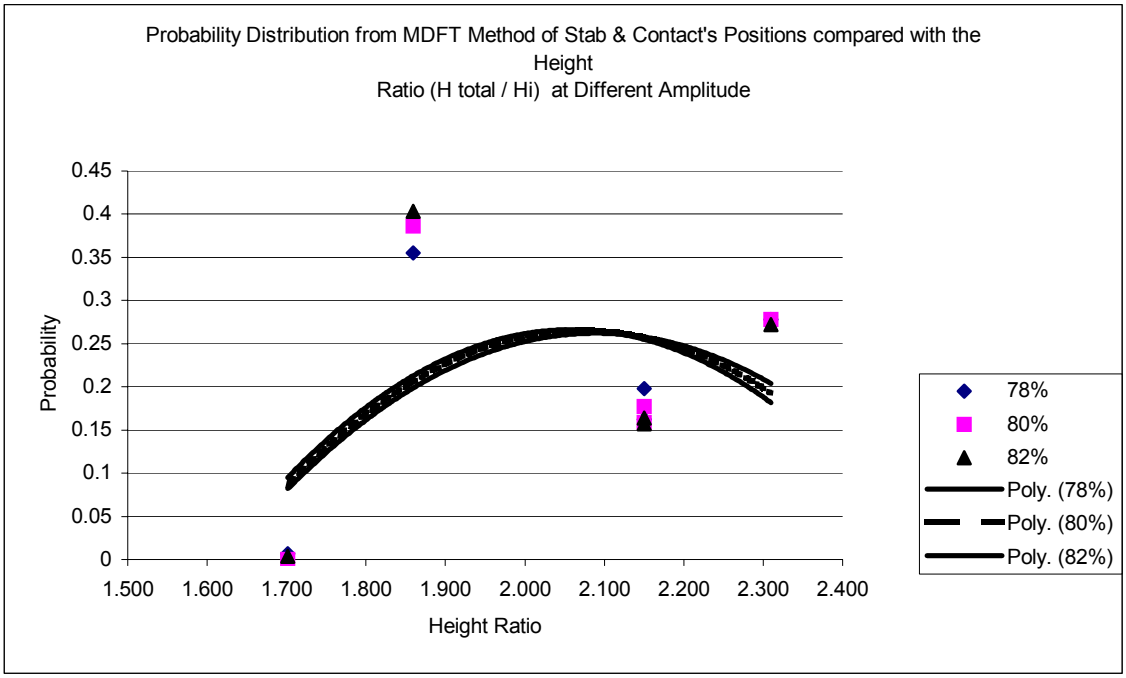

Figure C.22. Experimental Probability distribution from MDFT method of the stab & contact's aspects compared with the height ratio (h_{total}/ h_i).

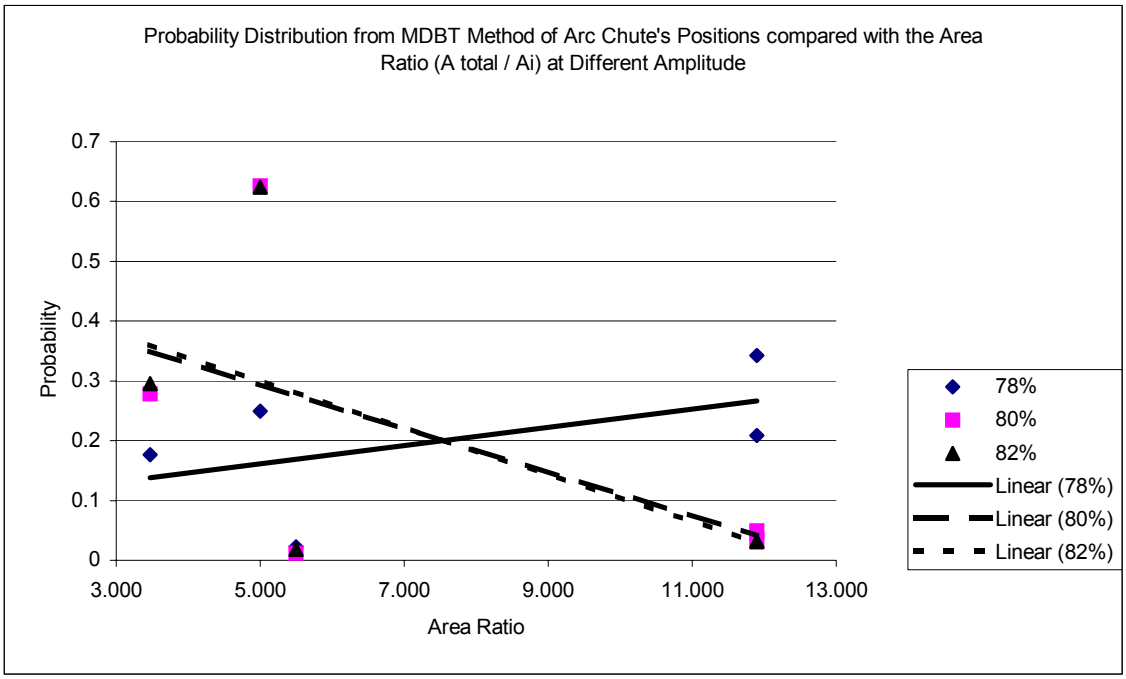

Figure C.23. Experimental Probability distribution from MDBT method of the arc chute's aspects compared with the area ratio (A_{total}/ A_i).

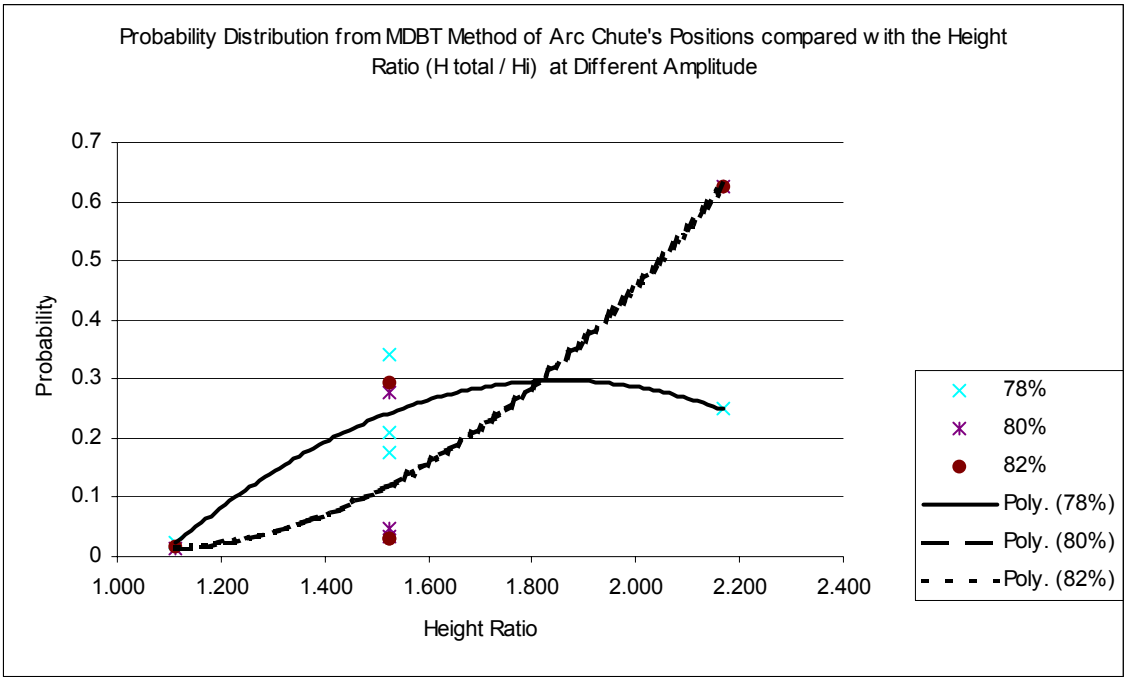

Figure C.24. Experimental Probability distribution from MDBT method of the arc chute's aspects compared with the height ratio (h_{total}/ h_i).

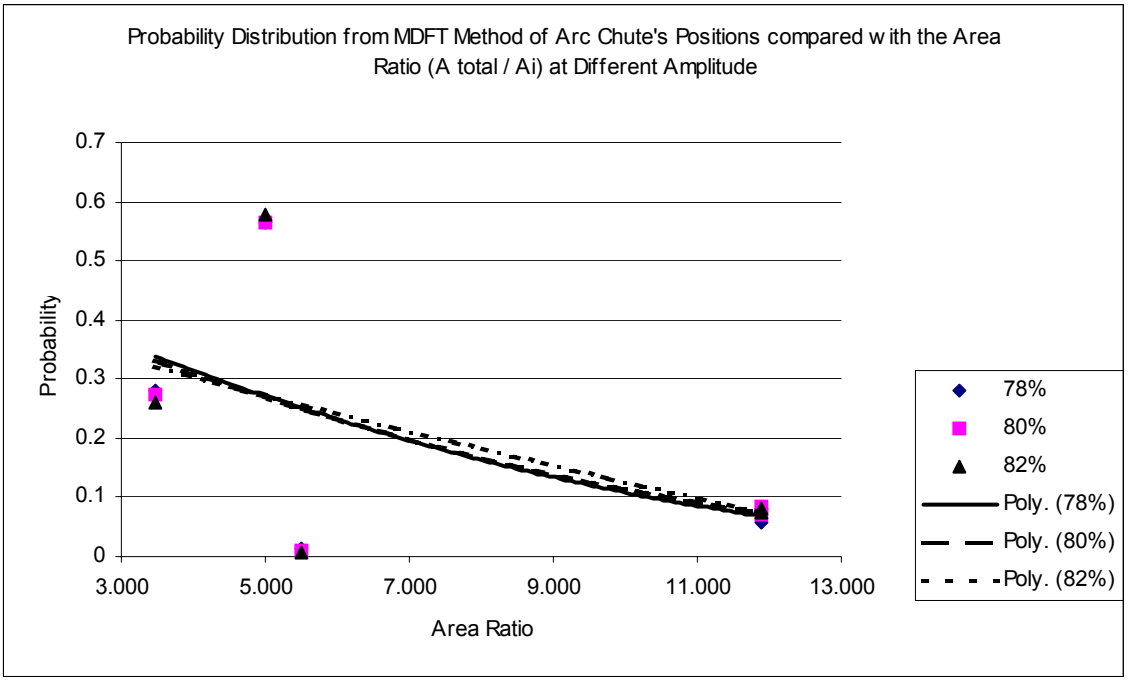

Figure C.25. Experimental Probability distribution from MDFT method of the arc chute's aspects compared with the area ratio (A_{total}/ A_i).

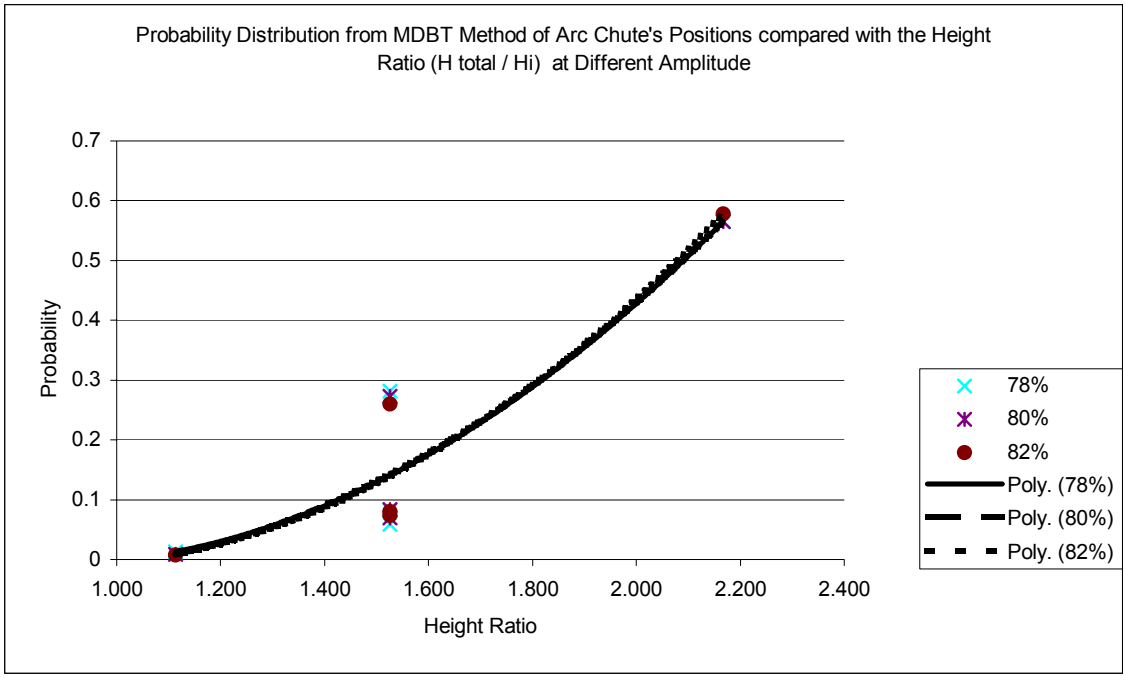

Figure C.26. Experimental Probability distribution from MDFT method of the arc chute's aspects compared with the height ratio (h_{total}/ h_i).

APPENDIX D

PEARSON'S X^2 TEST FOR GOODNESS OF FIT

For the latch part, taking $\propto = .05$, the computations for the x^2 statistic are shown in the following table, using the table of percentage points of x^2 distribution, $x^2_{.05} = 5.99$ with d.f = 2. Because the observed x^2 is larger than $x^2_{.05}$ value, the null hypothesis is rejected .

Table D.1. The x^2 Test for Goodness of Fit for Latch Part Data for MDBT versus CSA Method at 78% Amplitude.

Positions	1	2	3	Total
Observed frequency (O)	230	236	534	1000
Probability under Ho	0.066318	0.386732	0.546951	1
Expected frequency (E)	66.31759	386.7318	546.9506	1000
$\frac{(O-E)^2}{E}$	403.9944	58.74894	0.306641	463.05
				d.f.=2

Table D.2. The x^2 Test for Goodness of Fit for Latch Part Data for MDBT versus CSA Method at 80% Amplitude.

Positions	1	2	3	Total
Observed frequency (O)	277	225	498	1000
Probability under Ho	0.066318	0.386732	0.546951	1
Expected frequency (E)	66.31759	386.7318	546.9506	1000
$\frac{(O-E)^2}{E}$	669.3108	67.6365	4.380943	741.3283
				d.f.=2

Table D.3. The x^2 Test for Goodness of Fit for Latch Part Data for MDBT versus CSA Method at 82% Amplitude.

Positions	1	2	3	Total
Observed frequency (O)	306	208	486	1000
Probability under Ho	0.066318	0.386732	0.546951	1
Expected frequency (E)	66.31759	386.7318	546.9506	1000
$\frac{(O-E)^2}{E}$	866.2507	82.60263	6.792155	955.6455
				d.f.=2

Table D.4. The x^2 Test for Goodness of Fit for Latch Part Data for MDBT versus Stability Methods at 78% Amplitude.

Positions	1	2	3	Total
Observed frequency (O)	230	236	534	1000
Probability under Ho	0.074223	0.397398	0.528379	1
Expected frequency (E)	74.22262	397.3979	528.3795	1000
$\frac{(O-E)^2}{E}$	326.9433	65.54961	0.059787	392.5527
				d.f.=2

Table D.5. The x^2 Test for Goodness of Fit for Latch Part Data for MDBT versus Stability Methods at 80% Amplitude.

Positions	1	2	3	Total
Observed frequency (O)	277	225	498	1000
Probability under Ho	0.074223	0.397398	0.528379	1
Expected frequency (E)	74.22262	397.3979	528.3795	1000
$\frac{(O-E)^2}{E}$	553.991	74.7891	1.746687	630.5268
				d.f.=2

Table D.6. The x^2 Test for Goodness of Fit for Latch Part Data for MDBT versus Stability Method at 82% Amplitude.

Positions	1	2	3	Total
Observed frequency (O)	306	208	486	1000
Probability under Ho	0.074223	0.397398	0.528379	1
Expected frequency (E)	74.22262	397.3979	528.3795	1000
$\frac{(O-E)^2}{E}$	723.7787	90.2661	3.399113	817.4439
				d.f.=2

Table D.6. The x^2 Test for Goodness of Fit for Latch Part Data for MDFT versus CSA Method at 78% Amplitude.

Positions	1	2	3	Total
Observed frequency (O)	195	310	495	1000
Probability under Ho	0.066318	0.386732	0.546951	1
Expected frequency (E)	66.31759	386.7318	546.9506	1000
$\frac{(O-E)^2}{E}$	249.6949	15.22444	4.934381	269.8537
				d.f.=2

Table D.7. The x^2 Test for Goodness of Fit for Latch Part Data for MDFT versus CSA Method at 80% Amplitude.

Positions	1	2	3	Total
Observed frequency (O)	200	335	465	1000
Probability under Ho	0.066318	0.386732	0.546951	1
Expected frequency (E)	66.31759	386.7318	546.9506	1000
$\frac{(O-E)^2}{E}$	269.4758	6.919996	12.2788	288.6746
				d.f.=2

Table D.8. The x^2 Test for Goodness of Fit for Latch Part Data for MDFT versus CSA Method at 82% Amplitude.

Positions	1	2	3	Total
Observed frequency (O)	242	307	451	1000
Probability under Ho	0.066318	0.386732	0.546951	1
Expected frequency (E)	66.31759	386.7318	546.9506	1000
$\frac{(O-E)^2}{E}$	465.4016	16.43817	16.83244	498.6722
				d.f.=2

Table D.9. The x^2 Test for Goodness of Fit for Latch Part Data for MDFT versus Stability Method at 78% Amplitude.

Positions	1	2	3	Total
Observed frequency (O)	195	310	495	1000
Probability under Ho	0.074223	0.397398	0.528379	1
Expected frequency (E)	74.22262	397.3979	528.3795	1000
$\frac{(O-E)^2}{E}$	196.5327	19.22101	2.108694	217.8625
				d.f.=2

Table D.10. The x^2 Test for Goodness of Fit for Latch Part Data for MDFT versus Stability Method at 80% Amplitude.

Positions	1	2	3	Total
Observed frequency (O)	200	335	465	1000
Probability under Ho	0.074223	0.397398	0.528379	1
Expected frequency (E)	74.22262	397.3979	528.3795	1000
$\frac{(O-E)^2}{E}$	213.1419	9.797475	7.602416	230.5418
				d.f.=2

Table D.11. The x^2 Test for Goodness of Fit for Latch Part Data for MDFT versus Stability Method at 82% Amplitude.

Positions	1	2	3	Total
Observed frequency (O)	242	307	451	1000
Probability under Ho	0.074223	0.397398	0.528379	1
Expected frequency (E)	74.22262	397.3979	528.3795	1000
$\frac{(O-E)^2}{E}$	379.2543	20.56321	11.33198	411.1495
				d.f.=2

For the handle part, taking $\propto$ = .05, the computations for the x^2 statistic are shown in the following table, using the table of percentage points of x^2 distribution, $x^2_{.05}$ = 7.81 with d.f = 3. Because the observed x^2 is larger than $x^2_{.05}$ value, the null hypothesis is rejected.

Table D.12. The x^2 Test for Goodness of Fit for Handle Part Data for MDBT versus CSA Method at 78% Amplitude.

MDBT vs CSA at 78% Amplitude					
Positions	1	2	3	4	Total
Observed frequency (O)	268	267	228	237	1000
Probability under Ho	0.177262	0.190094	0.261398	0.371246	1
Expected frequency (E)	177.262	190.0944	261.3985	371.2455	1000
$\frac{(O-E)^2}{E}$	46.44754	31.11337	4.267269	48.54431	130.3725
					d.f.=3

Table D.13. The x^2 Test for Goodness of Fit for Handle Part Data for MDBT versus CSA Method at 80% Amplitude.

Positions	1	2	3	4	Total
Observed frequency (O)	274	238	221	267	1000
Probability under Ho	0.177262	0.190094	0.261398	0.371246	1
Expected frequency (E)	177.262	190.0944	261.3985	371.2455	1000
$\frac{(O-E)^2}{E}$	52.79327	12.07269	6.24348	29.27208	100.3815
					d.f.=3

Table D.14. The x^2 Test for Goodness of Fit for Handle Part Data for MDBT versus CSA Method at 82% Amplitude.

Positions	1	2	3	4	Total
Observed frequency (O)	244	244	244	268	1000
Probability under Ho	0.177262	0.190094	0.261398	0.371246	1
Expected frequency (E)	177.262	190.0944	261.3985	371.2455	1000
$\frac{(O-E)^2}{E}$	25.12643	15.28618	1.158027	28.71317	70.28381
					d.f.=3

Table D.15. The x^2 Test for Goodness of Fit for Handle Part Data for MDBT versus Stability Method at 78% Amplitude.

Positions	1	2	3	4	Total
Observed frequency (O)	268	267	228	237	1000
Probability under Ho	0.20116	0.20573	0.27022	0.32289	1
Expected frequency (E)	201.16	205.73	270.22	322.89	1000
$\frac{(O-E)^2}{E}$	22.20912	18.24728	6.596582	22.84708	69.90005
					d.f.=3

Table D.16. The x^2 Test for Goodness of Fit for Handle Part Data for MDBT versus Stability Method at 80% Amplitude.

Positions	1	2	3	4	Total
Observed frequency (O)	274	238	221	267	1000
Probability under Ho	0.20116	0.20573	0.27022	0.32289	1
Expected frequency (E)	201.16	205.73	270.22	322.89	1000
$\frac{(O-E)^2}{E}$	26.37535	5.061745	8.965319	9.674168	50.07658
					d.f.=3

Table D.17. The x^2 Test for Goodness of Fit for Handle Part Data for MDBT versus Stability Method at 82% Amplitude.

Positions	1	2	3	4	Total
Observed frequency (O)	244	244	244	268	1000
Probability under Ho	0.20116	0.20573	0.27022	0.32289	1
Expected frequency (E)	201.16	205.73	270.22	322.89	1000
$\frac{(O-E)^2}{E}$	9.123412	7.119005	2.54418	9.331079	28.11768
					d.f.=3

Table D.18. The x^2 Test for Goodness of Fit for Handle Part Data for MFBT versus CSA Method at 78% Amplitude.

MDFT vs CSA at 78% Amplitude					
Positions	1	2	3	4	Total
Observed frequency (O)	322	255	208	215	1000
Probability under Ho	0.177262	0.190094	0.261398	0.371246	1
Expected frequency (E)	177.262	190.0944	261.3985	371.2455	1000
$\frac{(O-E)^2}{E}$	118.1815	22.16132	10.90824	65.7588	217.0099
					d.f.=3

Table D.19. The x^2 Test for Goodness of Fit for Handle Part Data for MFBT versus CSA Method at 80% Amplitude.

Positions	1	2	3	4	Total
Observed frequency (O)	308	283	215	194	1000
Probability under Ho	0.177262	0.190094	0.261398	0.371246	1
Expected frequency (E)	177.262	190.0944	261.3985	371.2455	1000
$\frac{(O-E)^2}{E}$	96.42464	45.40617	8.23577	84.62317	226.454
					d.f.=3

Table D.20. The x^2 Test for Goodness of Fit for Handle Part Data for MFBT versus CSA Method at 82% Amplitude.

Positions	1	2	3	4	Total
Observed frequency (O)	350	244	207	199	1000
Probability under Ho	0.177262	0.190094	0.261398	0.371246	1
Expected frequency (E)	177.262	190.0944	261.3985	371.2455	1000
$\frac{(O-E)^2}{E}$	168.3295	15.28618	11.32062	79.91616	263.5318
					d.f.=3

Table D.21. The x^2 Test for Goodness of Fit for Handle Part Data for MFBT versus Stability Method at 78% Amplitude.

Positions	1	2	3	4	Total
Observed frequency (O)	322	255	208	215	1000
Probability under Ho	0.20116	0.20573	0.27022	0.32289	1
Expected frequency (E)	201.16	205.73	270.22	322.89	1000
$\frac{(O-E)^2}{E}$	72.5905	11.79961	14.32658	36.05021	134.7669
					d.f.=3

Table D.22. The x^2 Test for Goodness of Fit for Handle Part Data for MFBT versus Stability Method at 80% Amplitude.

Positions	1	2	3	4	Total
Observed frequency (O)	308	283	215	194	1000
Probability under Ho	0.20116	0.20573	0.27022	0.32289	1
Expected frequency (E)	201.16	205.73	270.22	322.89	1000
$\frac{(O-E)^2}{E}$	56.74481	29.02179	11.28432	51.44982	148.5007
					d.f.=3

Table D.23. The x^2 Test for Goodness of Fit for Handle Part Data for MFBT versus Stability Method at 82% Amplitude.

Positions	1	2	3	4	Total
Observed frequency (O)	350	244	207	199	1000
Probability under Ho	0.20116	0.20573	0.27022	0.32289	1
Expected frequency (E)	201.16	205.73	270.22	322.89	1000
$\frac{(O-E)^2}{E}$	110.128	7.119005	14.79079	47.53548	179.5733
					d.f.=3

For the magnet part, taking $\propto$ = .05, the computations for the x^2 statistic are shown in the following table, using the table of percentage points of x^2 distribution, $x^2_{.05}$ = 5.99 with d.f = 2. Because the observed x^2 is larger than $x^2_{.05}$ value, the null hypothesis is rejected.

Table D.24. The x^2 Test for Goodness of Fit for Magnet Part Data for MDBT versus CSA Method at 78% Amplitude.

Positions	1	2	3	Total
Observed frequency (O)	185	66	749	1000
Probability under Ho	0.110547	0.142769	0.746684	1
Expected frequency (E)	110.5473	142.7689	746.6839	1000
$\frac{(O-E)^2}{E}$	50.14332	41.27971	0.007184	91.43022
				d.f.=2

Table D.25. The x^2 Test for Goodness of Fit for Magnet Part Data for MDBT versus CSA Method at 80% Amplitude.

Positions	1	2	3	Total
Observed frequency (O)	171	58	771	1000
Probability under Ho	0.110547	0.142769	0.746684	1
Expected frequency (E)	110.5473	142.7689	746.6839	1000
$\frac{(O-E)^2}{E}$	33.05854	50.33142	0.791867	84.18182
				d.f.=2

Table D.26. The x^2 Test for Goodness of Fit for Magnet Part Data for MDBT versus CSA Method at 82% Amplitude.

Positions	1	2	3	Total
Observed frequency (O)	199	46	755	1000
Probability under Ho	0.110547	0.142769	0.746684	1
Expected frequency (E)	110.5473	142.7689	746.6839	1000
$\frac{(O-E)^2}{E}$	70.7741	65.59002	0.09262	136.4567
				d.f.=2

Table D.27. The x^2 Test for Goodness of Fit for Magnet Part Data for MDBT versus Stability Method at 78% Amplitude.

Positions	1	2	3	Total
Observed frequency (O)	185	66	749	1000
Probability under Ho	0.142001	0.14615	0.711849	1
Expected frequency (E)	142.0006	146.1503	711.8492	1000
$\frac{(O-E)^2}{E}$	13.02073	43.95519	1.938871	58.91479
				d.f.=2

Table D.28. The x^2 Test for Goodness of Fit for Magnet Part Data for MDBT versus Stability Method at 80% Amplitude.

Positions	1	2	3	Total
Observed frequency (O)	171	58	771	1000
Probability under Ho	0.142001	0.14615	0.711849	1
Expected frequency (E)	142.0006	146.1503	711.8492	1000
$\frac{(O-E)^2}{E}$	5.922278	53.16766	4.915114	64.00505
				d.f.=2

Table D.29. The x^2 Test for Goodness of Fit for Magnet Part Data for MDBT versus Stability Method at 82% Amplitude.

Positions	1	2	3	Total
Observed frequency (O)	199	46	755	1000
Probability under Ho	0.142001	0.14615	0.711849	1
Expected frequency (E)	142.0006	146.1503	711.8492	1000
$\frac{(O-E)^2}{E}$	22.87973	68.6285	2.615714	94.12395
				d.f.=2

Table D.30. The x^2 Test for Goodness of Fit for Magnet Part Data for MDFT versus CSA Method at 78% Amplitude.

Positions	1	2	3	Total
Observed frequency (O)	140	124	736	1000
Probability under Ho	0.110547	0.142769	0.746684	1
Expected frequency (E)	110.5473	142.7689	746.6839	1000
$\frac{(O-E)^2}{E}$	7.846985	2.467415	0.152869	10.46727
				d.f.=2

Table D.31. The x^2 Test for Goodness of Fit for Magnet Part Data for MDFT versus CSA Method at 80% Amplitude.

Positions	1	2	3	Total
Observed frequency (O)	166	125	709	1000
Probability under Ho	0.110547	0.142769	0.746684	1
Expected frequency (E)	110.5473	142.7689	746.6839	1000
$\frac{(O-E)^2}{E}$	27.81619	2.211492	1.901841	31.92953
				d.f.=2

Table D.32. The x^2 Test for Goodness of Fit for Magnet Part Data for MDFT versus CSA Method at 82% Amplitude.

MDFT vs CSA at 82% Amplitude				
Positions	1	2	3	Total
Observed frequency (O)	157	117	726	1000
Probability under Ho	0.110547	0.142769	0.746684	1
Expected frequency (E)	110.5473	142.7689	746.6839	1000
$\frac{(O-E)^2}{E}$	19.51975	4.651112	0.572963	24.74383
				d.f.=2

Table D.33. The x^2 Test for Goodness of Fit for Magnet Part Data for MDFT versus Stability Method at 78% Amplitude.

MDFT vs Stability at 78% Amplitude				
Positions	1	2	3	Total
Observed frequency (O)	140	124	736	1000
Probability under Ho	0.142001	0.14615	0.711849	1
Expected frequency (E)	142.0006	146.1503	711.8492	1000
$\frac{(O-E)^2}{E}$	0.028185	3.357049	0.819362	4.204597
				d.f.=2

Table D.34. The x^2 Test for Goodness of Fit for Magnet Part Data for MDFT versus Stability Method at 80% Amplitude.

MDFT vs Stability at 80% Amplitude				
Positions	1	2	3	Total
Observed frequency (O)	166	125	709	1000
Probability under Ho	0.142001	0.14615	0.711849	1
Expected frequency (E)	142.0006	146.1503	711.8492	1000
$\frac{(O-E)^2}{E}$	4.056128	3.060776	0.011404	7.128308
				d.f.=2

Table D.35. The x^2 Test for Goodness of Fit for Magnet Part Data for MDFT versus Stability Method at 82% Amplitude.

Positions	1	2	3	Total
Observed frequency (O)	157	117	726	1000
Probability under Ho	0.142001	0.14615	0.711849	1
Expected frequency (E)	142.0006	146.1503	711.8492	1000
$\frac{(O-E)^2}{E}$	1.58438	5.814134	0.281304	7.679817
				d.f.=2

For the stab & contact part, taking $\propto$ = .05, the computations for the x^2 statistic are shown in the following table, using the table of percentage points of x^2 distribution, $x^2_{.05}$ = 9.49 with d.f = 4. Because the observed x^2 is larger than $x^2_{.05}$ value, the null hypothesis is rejected.

Table D.36. The x^2 Test for Goodness of Fit for Stab & Contact Part Data for MDBT versus CSA Method at 78% Amplitude.

Positions	1	2	3	4	5	Total
Observed frequency (O)	22	343	209	177	249	1000
Probability under Ho	0.112575	0.137629	0.223654	0.223757	0.302385	1
Expected frequency (E)	112.5749	137.6293	223.654	223.7565	302.3854	1000
$\frac{(O-E)^2}{E}$	72.87422	306.4546	0.960139	9.770312	9.425049	399.4843
						d.f.=4

Table D.37. The x^2 Test for Goodness of Fit for Stab & Contact Part Data for MDBT versus CSA Method at 80% Amplitude.

Positions	1	2	3	4	5	Total
Observed frequency (O)	30	332	198	183	257	1000
Probability under Ho	0.112575	0.137629	0.223654	0.223757	0.302385	1
Expected frequency (E)	112.5749	137.6293	223.654	223.7565	302.3854	1000
$\frac{(O-E)^2}{E}$	60.56954	274.5053	2.942609	7.423662	6.811941	352.253
						d.f.=4

Table D.38. The x^2 Test for Goodness of Fit for Stab & Contact Part Data for MDBT versus CSA Method at 82% Amplitude.

Positions	1	2	3	4	5	Total
Observed frequency (O)	25	363	200	163	249	1000
Probability under Ho	0.112575	0.137629	0.223654	0.223757	0.302385	1
Expected frequency (E)	112.5749	137.6293	223.654	223.7565	302.3854	1000
$\frac{(O-E)^2}{E}$	68.12672	369.049	2.501679	16.49719	9.425049	465.5996
						d.f.=4

Table D.39. The x^2 Test for Goodness of Fit for Stab & Contact Part Data for MDBT versus Stability Method at 78% Amplitude.

Positions	1	2	3	4	5	Total
Observed frequency (O)	22	343	209	177	249	1000
Probability under Ho	0.137692	0.111096	0.221871	0.221871	0.307469	1
Expected frequency (E)	137.6919	111.0961	221.8714	221.8714	307.4692	1000
$\frac{(O-E)^2}{E}$	97.20702	484.0802	0.746708	9.074821	11.11865	602.2274
						d.f.=4

Table D.40. The x^2 Test for Goodness of Fit for Stab & Contact Part Data for MDBT versus Stability Method at 80% Amplitude.

Positions	1	2	3	4	5	Total
Observed frequency (O)	30	332	198	183	257	1000
Probability under Ho	0.137692	0.111096	0.221871	0.221871	0.307469	1
Expected frequency (E)	137.6919	111.0961	221.8714	221.8714	307.4692	1000
$\frac{(O-E)^2}{E}$	84.22826	439.2462	2.568353	6.81019	8.284254	541.1372
						d.f.=4

Table D.41. The x^2 Test for Goodness of Fit for Stab & Contact Part Data for MDBT versus Stability Method at 82% Amplitude.

Positions	1	2	3	4	5	Total
Observed frequency (O)	25	363	200	163	249	1000
Probability under Ho	0.137692	0.111096	0.221871	0.221871	0.307469	1
Expected frequency (E)	137.6919	111.0961	221.8714	221.8714	307.4692	1000
$\frac{(O-E)^2}{E}$	92.23105	571.1774	2.156017	15.62095	11.11865	692.304
						d.f.=4

Table D.42. The x^2 Test for Goodness of Fit for Stab & Contact Part Data for MDFT versus CSA Method at 78% Amplitude.

Positions	1	2	3	4	5	Total
Observed frequency (O)	7	335	198	162	278	980
Probability under Ho	0.112575	0.137629	0.223654	0.223757	0.302385	1
Expected frequency (E)	112.5749	137.6293	223.654	223.7565	302.3854	1000
$\frac{(O-E)^2}{E}$	99.01013	283.0443	2.942609	17.04472	1.966517	404.0083
						d.f.=4

Table D.43. The x^2 Test for Goodness of Fit for Stab & Contact Part Data for MDFT versus CSA Method at 80% Amplitude.

Positions	1	2	3	4	5	Total
Observed frequency (O)	0	386	177	159	278	1000
Probability under Ho	0.112575	0.137629	0.223654	0.223757	0.302385	1
Expected frequency (E)	112.5749	137.6293	223.654	223.7565	302.3854	1000
$\frac{(O-E)^2}{E}$	112.5749	448.2186	9.731967	18.74093	1.966517	591.2328
						d.f.=4

Table D.44. The x^2 Test for Goodness of Fit for Stab & Contact Part Data for MDFT versus CSA Method at 82% Amplitude.

Positions	1	2	3	4	5	Total
Observed frequency (O)	4	403	164	157	272	1000
Probability under Ho	0.112575	0.137629	0.223654	0.223757	0.302385	1
Expected frequency (E)	112.5749	137.6293	223.654	223.7565	302.3854	1000
$\frac{(O-E)^2}{E}$	104.717	511.676	15.91117	19.91643	3.05329	655.2739
						d.f.=4

Table D.45. The x^2 Test for Goodness of Fit for Stab & Contact Part Data for MDFT versus Stability Method at 78% Amplitude.

Positions	1	2	3	4	5	Total
Observed frequency (O)	7	355	198	162	278	1000
Probability under Ho	0.137692	0.111096	0.221871	0.221871	0.307469	1
Expected frequency (E)	137.6919	111.0961	221.8714	221.8714	307.4692	1000
$\frac{(O-E)^2}{E}$	124.0478	451.2576	2.568353	16.15614	2.82445	596.8543
						d.f.=4

Table D.46. The x^2 Test for Goodness of Fit for Stab & Contact Part Data for MDFT versus Stability Method at 80% Amplitude.

Positions	1	2	3	4	5	Total
Observed frequency (O)	0	386	177	159	278	1000
Probability under Ho	0.137692	0.111096	0.221871	0.221871	0.307469	1
Expected frequency (E)	137.6919	111.0961	221.8714	221.8714	307.4692	1000
$\frac{(O-E)^2}{E}$	137.6919	680.2413	9.074821	17.81579	2.82445	847.6483
						d.f.=4

Table D.47. The x^2 Test for Goodness of Fit for Stab & Contact Part Data for MDFT versus Stability Method at 82% Amplitude.

MDFT vs Stability at 82% Amplitude						
Positions	1	2	3	4	5	Total
Observed frequency (O)	4	403	164	157	272	1000
Probability under Ho	0.137692	0.111096	0.221871	0.221871	0.307469	1
Expected frequency (E)	137.6919	111.0961	221.8714	221.8714	307.4692	1000
$\frac{(O-E)^2}{E}$	129.8081	766.9747	15.09478	18.96729	4.091667	934.9365
						d.f.=4

For the arc chute part, taking $\propto$ = .05, the computations for the x^2 statistic are shown in the following table, using the table of percentage points of x^2 distribution, $x^2_{.05}$ = 9.49 with d.f = 4. Because the observed x^2 is larger than $x^2_{.05}$ value, the null hypothesis is rejected.

Table D.48. The x^2 Test for Goodness of Fit for Arc Chute Part Data for MDBT versus CSA Method at 78% Amplitude.

Positions	1	2	3	4	5	Total
Observed frequency (O)	22	343	209	177	249	1000
Probability under Ho	0.081344	0.18421	0.184210.224287		0.32595	1.000001
Expected frequency (E)	81.34353	184.2101	184.2101	224.2872	325.95	1000.001
$\frac{(O-E)^2}{E}$	43.2936	136.8775	3.336074	9.96973	18.16629	211.6432
						d.f.=4

Table D.49. The x^2 Test for Goodness of Fit for Arc Chute Part Data for MDBT versus CSA Method at 80% Amplitude.

Positions	1	2	3	4	5	Total
Observed frequency (O)	12	35	49	278	626	1000
Probability under Ho	0.081344	0.18421	0.184210	0.224287	0.32595	1.000001
Expected frequency (E)	81.34353	184.2101	184.2101	224.2872	325.95	1000.001
$\frac{(O-E)^2}{E}$	59.1138	120.8601	99.24414	12.86324	276.208	568.2893
						d.f.=4

Table D.50. The x^2 Test for Goodness of Fit for Arc Chute Part Data for MDBT versus CSA Method at 82% Amplitude.

Positions	1	2	3	4	5	Total
Observed frequency (O)	18	32	31	295	624	1000
Probability under Ho	0.081344	0.18421	0.184210	0.224287	0.32595	1.000001
Expected frequency (E)	81.34353	184.2101	184.2101	224.2872	325.95	1000.001
$\frac{(O-E)^2}{E}$	49.32663	125.769	127.427	22.29415	272.5381	597.3549
						d.f.=4

Table D.51. The x^2 Test for Goodness of Fit for Arc Chute Part Data for MDBT versus Stability Method at 78% Amplitude.

MDBT vs Stability at 78% Amplitude						
Positions	1	2	3	4	5	Total
Observed frequency (O)	22	343	209	177	249	1000
Probability under Ho	0.152112	0.096241	0.096241	0.330144	0.325261	1
Expected frequency (E)	152.112	96.24144	96.24144	330.1441	325.2611	1000
$\frac{(O-E)^2}{E}$	111.2938	632.6775	132.1104	71.03901	17.88026	965.001
						d.f.=4

Table D.52. The x^2 Test for Goodness of Fit for Arc Chute Part Data for MDBT versus Stability Method at 80% Amplitude.

Positions	1	2	3	4	5	Total
Observed frequency (O)	12	35	49	278	626	1000
Probability under Ho	0.152112	0.096241	0.096241	0.330144	0.325261	1
Expected frequency (E)	152.112	96.24144	96.24144	330.1441	325.2611	1000
$\frac{(O-E)^2}{E}$	129.0586	38.96984	23.18911	8.235814	278.0655	477.519
						d.f.=4

Table D.53. The x^2 Test for Goodness of Fit for Arc Chute Part Data for MDBT versus Stability Method at 82% Amplitude.

Positions	1	2	3	4	5	Total
Observed frequency (O)	18	32	31	295	624	1000
Probability under Ho	0.152112	0.096241	0.096241	0.330144	0.325261	1
Expected frequency (E)	152.112	96.24144	96.24144	330.1441	325.2611	1000
$\frac{(O-E)^2}{E}$	118.242	42.88134	44.22674	3.741113	274.3794	483.4706
						d.f.=4

Table D.54. The x^2 Test for Goodness of Fit for Arc Chute Part Data for MDFT versus CSA Method at 78% Amplitude.

Positions	1	2	3	4	5	Total
Observed frequency (O)	13	59	82	281	565	1000
Probability under Ho	0.081344	0.18421	0.184210.224287		0.32595	1.000001
Expected frequency (E)	81.34353	184.2101	184.2101	224.2872	325.95	1000.001
$\frac{(O-E)^2}{E}$	57.42113	85.10701	56.71191	14.34026	175.318	388.8983
						d.f.=4

Table D.55. The x^2 Test for Goodness of Fit for Arc Chute Part Data for MDFT versus CSA Method at 80% Amplitude.

Positions	1	2	3	4	5	Total
Observed frequency (O)	9	70	83	273	565	1000
Probability under Ho	0.081344	0.18421	0.184210	0.224287	0.32595	1.000001
Expected frequency (E)	81.34353	184.2101	184.2101	224.2872	325.95	1000.001
$\frac{(O-E)^2}{E}$	64.3393	70.81017	55.60763	10.57988	175.318	376.655
						d.f.=4

Table D.56. The x^2 Test for Goodness of Fit for Arc Chute Part Data for MDFT versus CSA Method at 82% Amplitude.

Positions	1	2	3	4	5	Total
Observed frequency (O)	8	74	80	260	578	1000
Probability under Ho	0.081344	0.18421	0.184210	0.224287	0.32595	1.000001
Expected frequency (E)	81.34353	184.2101	184.2101	224.2872	325.95	1000.001
$\frac{(O-E)^2}{E}$	66.13031	65.93704	58.95305	5.686463	194.9047	391.6116
						d.f.=4

Table D.57. The x^2 Test for Goodness of Fit for Arc Chute Part Data for MDFT versus Stability Method at 78% Amplitude.

Positions	1	2	3	4	5	Total
Observed frequency (O)	13	59	82	281	565	1000
Probability under Ho	0.152112	0.096241	0.096241	0.330144	0.325261	1
Expected frequency (E)	152.112	96.24144	96.24144	330.1441	325.2611	1000
$\frac{(O-E)^2}{E}$	127.223	14.41089	2.107393	7.315414	176.7034	327.7601
						d.f.=4

Table D.58. The x^2 Test for Goodness of Fit for Arc Chute Part Data for MDFT versus Stability Method at 80% Amplitude.

MDFT vs Stability at 80% Amplitude						
Positions	1	2	3	4	5	Total
Observed frequency (O)	9	70	83	273	565	1000
Probability under Ho	0.152112	0.096241	0.096241	0.330144	0.325261	1
Expected frequency (E)	152.112	96.24144	96.24144	330.1441	325.2611	1000
$\frac{(O-E)^2}{E}$	134.6445	7.155057	1.821831	9.890972	176.7034	330.2158
						d.f.=4

Table D.59. The x^2 Test for Goodness of Fit for Arc Chute Part Data for MDFT versus Stability Method at 82% Amplitude.

MDFT vs Stability at 82% Amplitude						
Positions	1	2	3	4	5	Total
Observed frequency (O)	8	74	80	260	578	1000
Probability under Ho	0.152112	0.096241	0.096241	0.330144	0.325261	1
Expected frequency (E)	152.112	96.24144	96.24144	330.1441	325.2611	1000
$\frac{(O-E)^2}{E}$	136.5327	5.140005	2.740859	14.90317	196.3867	355.7035
						d.f.=4